

# **UNIVERSIDAD DE CÓRDOBA**

**ESCUELA TÉCNICA SUPERIOR DE INGENIEROS  
AGRÓNOMOS Y MONTES**

**DEPARTAMENTO DE AGRONOMÍA**

## **SIMULACIÓN DEL TRANSPORTE DE AGUA Y SOLUTOS EN SUELOS VOLCÁNICOS, BASADA EN TÉCNICAS DE OPTIMIZACIÓN INVERSA, PARA LA EVALUACIÓN DEL EFECTO DE LAS PRÁCTICAS AGRONÓMICAS**

Tesis Doctoral presentada por Axel Ritter Rodríguez, en satisfacción de los requisitos necesarios para optar al grado de Doctor Ingeniero Agrónomo, y dirigida por el Dr. Rafael Muñoz Carpena, profesor del Departamento de Ingeniería Agrícola (Agricultural Engineering Department), University of Florida (USA).

El director:

El doctorando:

Fdo.: Dr. Rafael Muñoz Carpena

Fdo.: Axel Ritter Rodríguez

Córdoba, Octubre de 2002

## RESUMEN

El presente trabajo trata del estudio de los procesos de flujo y transporte de solutos a través de suelos volcánicos cultivados. La caracterización de dichos suelos proporciona información sobre sus propiedades físicas atípicas y la relevancia de éstas de cara a los procesos estudiados. En concreto, el alto contenido en oxihidróxidos de hierro y la presencia de arcillas alofanas da lugar a una fuerte micro-agregación del suelo que se traduce en la existencia de diferentes fases o regiones de agua, así como porosidad, conductividad hidráulica y retención de humedad altas. Estas características pueden condicionar tanto las predicciones de transporte a través de estos suelos, como las técnicas para la medida y estimación del potencial contaminante a través de los mismos.

El estudio detallado en campo durante 2 años de una parcela comercial de platanera en el Norte de Tenerife (Canarias) regada con un sistema de aspersión de gran volumen mostró lo inadecuado que resulta este sistema de riego obsoleto en el cultivo, donde el 48-52% del nitrógeno total aplicado al cultivo se perdió por lixiviación a través del suelo. Debido a la hidrogeología de la zona (basalto fracturado), el volumen lixiviado tiene el potencial de recargar rápidamente el acuífero y por lo tanto contaminarlo. Este es un problema de especial gravedad por la gran lentitud que la renovación natural de agua tiene en estos acuíferos compartimentados. El análisis de los requerimientos de lavado del cultivo según la salinidad del suelo indica que la solución al problema debe centrarse en la reducción (cambio) y fraccionamiento del fertilizante y sistema de riego, y no en la reducción de la fracción de lavado.

La enorme complejidad que presenta la estimación de los flujos y del potencial contaminante del medio agrícola apunta a que los modelos de simulación, suficientemente contrastados, pueden ser una herramienta potente para el análisis del problema y la elaboración de escenarios alternativos que permitan la reducción del impacto negativo.

No obstante, la aplicación y contrastación (calibración y validación) de dichos modelos es una tarea ardua y compleja. La medida del enorme número de parámetros que intervienen en la simulación de dichos procesos es impráctica y en muchos casos no conclusiva. Aunque idealmente debe contarse con el rango de las propiedades más significativas que condicionan cada proceso, la identificación del valor efectivo de las mismas suele obtenerse durante la contrastación del modelo frente a valores experimentales obtenidos en el lugar donde pretende aplicarse el mismo. Tradicionalmente, a través de prueba y error, variando los rangos de los parámetros que condicionan la salida del modelo, el experto podía encontrar el valor efectivo de dichos parámetros. Sin embargo, este procedimiento no es recomendable por ser muy subjetivo, consumir bastante tiempo y no asegurar la obtención del mejor conjunto de parámetros. Las técnicas de optimización inversa se presentan como una alternativa prometedora para estimar de forma automática los parámetros óptimos. Este procedimiento requiere el uso de un algoritmo de optimización así como datos de calidad medidos en condiciones de campo o de laboratorio en suelo inalterado. En este trabajo se utiliza un algoritmo de tipo global (evitando los mínimos locales) desarrollado recientemente y el modelo numérico para simulación de flujo y transporte en el suelo, WAVE. Aplicando esta técnica con los datos recogidos en la parcela de platanera se demuestra su eficiencia frente al procedimiento de calibrado tradicional.

A la hora de plantear el seguimiento complejo de estos procesos, resulta de gran interés el poder minimizar el esfuerzo y coste de esta actividad al mismo tiempo que se garantiza el éxito del método. Esto puede obtenerse con la nueva herramienta de optimización inversa planteada y la comparación de diferentes estrategias para generar los datos que requiere la

técnica. Así, cada estrategia resulta de la combinación de un cierto número de profundidades de medida y de distintas variables a medir. La estrategia más adecuada será aquella que, para satisfacer los criterios de bondad de ajuste de la simulación, requiera el mínimo de variables y de profundidades a medir. Este procedimiento para obtener la estrategia de mínimo coste puede utilizarse a priori como una herramienta de diseño experimental utilizando datos de simulación sintéticos. Éstos se generan con el modelo a partir de una primera estimación aproximada de los parámetros de la zona a estudiar. Para facilitar la comparación de dichas alternativas, se propone así mismo un índice de evaluación (FEI).

La validación de este procedimiento se hizo con datos de flujo de agua a través del suelo durante varios riegos obtenidos en el laboratorio, en una columna de suelo inalterado de grandes dimensiones ( $\varnothing 45 \times 70$  cm). Este monolito se instrumentó intensivamente en 7 profundidades, cada una de las cuales disponía de 1 tensiómetro digital, 3 sondas de TDR y 2 extractores de solución de suelo. En los extremos de la columna se instaló un simulador de lluvia en la parte superior, y en la base, un controlador de la succión y un sistema para el registro del flujo de salida de la columna. El sistema de recogida de datos con tensiómetros, TDR y flujo en la base se automatizó mediante un PC. Las estrategias de medida experimental planteadas se basaron en la combinación de distinto número de profundidades de medida (3, 4 y 7), así como de variables de estado (potencial mátrico- $h$ , contenido de humedad- $\theta$  y flujo en la base del monolito- $q$ ). Aplicando el índice de evaluación propuesto a los resultados de la optimización inversa obtenidos con cada estrategia, se deduce que, para el experimento en laboratorio, 4 profundidades y la combinación de  $h\theta$  o  $\theta q$  son suficientes para garantizar simulaciones de calidad con el modelo calibrado. Debido a la dificultad que implica la medida de  $q$  en campo, se sugiere la combinación  $h\theta$  si ese fuera el caso.

Actualmente, con las técnicas disponibles, el análisis de la dinámica de transporte en suelos volcánicos puede realizarse de forma similar al estudio de sus propiedades hidráulicas. La descripción del movimiento de solutos en estos suelos con los procedimientos clásicos (ecuación convección-dispersión CDE) puede presentar dificultades derivadas de la fuerte micro-agregación del suelo, donde se plantea la existencia de dos fracciones de agua, una inmóvil asociada al interior de los micro-agregados y otra móvil entre agregados. En estos casos, considerar un proceso de transporte con fase móvil-fase inmóvil (“mobile-immobile-model”, MIM) puede resultar más conveniente. La aplicación del procedimiento de optimización inversa con el modelo WAVE, que incluye ambas alternativas de transporte, permite identificar la significación de este factor desde un punto de vista práctico. Esta hipótesis se comprueba con datos obtenidos en la columna de laboratorio durante un experimento de riego con una solución de trazador bromuro. En este experimento se aplica una técnica novedosa de análisis de la señal de TDR (Time Domain Reflectometry) que permite estimar la concentración del trazador salino en las distintas profundidades y por lo tanto obtener las curvas de ruptura automáticamente. Estos experimentos indican sin embargo que, bajo el régimen de humedad contemplado, no hay diferencias importantes entre ambas alternativas de transporte. El desplazamiento del soluto resulta principalmente por convección. El frente abrupto que presentan las curvas sugieren la presencia de flujo preferencial. En consecuencia el potencial contaminante de productos agroquímicos aplicados a estos suelos volcánicos se espera que sea mayor.

# ÍNDICE

Resumen .....	2
Introducción .....	5
Objetivos .....	6
Capítulo 1: <i>Nitrogen evolution and fate in a Canary Islands (Spain) sprinkler fertigated banana plot</i> .....	8
Capítulo 2: <i>Using inverse methods for estimating soil hydraulic properties from field data as an alternative to direct methods</i> .....	35
Capítulo 3: <i>Analysis of alternative measurement strategies for the inverse optimization of the hydraulic properties of a volcanic soil</i> .....	61
Capítulo 4: <i>Characterization of solute transport properties in an agricultural volcanic soil using TDR and inverse modeling</i> .....	89
Discusión .....	109
Conclusiones .....	118

## INTRODUCCIÓN

El constante crecimiento de la población y el aumento del nivel de vida han conducido a una intensificación de los métodos de producción agrarios, con el inconveniente de la reducción de la calidad de recursos escasos como son el suelo y el agua. En Canarias esta situación adquiere especial interés. Por un lado, el suelo agrícola es insuficiente y por otro lado, el bajo régimen de precipitaciones y las características geológicas de las Islas hacen que el agua sea un recurso escaso. Este problema se agrava por la acción contaminante de la actividad agrícola, que además es el principal consumidor de agua en las Islas. La degradación de estos recursos exige la evaluación de las prácticas agrícolas y su mejora para minimizar el impacto negativo que éstas ejercen sobre el medio. Previamente es recomendable obtener una descripción lo más detallada posible de las propiedades del medio para facilitar la interpretación y comprensión de los procesos que en él ocurren.

En este contexto, actualmente disponemos de herramientas útiles. Por un lado, los avances tecnológicos han conducido al desarrollo de instrumentación que permite realizar el seguimiento y obtener información sobre el funcionamiento hidrológico y el transporte de contaminantes en escenarios agrícolas. El comportamiento hidrológico no sólo influye en la eficiencia del uso del agua, sino en el transporte de las sustancias químicas aplicadas al suelo. En este sentido, los procesos hidrológicos y de transporte en suelos volcánicos, como los que se encuentran en las Islas Canarias, están condicionados por las propiedades particulares (ándicas) de estos suelos. Aunque los suelos volcánicos cubren sólo el 0.84% de la superficie terrestre, éstos tienen gran importancia, porque se encuentran entre los suelos más productivos del Mundo, debido a su elevada fertilidad y capacidad de retención de agua. En el caso de Canarias estos suelos toman aún mayor relevancia dado que el 90% de los principales cultivos (plátano y tomate) se realiza en sorribas construidas con suelos que exhiben propiedades ándicas.

Por otro lado, contamos con modelos de simulación. Las medidas de control que se contemplan en la directiva 91/676/CEE y que se recogen en España mediante el Real Decreto 261/1996 del 16.02.1996 están basadas en pobres estimaciones del riesgo de lixiviación de los distintos agroquímicos, sin considerar las interacciones entre clima, cultivos, suelo e hidrogeología de la zona. El uso de modelos para la simulación del transporte de aguas y solutos en el suelo facilita la evaluación del impacto negativo sobre los recursos mencionados; puede ayudar en la toma de decisiones y desarrollo de normas y leyes para

reducir el mismo y resulta mucho menos costoso que la propia investigación experimental. Además, en la directiva 91/414/CEE sobre evaluación del riesgo de lixiviados, se sugiere la realización de estudios de simulación usando modelos suficientemente contrastados.

El uso de modelos presenta, sin embargo, limitaciones debido a la necesidad de estimar los parámetros que éste requiere y que caracterizan las condiciones en las que se pretende aplicar. Este proceso, denominado calibración es crítico, porque de él depende el éxito de la aplicabilidad del modelo de simulación. Existen varias técnicas para determinación de parámetros o propiedades del medio. Éstos pueden obtenerse por métodos directos, pero suelen ser laboriosos, caros y consumir mucho tiempo. Como alternativa, tenemos los métodos indirectos, en los que los parámetros se estiman en un proceso basado en reducir las diferencias entre los valores medidos y simulados de alguna variable de estado del sistema. Esta técnica puede realizarse por el procedimiento de “prueba y error” o bien usando herramientas de optimización más complejas y elaboradas.

Estos temas se abordan en el presente documento cuya estructura se divide en cuatro artículos, cada uno de los cuales se centra en un objetivo diferente.

## **OBJETIVOS**

Para cada artículo, los objetivos que se persiguen son los siguientes:

1. Estudio del funcionamiento hidrológico de un escenario típico agrícola canario a partir de información obtenida mediante muestreos intensivos y técnicas avanzadas de instrumentación en un cultivo de plátanos. Se evalúa el uso del agua de riego y se cuantifica el efecto contaminante de los fertilizantes nitrogenados aplicados.
2. Con los datos obtenidos, se estudia la aplicación de un modelo para la simulación del movimiento de agua en condiciones de campo en un escenario típico agrícola canario. Se evalúan tres procedimientos para la estimación de parámetros: método directo, método indirecto por “prueba y error” y calibración por optimización inversa.
3. Visto el potencial y las limitaciones de la optimización inversa se propone un procedimiento para analizar diferentes alternativas de toma de datos y establecer de esta forma los requerimientos mínimos de información (datos) necesarios para la estimación de parámetros hidráulicos por este método.

4. Conocidas las propiedades hidráulicas, se procede al estudio de la dinámica de transporte en este suelo volcánico. Para ello se emplea la técnica de TDR (Time Domain Reflectometry) que permite el seguimiento simultáneo del contenido de humedad del suelo y de la concentración de un soluto salino. Para la estimación de los parámetros que rigen el movimiento de solutos en el suelo se aplica el procedimiento de simulación inversa.

## **Capítulo 1**

### **Nitrogen evolution and fate in a Canary Islands (Spain) sprinkler fertigated banana plot**

*Agricultural Water Management* 52 (2002): 93-117

## **Abstract**

Banana and other horticultural produce cultivation, together with the population increase, has led to coastal aquifer degradation in the Canary Islands. A detailed field study to track nitrogen degradation and transport through a banana plantation soil into the aquifer is presented. The main objective of the study is to understand and quantify the hydrological behavior of the system, and quantify nitrogen leaching. The hydrogeological study of the area shows that the thin terraced soil is set on top of several layers of fractured basalt down to a massive formation where the polluted aquifer is found. When water leaves the soil profile, it is likely to quickly percolate along the preferential paths (cracks) through the basaltic layers and it is intercepted by lateral interflow in a mixing ratio of 25% irrigation drainage plus 75% interflow, before it reaches the aquifer. The soil water balance shows that most of the drainage (18% of the total irrigation+rainfall) is produced during the crop highest water demand period and during the short rainy season when no irrigation is applied. Monitoring of the soil solution showed that very high nitrate concentrations (50-120 mg/l N-NO<sub>3</sub>) are present throughout the experimental period. The high water fluxes and nitrate concentration at the bottom of the soil profile produce a yearly loss of 48-52% of the total N applied (202-218 kg N/ha per year). Monitoring of water from springs below the experimental area shows that the nitrate lixiviates are diluted around 60% before reaching the aquifer, after mixing with the lateral flow. Smaller and more frequent applications of both N and water would help to reduce the environmental impact of the system.

*Keywords:* Ammonium; Bananas; Contaminant; Environment; Fertigation; Hydrology; Nitrate; Pollution; Volcanic soil; Water; Suction cups.

## 1. Introduction

Although income from bananas is about 2% of the gross regional income in the Canary Islands (COAP, 1995), its cultivation and trade are very important for economic, cultural and social reasons, employing 6% of the active population. The climatic and physiographic variability of the islands impose irrigation on the crop for most of its year-around cycle to cover monthly water deficits as high as 130 mm. The introduction of fertigation and micro-irrigation techniques has allowed the expansion of the crop to areas with reduced water quantity and quality. The intensity of the banana and other horticultural crops coexisting in the same areas, demanding high inputs of water and agrochemicals, together with rural population increase, has resulted in degradation of the coastal aquifers.

The global hydrological balance in the two most populated islands (Tenerife and Gran Canaria) and the region is presented in Table 1. Evapotranspiration plus infiltration account for up to 85-98% of the total rainfall. This means surface water is a scarce resource, and the islands rely heavily on groundwater resources (95% of total water supply).

Table 1. Components of the hydrological cycle in the Canary Islands

Factor <sup>1</sup>	Gran Canaria			Tenerife			Canary Islands		
	hm <sup>3</sup> /year	mm/year	%	hm <sup>3</sup> /year	mm/year	%	hm <sup>3</sup> /year	mm/year	%
P	466	300	100	865	425	100	2535	507	100
ET	304	195	65	606	298	70	1665	333	66
I	87	56	19	239	117	28	590	118	23
Es	73	47	16	20	10	2	280	56	11

<sup>1</sup> P= Precipitation; ET= Evapotranspiration; I= Infiltration; Es= Surface Runoff.

Rainfall varies significantly within each island depending on orientation and altitude. Northern areas are wetter than southern ones, and precipitation also increases with elevation. Bananas are grown on the lower, drier coastal areas, where precipitation can be as low as 100 mm/year or even less. Water consumption from both agricultural and human uses is increasing, exceeding in some instances the net groundwater recharge. This situation is forcing the introduction of expensive non-traditional water resources such as desalinization and water treatment and reuse, as proposed by the Canary Islands's Hydrological Plans (DGA-SPH, 1993; CIAGC, 1995). Water use statistics by economic activity show agriculture to be the major consumer, using 60-80% of available resources. Among crops, bananas alone consume up to 60% of the agricultural water resources (SYSCONSULT-AICASA,1987). The scarcity of water imposes the need to conserve the resource and to use it efficiently. This

concern is illustrated by the fact that the Canaries pioneered the introduction of micro-irrigation systems at both national and European levels (Sanchez Padrón, 1993).

Water management and use in the islands is threatened by pollution from human sources (agriculture and others). A recent study (DGA-SPH, 1993) shows that most of the traditional agricultural areas are already polluted. In a limited area such as an island, a polluted aquifer is a lost aquifer, thus imposing the need to resort to expensive non-traditional resources that compromise the sustainability of the system.

There are three mayor classes of groundwater pollution present in the islands: i) volcanic activity; ii) sea water intrusion caused by over-exploitation; and iii) drainage from agricultural lands and rural septic systems. As a result, the quality of available resources varies depending on their source. The two most common groundwater extraction systems on the islands are regular (vertical) wells and “galleries” (horizontal wells). Well water typically bears a high sodium chloride content, up to 2000 mg/l Cl and 1250 mg/l Na, with neutral pH and  $EC_{25} > 5$  dS/m. Gallery water is characterized as sodium bicarbonated, with  $pH > 8$ , and, in some cases, reaching up to 2000 mg/l  $HCO_3$  and 500 mg/l Na. The water usually has a high silica content (50-110 mg/l  $SiO_2$ ) caused by prolonged contact with the aquifer materials (fossil waters); in some areas it can also have a very high fluoride content (up to 9 mg/l).

Dumping of domestic untreated effluents and agricultural lixiviates from intensive crops are the main nitrate sources to the aquifer. In general, the affected areas correspond to those where salt water intrusion is already present. These areas in Tenerife are represented by a high density of nitrate (mg/l  $NO_3$ ) concentration isolines (Figure 1). The average nitrate concentration in the main agricultural valleys of the island ranges 9-11 mg/l N- $NO_3$  (40-50 mg/l  $NO_3$ ), but exceeds 25 mg/l N- $NO_3$  in some areas ( $>110$  mg/l  $NO_3$ ).

The Hydrological Plan of Tenerife (DGA-SPH, 1993) indicates that most of the nitrate comes from crop fertilization rather than septic systems. The study concludes that in the short and mid term, the groundwater resources of the island will continue to degrade as: i) volcanism is a permanent process; ii) there is not an abundant resource available in the short term that will prevent aquifer over-exploitation in the coastal areas, although a significant increase in alternative sources is expected; iii) nitrate leaching will eventually be reduced by non-point source pollution control programs but the existing levels will persist for a long time due to the slow recharge rate of the aquifer. The conclusions of the study can be

extrapolated to other islands of the Archipelago, with some differences regarding salinity levels - lower in the wetter islands - but with nitrate levels still high.

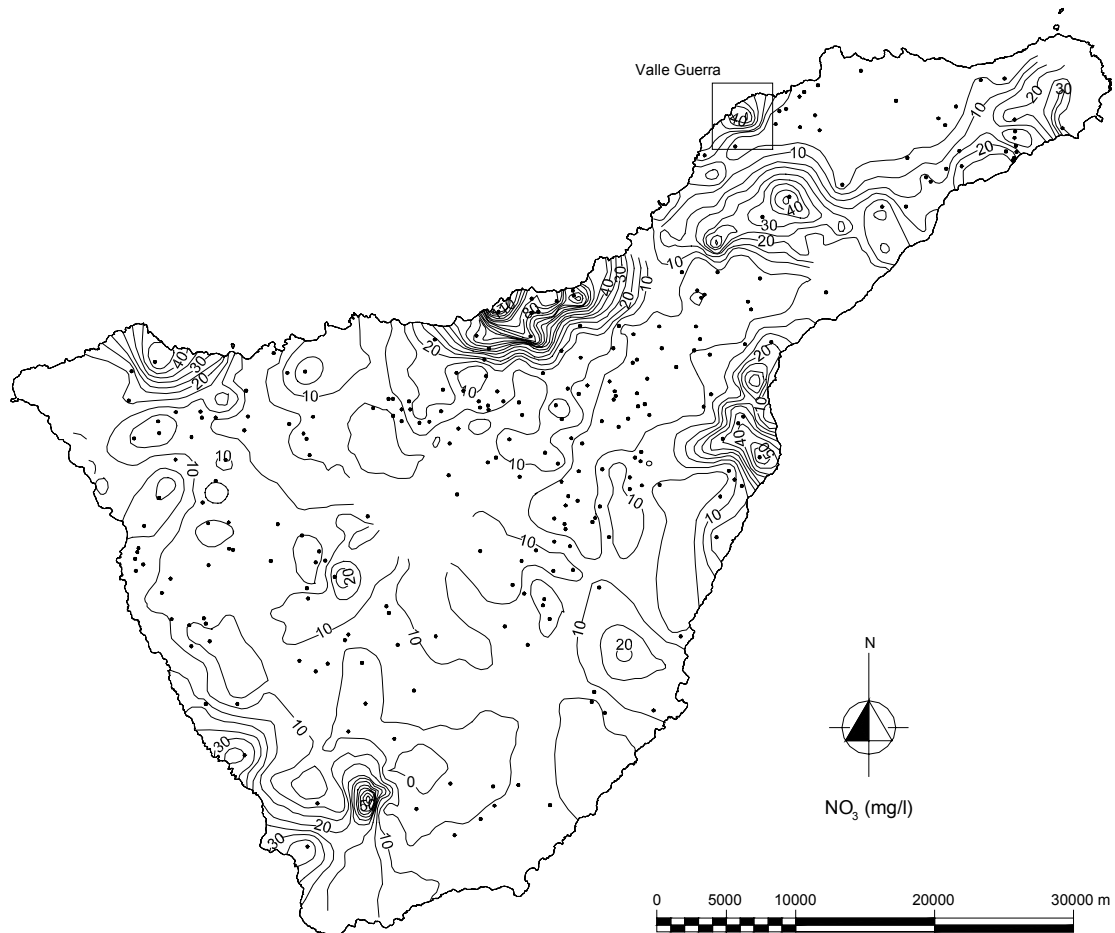


Figure 1. Nitrate concentration isolines ( $\text{NO}_3$  mg/l) in the island of Tenerife (DGA-SPH, 1993).

The following experimental study deals with water and nutrient hydrological transport processes that take place in a fertigated banana plot, and that ultimately lead to soil and water pollution. The results will help agronomists to identify alternative management schemes that reduce environmental impact. The data obtained is also being used in field testing of a numerical model that will aid in the assessment of the proposed management schemes.

## 2. Methodology

### 2.1. Selection of experimental area

A 4800 m<sup>2</sup> field plot was selected within an intensive agricultural area, the valley of Valle Guerra, in the north of Tenerife (the largest island, 2057 km<sup>2</sup>). The valley is enclosed by the Anaga Mountain range (altitude over 2000 m) on its NE side and is open to the Atlantic Ocean on its NW exposure, ending in a cliff 70 m high. The mean annual temperature for the area is 20°C (minimum of 15°C in winter), and annual precipitation and crop evapotranspiration measured at the plot are around 380 and 1000 mm, respectively.

The main crops in the valley are bananas and other horticultural and ornamental crops (under greenhouse and open air systems). The experimental plot was selected inside a 42 ha banana plantation (Las Cuevas) owned and operated by a private company. The plot was chosen to represent the average conditions of the area (fertigation and cultural practices) at the time. The plantation, located on fairly steep ground in the lower part of the valley, is terraced all the way down to the edge of the cliff, 70 m above sea level. One major spring present in the cliff face directly below the plantation (at 10 m above sea level) was also used in the experimental study.

The fertigation system used by the company for this plantation (Table 2) is of the type employed in around 13% of the total banana surface in the Canary Islands.

Table 2. Characteristics of the fertigation system

Distribution system	Emitter type	Summer application (m <sup>3</sup> /ha)	Annual application (m <sup>3</sup> /ha per year)	Efficiency (%) <sup>1</sup>	Fertigation equipment	% of banana area <sup>2</sup>
Buried PVC pipes	800 l/h placed 1 m high, precipitation: 40-80 mm/h	500 per week	14000	50	Venturi	13.24

<sup>1</sup> From: Ingenieros Asociados de Tenerife, S.L. (1983). <sup>2</sup> Data extrapolated from AGRIMAC S.L.(1995).

Banana fertilization guidelines in the area are as follows (g/plant-year): a) applied with the irrigation system: 250-300 N, 80-100 P<sub>2</sub>O<sub>5</sub>, 350-400 K<sub>2</sub>O; b) applied to the soil in solid form: 80-150 CaO. The density of plants in the area is about 1800 plants/ha. In the south of the island, density goes up to 2000 plants/ha, which can be increased by a further 20-30% if micro-irrigation, new cultivars, and greenhouses are used.

## 2.2. Hydrogeology of the area

A detailed hydrogeological study was conducted on site (Poncela, 1994). The area was formed as a series of fractured lava layers from the Quaternary period (Series III) on top of an older massive basaltic foundation (Series I) closed to sea level. If enough time passed between volcanic eruptions, soil was formed so that the lava layers are alternated by these continuous impermeable layers of baked soil called “almagre” (Figure 2).

The unsaturated zone is constituted by two types of materials: a) thin soil layer at the surface, 0.6 m thick; and b) fractured Series III basaltic materials down to the water table, with a variable thickness of up to 70 m. There are only a few wells in production in the lower coastal areas due to salinization (sodium chloride) and deep water tables. Most of the irrigation water comes from galleries or a mixture of both types. The samples obtained from the network of wells around the experimental area show that nitrate pollution is present, with values above 11 mg/l N-NO<sub>3</sub> (50 mg/l NO<sub>3</sub>) in some instances (Muñoz-Carpena et al, 1996a).

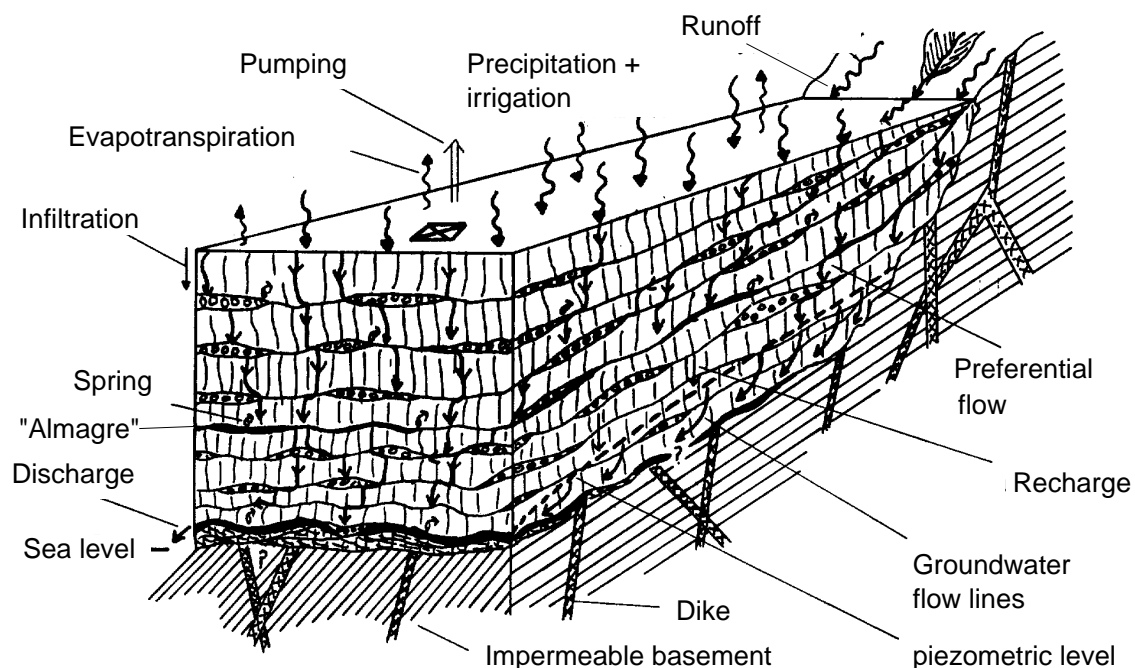


Figure 2. Hydrogeological model at the experimental area.

Water flow to the aquifer comes from two major sources: a) general interflow from the adjacent mountains; b) drainage from agricultural lands. This flow to the aquifer is intercepted by “almagres” and conducted laterally where it frequently appears as a spring flowing from the cliff side. The isotopic and hydrogeological study conducted using water samples (irrigation, spring and well water) from one sampling date shows that the water

finally reaching the aquifer is a complex mix of about 25% drainage from agriculture and 75% general groundwater interflow.

### *2.3. Soil characterization*

It is generally agreed that the lower limiting temperature for banana growth is 15 °C. Since those conditions are only met in the lower coastal areas of the islands (preferably along the southern shores), two practical problems arise for banana (and other horticultural crops) production. First, generally speaking, the natural soil profile in the area is too thin to sustain banana cultivation due to its recent volcanic origin, and the dry and uniform climate of the lower coastal areas. Second, the fact that the landscape of the area is typically formed by steep slopes, sometimes over 10%. These conditions have resulted in the typical agricultural landscape of the islands, the “sorriba”, terraces built across the steep slopes with rock retaining walls filled with soils imported from the high mountain areas where changes in humidity and temperature have allowed weathering of the volcanic materials and produced well developed soils. Traditionally these soils are put over a drainage layer of gross material, which lays on top of the fractured rock that constitutes the subsoil. From the soils standpoint the implications are clear: conditions at any given terrace or plot should not necessarily correspond to those found in adjacent plots, since the soil might have different characteristics depending on its origin. This imposes the need of a careful on-site soil characterization. In our case, the “sorribas” of the plantation (42 ha) were built by the owner during the same period (over 50 years ago) from the same soil sources, but they might not agree with soils from adjacent plantations.

In June 1994 a soil depth survey was conducted at the experimental plot by means of thin soil borer on a grid of 110 points (Figure 3). Seven soil pits were excavated on the plot with the aim of describing (Soil Survey Staff, 1978) and sampling the soil profile to determine variability (in depth and area) of the main soil characteristics. Soil samples, both disturbed samples and undisturbed soil cores, were taken at three depths (15, 30, 60 cm) in each pit. Physical and chemical properties were determined following standard methods (Klute, 1986). The mineral content was studied with the aid of X-diffraction techniques.

The soil saturated hydraulic conductivity ( $K_s$ ) and characteristic (moisture) curves were measured using undisturbed soil cores (Klute, 1986). The soil characteristic curves were then fitted to the van Genuchten’s equation (van Genuchten, 1980). Sorption properties for

ammonium were measured in the laboratory by means of batch studies (Muñoz-Carpena et al., 1996a) and the comparison of field values of ammonium sorbed in the soil vs. soil solution values. These values will help to establish the nitrogen cycle and transport at the site in concurrent modeling efforts.

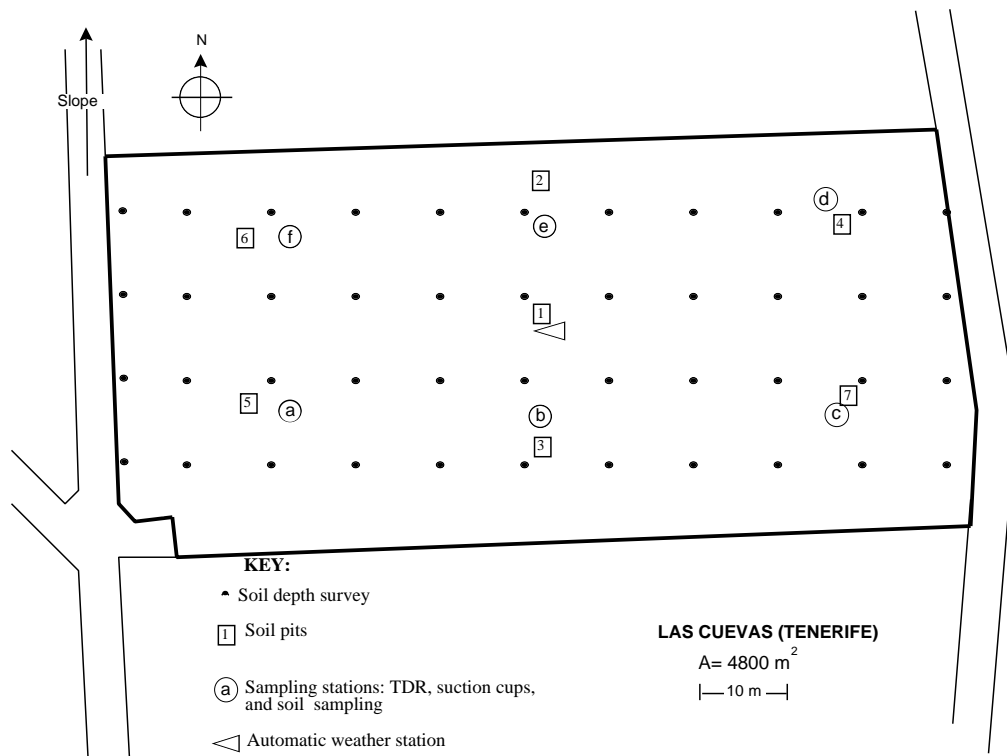


Figure 3. Experimental field setup.

#### 2.4. Experimental design and sampling protocol

The experimental setup at the plot was designed to obtain soil and water samples from the soil section of the unsaturated zone, record the variation of the hydrologic components, and register the cultural practices and crop data at the experimental plot. Fertigation and other cultural practices were carried out by the farm following usual calendars in the area, since the intent of the experiment was to evaluate existing practices rather than to alter these experimentally.

A total of 1725 samples were collected and analyzed during the 1.5 years experimental period (8/1995-9/1996). Soil and water samples were taken at six different points in the plot to assess spatial variability (Figure 3). Nitrogen movement was tracked by sampling the soil profile at three depths (15, 30, 60 cm). The sampling depth of 60 cm was selected to capture nitrogen content at the interface between the soil and the underlying drainage layer. Sampling

took place weekly or after each irrigation event when the crop was irrigated more than once a week. Four types of samples were collected in each of the six sampling stations: i) soil at three depths (15, 30, 60 cm); ii) soil solution taken by ceramic suction samplers at the same three depths; iii) effective precipitation (rainfall and irrigation) and incoming nitrogen into the soil captured by a set of ground level pluviometers, one in each of the sampling stations (Figure 3); and iv) water from the spring on the cliff.

The porous ceramic cups used were 60.5 mm long with an outside diameter 48.3 mm and a 2 bar (200 kPa) air-entry value (SoilMoisture 653X01-B02M2, 2 bar, high flow). They were mounted on 4.8 cm outside diameter PVC tube of 15-61 cm length, closed at the top with a Santoprene stopper. Neoprene tubing was used as an access port for sample extraction and suction application. The devices were inserted vertically in clusters of three (Figure 4), and the PVC pipes were sealed with bentonite at the surface to prevent downward water movement along the external surface of the pipe. A suction of 0.60 bar (60 kPa) was applied two days prior to sampling. The water was collected during the period in which the suction head decreases as water enters the cup (falling head method). Suction cups are one of the early methods proposed for sampling soil water (Briggs and McCall, 1904; Wagner, 1962). The advantages of the method (nondestructive, low-cost, easiness of use) have made it one of the most widely used nowadays. The method however presents limitations and can yield contradictory results. Alberts et al. (1977) studied the temporal variation on the soil N-NO<sub>3</sub> content by comparing soil sample extractions with 1M KCl with suction cup samples. Generally they found similar values between both types of samples, but in some instances large differences were attributed to the soil intrinsic variability and the limited number of repetitions. Overall, the authors concluded that this was an acceptable sampling method. Bernhard and Schenck (1986) also found an acceptable correlation ( $R^2 = 0.5-0.7$ ) between both types of samples. Other studies show that the sample volume and concentration are not reproducible on an experimental setup, depending on the contaminant studied, material of which the suction lysimeter is made of, and the soil variability and type. Hansen and Harris (1975) in a nitrate and phosphate monitoring study observed that the variability among samplers placed close to each other was at least 30%. They explained this sample variability in terms of: i) sorption, diffusion, washing and filtering through the cup; ii) changes in cup permeability caused by the deposition of the fine soil particles in the small cup pores; iii) spatial variability of the soil horizons; iv) and differences in lysimeter management such as vacuum level applied or installation. On another contaminant tracking and monitoring study

of pesticides (atrazine and alachlor), using bromide as a tracer, Smith and Thomas (1990) found a coefficient of variation among nearby samples ranging from 23-200%. The effect of soil texture and structure on suction cup samples was studied by Shaffer et al. (1979), Barbee and Brown (1986), and Djurhuus and Jacobsen (1995). These researchers compared soil and suction cup samples obtained from soils with different textures and concluded that the method is well suited for sandy soils if the sample is taken on the same irrigation or rainfall day. For clay structured soils sample variability is high, specially when a large volume of water is applied and water moves rapidly through cracks or macropores. Djurhuus and Jacobsen (1995) concluded that in the case of structured soils, such as the one in this study, the suction cups should be preferred to soil sampling when the aim is to estimate nitrate leaching. Preferential flow through macropores in soils may affect the composition of the soil solution sampled if seepage water bypasses the suction cup (Shaffer et al., 1979, Barbee and Brown, 1986). This problem is partly a problem of spatial variability of the soils and should be addressed as such by an intensive sampling and repetition scheme. Some chemicals are adsorbed to the porous cups during the sampling process. Nagpal (1982) found very low adsorption for  $\text{NO}_2$  and  $\text{NO}_3$  when passing a standard solution through the cup, so that there are no limitations to its use from this point of view.

Water samples (from suction cups, pluviometers and the spring) were collected in dark glass bottles with teflon caps. Soil and water were immediately cooled down to 5 °C in the field for transportation to the lab.

A typical analysis of a soil sample consisted of pH,  $\text{EC}_{25}$ , soluble N- $\text{NO}_3$  and N- $\text{NH}_4$ , and total N. The N- $\text{NO}_3$  and N- $\text{NH}_4$  were analyzed using a Technicon autoanalyzer and total N by Kjeldahl's method. Water samples were analyzed in a similar manner (pH,  $\text{EC}_{25}$ , soluble N- $\text{NO}_3$  and N- $\text{NH}_4$ ) with the exception of the suction cups samples, where ammonium was not determined since it is known to be retained at the ceramic cup (Muñoz-Carpena et al., 1995).

An automatic weather station was installed on site (Muñoz-Carpena et al., 1996b) to estimate reference evapotranspiration for the crop at intervals of 15 minutes (1 min data average) and record rainfall and soil temperature changes. Daily soil moisture content was monitored using a time domain reflectometry system (TDR). Sensors were placed at the same three depths in all six sampling stations (Figure 4). Suction lysimeters, TDR equipment and pluviometers were protected by a mesh cage in each of the sampling stations. Soil samples

were taken in a spiral fashion around the equipment cage and the sampling spot was marked with a survey flag to avoid taking a sample on disturbed soil.

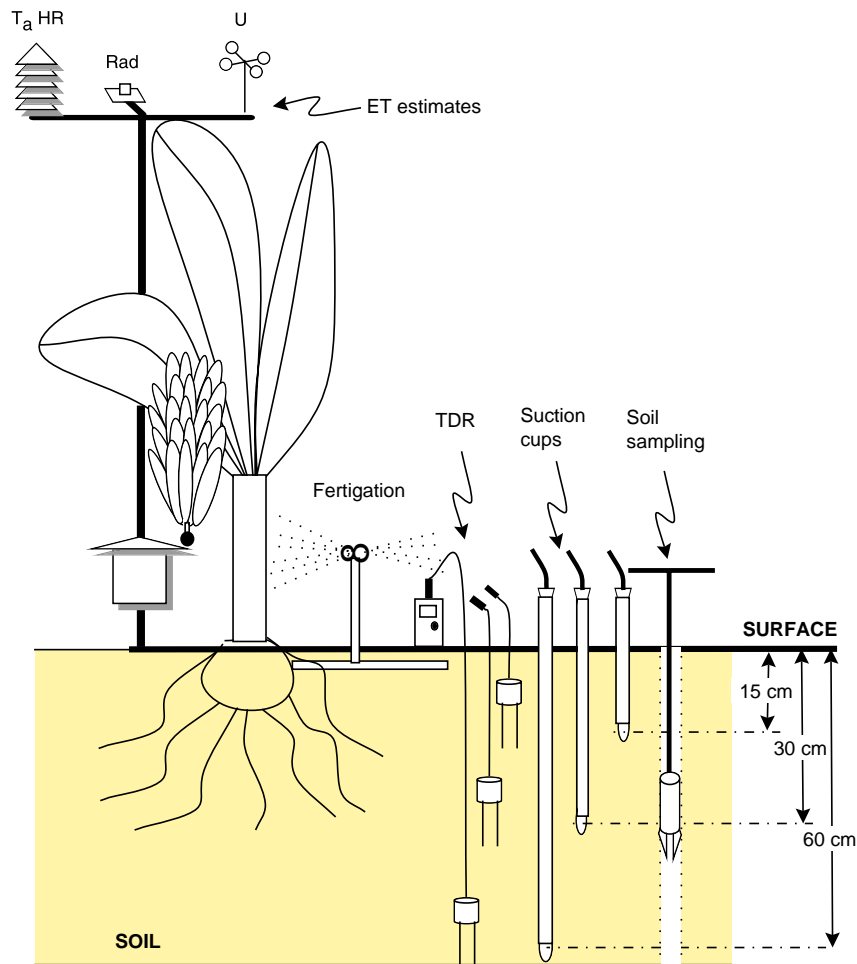


Figure 4. Details of the sampling and monitoring equipment used in a sampling station.

### 2.5. Balances

A monthly water balance was established based on Penman (1950a, b) and taking the sum of daily data of precipitation, irrigation and crop evapotranspiration. Monthly average soil water content values for the whole profile were determined using the daily values of soil water content measured with TDR. Soil water content variation was calculated as the difference between consecutive monthly values. Assuming no runoff for the terraced soil, the water balance and drainage to the aquifer are given by,

$$BAL = (P + R) - (ET_c + \Delta W) \quad (1)$$

where  $BAL$  stands for water balance,  $P$  for precipitation,  $R$  for irrigation,  $ET_c$  for crop potential evapotranspiration and  $\Delta W$  for moisture variation.

$$D = \begin{cases} BAL; & BAL \geq 0 \\ 0; & BAL < 0 \end{cases} \quad (2)$$

where  $D$  stands for drainage.

If Eq. (1) gives negatives values, there is no drainage and actual evapotranspiration ( $ET_a$ ) is set to be less than the potential evapotranspiration.

$$ET_a = \begin{cases} ET_c; & BAL \geq 0 \\ P + R + \Delta W; & BAL < 0 \end{cases} \quad (3)$$

where  $ET_a$  is crop actual evapotranspiration.

A monthly nitrogen balance was also made. N-NH<sub>4</sub> and N-NO<sub>3</sub> inputs coming from the rain and irrigation water were calculated from the analysis of field samples. Those inputs coming via fertigation were determined based on water samples taken from the sprinklers during fertigation. An estimation of the total nitrogen extraction by the crop was made combining data of banana production at the experimental plot for the period studied, foliar analyses, and considering average values found in the literature (Table 3).

Table 3. Annual average matter and nitrogen content of a banana plant of the Cavendish group (cv. “Grand Naine”) (Soto Ballesteros, 1990)

Part of banana plant	Fresh matter (%)	Dry matter (%)	N (%)
Bunch <sup>1</sup>	26.85	18.2	0.87
Whole plant <sup>2</sup>	91.56	11.2	1.06
Shoot <sup>3</sup>	8.44	7.7	1.61
Whole plant + Shoot	100.00	10.9	1.06

<sup>1</sup> Includes: petiole, rib and limb. <sup>2</sup> Includes: bunch, pseudostem and stalk. <sup>3</sup> Includes: whole leaves, pseudostem, immature leave and stalk.

A fraction of this total N extraction is assumed to return into the soil by mineralization of the crop residues left on the plot. N-NO<sub>3</sub> and N-NH<sub>4</sub> soil concentrations were obtained from soil samples, combining them with soil water content values measured with TDR. The monthly variation of soil nitrogen concentration was calculated by monthly averaging the daily values (estimated by linear interpolation between weekly sample values). Taking all

these factors into account, the amount of nitrogen that is lost by leaching from the soil ( $N_L$ ) is given by the following balance:

$$N_L = (N_P + N_R + N_F + N_{MIN}) - (N_{EX} + \Delta N_S + N_{IN}) \quad (4)$$

where  $N_L$  is the nitrogen losses by leaching obtained with the balance method,  $N_P$  the nitrogen content in the rain,  $N_R$  the nitrogen content in irrigation water,  $N_F$  the nitrogen content of fertilizer,  $N_{MIN}$  the nitrogen content of the crop residues that are mineralized,  $N_{EX}$  the total nitrogen extracted by the crop,  $\Delta N_S$  the soil nitrogen content variation and  $N_{IN}$  the nitrogen content immobilized by soil microorganisms.

Nitrogen losses by leaching will only take place in those months where drainage is observed. If the balance gives a positive value and there is no drainage, it is assumed that the nitrogen has been temporally immobilized by soil microorganisms (Gros, 1976), and the quantity is supposed to leave the soil by leaching the next month that drainage takes place.

Nitrogen losses values were compared with those independently obtained by multiplying the monthly drainage values from the water balance (Eq. (2)) by the monthly average nitrogen concentration of the soil solution in the interface of the soil and fractured rock (60 cm),

$$N_{L60} = 0.01D\bar{C} \quad (5)$$

where  $N_{L60}$  is the nitrogen losses by leaching at the interface of the soil and the drainage layer (kg/ha),  $D$  the drainage (l/m<sup>2</sup>) and  $\bar{C}$  the monthly average nitrogen concentration at 60 cm (mg/l).

### 3. Results and discussion

The results of the soil depth survey showed that the average soil depth in the experimental plot was 60 cm, with a range of 50-80 cm, below which a net contact with the fractured basaltic rock was found. Average values and their standard deviations of the soil physical and chemical properties are summarized in Tables 4 and 5. The mineral content shows presence of volcanic amorphous materials, ferric minerals (hematites and goethite) and 1:1 clays with

pH dependent charge (halloysite) and 1:2 (nontronite). The soil displays andic properties (Soil Survey Staff, 1978).

Table 4. Physical properties of the soil at the experimental site<sup>1</sup>

Depth (cm)	Hydraulic conductivity, $K_s$ (cm/h)	Bulk density, $\rho_b$ (g/cm <sup>3</sup> )	Specific density, $\rho_s$ (g/cm <sup>3</sup> )	Porosity, $P$ (cm <sup>3</sup> /cm <sup>3</sup> )	van Genuchten's parameters			Texture (USDA) <sup>2</sup>
					$\alpha$	$n$	$\theta_r$	
15	13.0 ± 3.77	1.09 ± 0.06	2.51 ± 0.19	0.55 ± 0.02	0.28 ± 0.04	1.38 ± 0.05	0.32 ± 0.03	C
30	8.38 ± 2.08	1.18 ± 0.06	2.49 ± 0.06	0.52 ± 0.03	0.22 ± 0.04	1.41 ± 0.05	0.32 ± 0.03	C
60	7.65 ± 2.18	1.09 ± 0.10	2.34 ± 0.20	0.49 ± 0.03	0.19 ± 0.04	1.29 ± 0.05	0.25 ± 0.03	C-L

<sup>1</sup> Values shown are  $\bar{X} \pm S_x$ , number of samples = 7. <sup>2</sup> C= Clay; L= Loam.

The particle analysis shows that the soil has a clay percentage above 40% (USDA texture from Clay to Clay-Loam).  $K_s$  literature values for these soil textures are 0.06-0.2 cm/h (Rawls and Brakensiek, 1983) or 1.07-3.63 cm/h (McCuen, 1981). Our soils give values around 5 times higher than those reported in the literature ( $K_s=7.65-13.0$  cm/h). This may be explained in terms of the high Fe-oxyhydroxides content in volcanic soils that leads to strong particle aggregation. This is consistent with a dual-porosity soil model revealing a slow flow-diffusive transport region inside the aggregates and a fast flow-convective transport region in between aggregates, as proposed for this soil by Regalado et al. (2001). This preferential flow process is widespread and leads to high effective  $K_s$  values, well above standard levels for their texture, and also to the soil fast response to inputs in the system (water and solutes).

The higher clay content in the surficial layers results in an increased moisture retention capacity as shown in Figure 5. Values for pH and  $EC_{25}$  remain constant with depth, but organic matter (OM) is high on the surface layer due to the large amount of leaves that bananas produce, which are typically left on site after harvest.

Table 5. Average chemical properties of the soil at the experimental site at two different times<sup>1</sup>

Depth (cm)	Organic matter (%) December 1995	$EC_{25}$ (dS/m)		pH		CEC (meq/100g)	Sorption $K_d$ NH <sub>4</sub>
		December 1995	October 1996	December 1995	October 1996		
15	2.32 ± 0.79	1.85 ± 0.16	1.08 ± 0.04	6.92 ± 0.16	7.07 ± 0.21	37.1 ± 3.4	10.1 ± 2.8
30	1.70 ± 0.63	1.88 ± 0.13	1.02 ± 0.05	6.98 ± 0.11	7.17 ± 0.09	33.7 ± 2.24	13.3 ± 3.6
60	1.03 ± 0.24	1.65 ± 0.13	1.23 ± 0.09	7.25 ± 0.08	7.35 ± 0.11	32.0 ± 2.75	18.9 ± 4.1

<sup>1</sup> Values shown are  $\bar{X} \pm S_x$ , number of samples = 7.

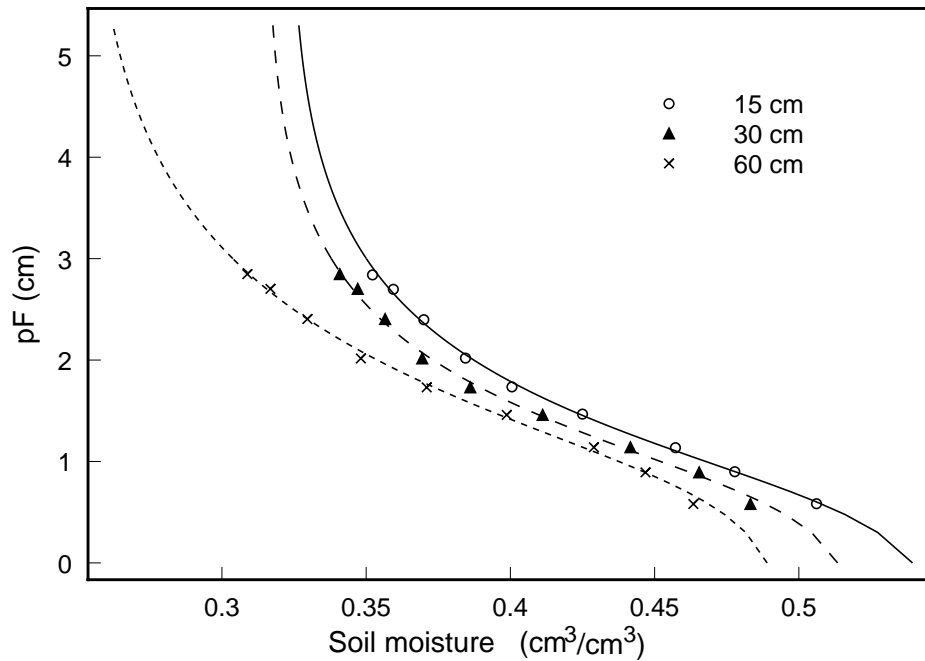


Figure 5. Average suction curves at the experimental site (lines: van Genuchten equation; symbols: data).

The evolution of the soil water content for the period studied (01/08/95–30/09/96) is shown in Figure 6. It represents the average daily moisture variation at each soil depth in response to water exchanges from the soil ( $R$ ,  $P$ ,  $ET_a$ ,  $D$ ). The average coefficients of variation among sampling stations for each soil depth TDR readings were 21.2, 16.6, 18.3% for 15, 30 and 60 cm, respectively. The rainy period at the end of 1995 and beginning of 1996 results in a noticeable increase in average soil moisture content in the soil profile. Average moisture content begins to drop after that date, especially between March and June (when irrigation decreases). At 60 cm there is less depletion in soil water content. The increase of the irrigation volume in the following months re-establishes the water content of the superficial layers to the average levels.

Figure 7 shows the components of the monthly water balance for the period studied. Potential and actual crop evapotranspiration for the period studied was 1177 and 1059 mm respectively. The total drainage reaches 237 mm/year, which corresponds to 18% of the rain and irrigation applied in the plot during a year (439 and 873 mm, respectively). This amount is not uniformly distributed, but it takes place after long periods of precipitation or frequent irrigation. Between November and March there is less evapotranspiration and therefore the input of water by irrigation and rain results in the largest amounts of drainage. Irrigation excess produces also some drainage in April, May and July of 1996.

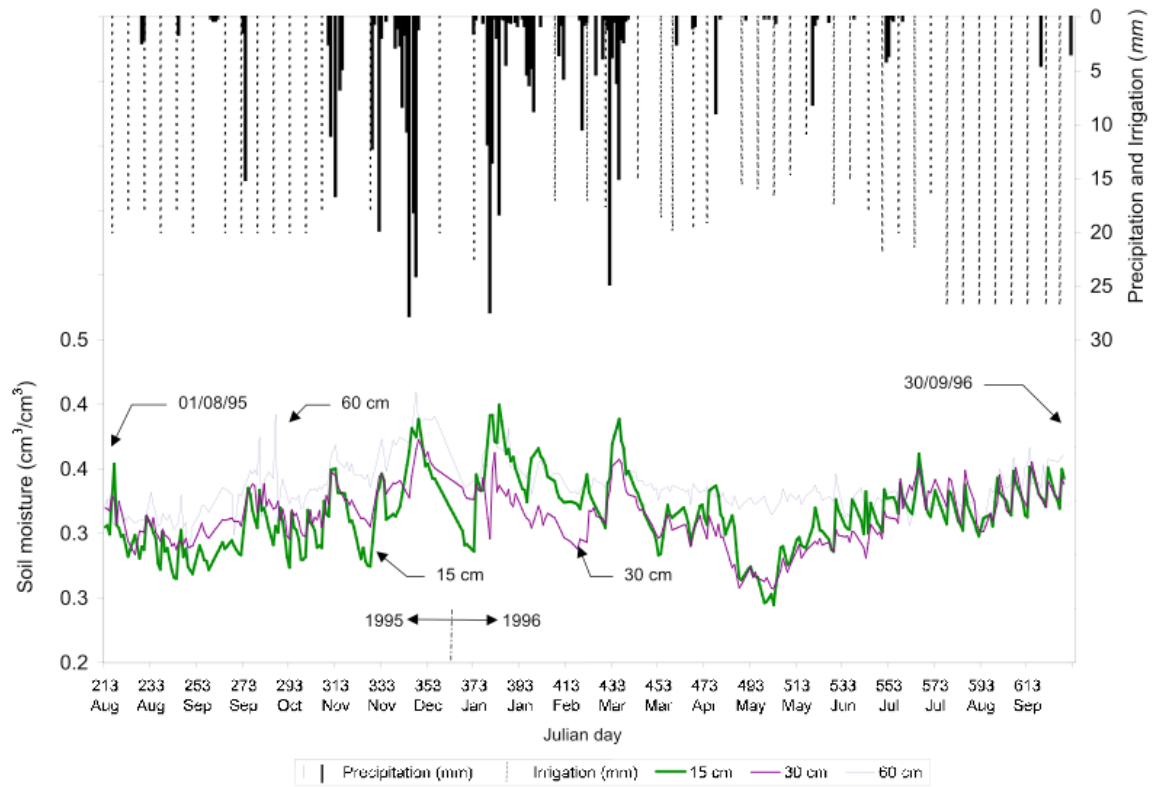


Figure 6. Soil moisture variation at the experimental plot.

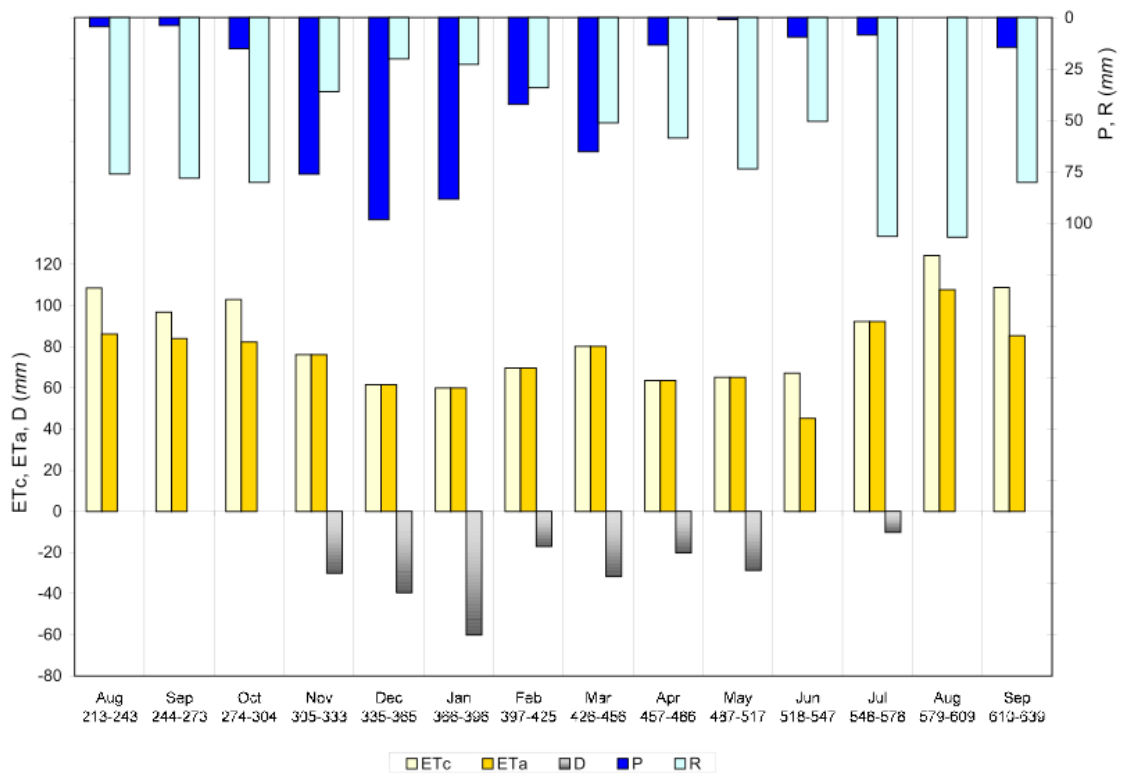


Figure 7. Water balance at the experimental plot.

Figure 8 shows the nitrogen content in the soil solution during the year. The average coefficients of variation of N-NO<sub>3</sub> among sampling stations for each soil depth were 37.6, 34.2 and 25.0% for 15, 30 and 60 cm, respectively. Likewise 49.9, 41.2 and 47.2% are the average coefficients of variation of N-NH<sub>4</sub> at those depths. While fertilization increases nitrogen in the whole profile, there is a marked reduction in the surficial horizon (15 cm) due mostly to plant extraction (roots found at 1-40 cm depth) and to leaching downwards.

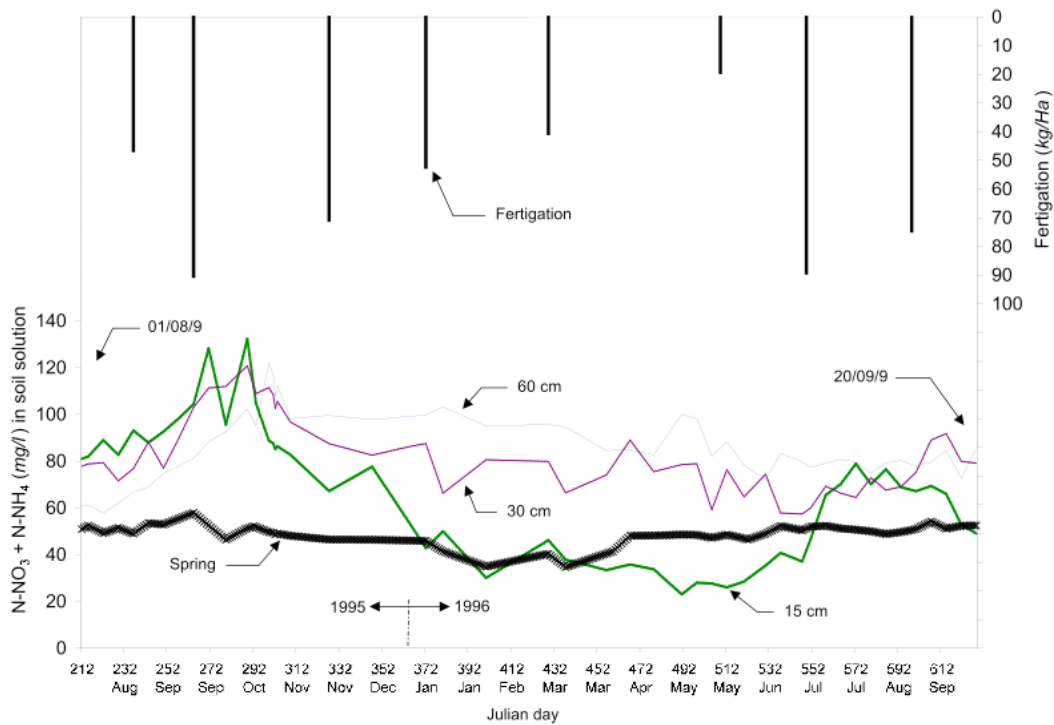


Figure 8. Nitrogen content variation measured at the experimental plot and in the spring water samples.

Table 6 presents annual nitrogen content and fresh and dry matter distribution among the different parts of the banana plant at the end of the year based on Table 3 and a yield 46.7 Tm/ha per year. Figure 9 presents the net nitrogen extraction curve by the crop, i.e. discounting the fraction which returns into the soil by mineralization of the crop residues left on the plot. In January and August maximal extraction is observed, while in May and November the nitrogen uptake is the smallest.

Table 6. Fresh and dry matter and N-uptake of the crop for the experimental period studied (46.7 Tm/ha yield)

Part of banana plant	Fresh matter (kg/ha)	Dry matter (kg/ha)	N (kg/ha)
Bunch <sup>1</sup>	46679.38	8495.65	73.91
Whole plant <sup>2</sup>	159176.47	17827.76	188.97
Shoot <sup>3</sup>	14676.49	1130.09	18.19
Whole plant + Shoot	173852.96	18949.97	199.14

<sup>1</sup> Includes: petiole, rib and limb. <sup>2</sup> Includes: bunch, pseudostem and stalk. <sup>3</sup> Includes: whole leaves, pseudostem, immature leaf and stalk.

Figure 10 summarizes the monthly nitrogen balance for the period. Nitrogen losses by leaching reach 202 kg/ha per year, which represents 48% of total nitrogen applied as fertilizer. Comparison of Figures 7 and 10 shows that these losses are caused by excessive fertigation at times when leaching was produced by rainy periods or intensive irrigation. In October 1995, August and September 1996, there is no drainage so that the nitrogen excess stays immobilized in the soil profile. There are two possible explanations to the origin of the excessive N-applied. One explanation could lay on poor knowledge (or unrealistic expectations) of the N requirement by the crop, so that excess N is being applied even when no extra yield will be obtained. Alternatively, it could be the case where increased nitrogen levels do produce higher yields and so a reduction for environmental reasons would have economic implications. Although experience shows that in general unrealistic yield expectations (limited by micro-meteorological conditions, plant material and cultural practices) might be the key to the problem, further agronomic studies beyond the scope of this work (i.e. plant responses to different N-fertilization levels, timing and application technique), might be needed to establish the probable cause.

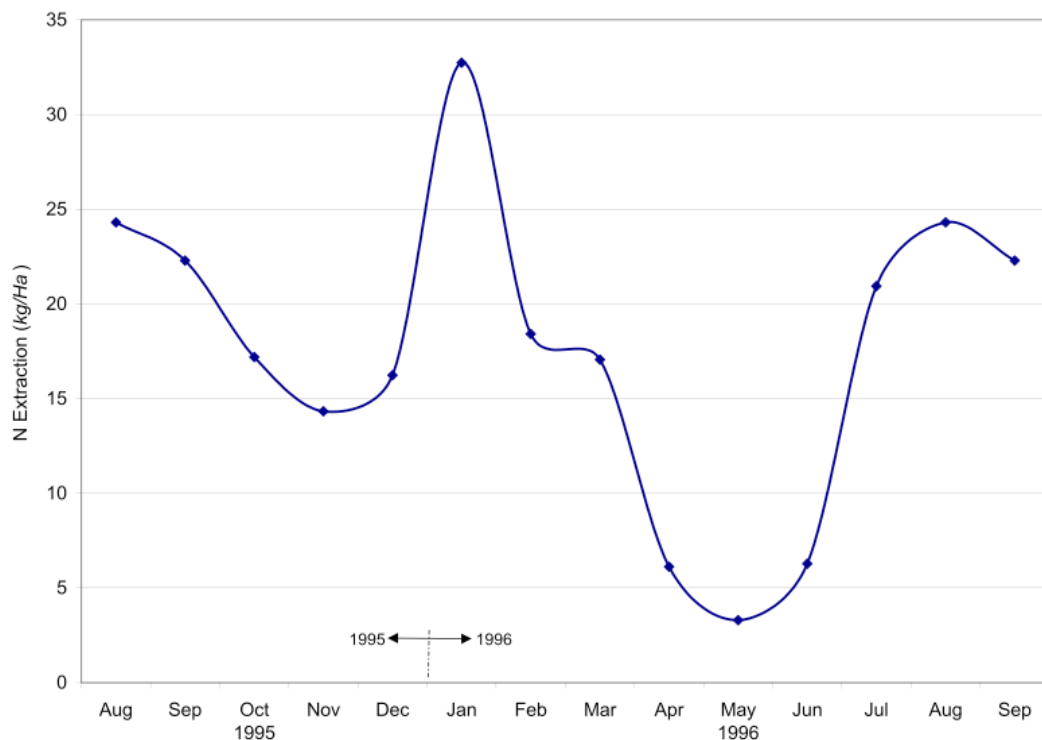


Figure 9. Nitrogen extraction from the soil by the crop.

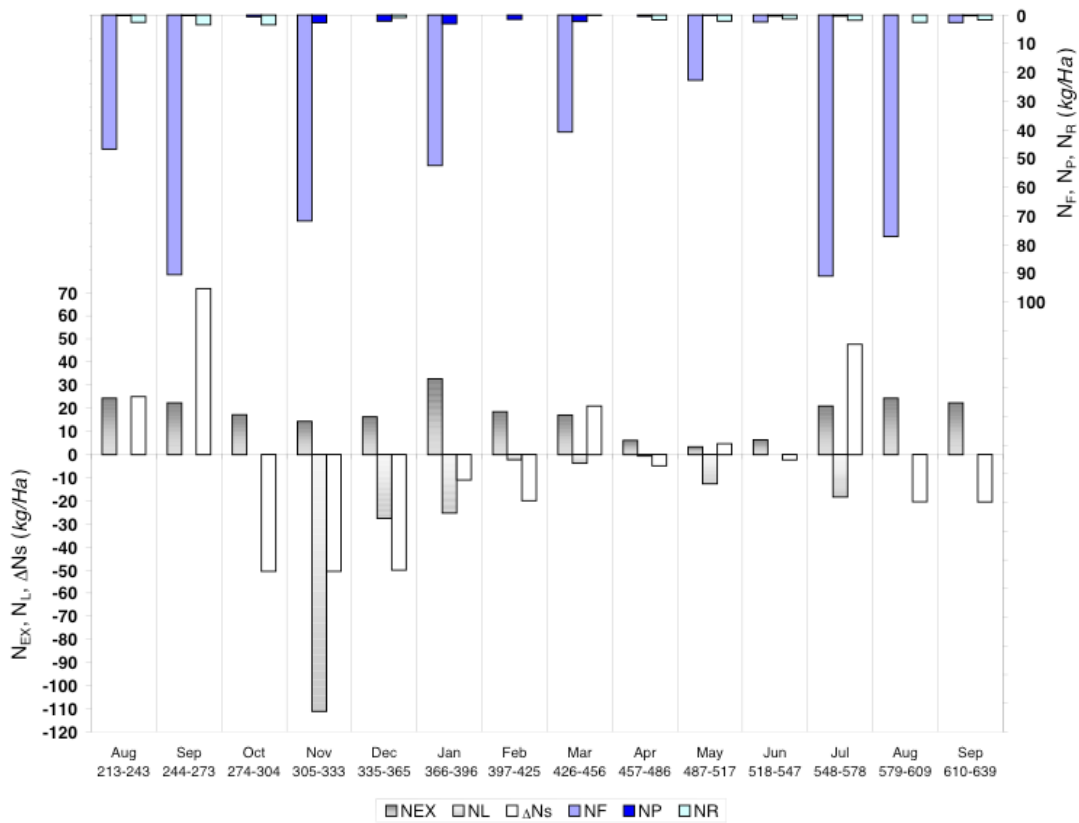


Figure 10. Nitrogen balance in the soil.

An alternative to reduce nitrogen leaching could be to decrease soil drainage. There are practical limitations to this option based on salt leaching requirements. Leaching requirements (LR) are expressed as the additional percentage of water to irrigate, above that needed to satisfy crop water needs, in order to maintain salinity in the root environment at acceptable levels. For a sprinkler irrigation system LR can be calculated following Ayers and Westcot (1976) as  $LR = EC_w / (5 \cdot EC_e - EC_w)$ , where  $EC_w$  is the electrical conductivity of the irrigation water used and  $EC_e$  is the maximum soil extract electrical conductivity for different potential crop yields (Y). Based on weekly analyses, irrigation water used in the plot during the experimental period had an  $EC_w$  range of 0.7-1.4 dS/m with an average of 0.93 dS/m. Following work by Israeli et al (1986) with bananas of the same variety,  $EC_e$  values for Y=100% and 90% are 1.8 and 2.5 dS/m, respectively. This translates in average leaching requirements in excess of 12% for maximum potential yield and of 8% at 90% potential yield. Results from our water balance show the actual annual LR=18%. The effect of this LR on salinity levels at the plot is shown in Figure 11. Weekly values for  $EC_e$  were calculated from soil solution (suction cups) electrical conductivity values ( $EC_{sw}$ ) using the relationship proposed by Ayers and Westcot (1976) where  $EC_e = 0.5 EC_{sw}$ . The Figure shows that EC

values in the root zone (15 and 30 cm) are always maintained below those for maximum potential yield and are only over that in a few instances for the deeper soil layer (but always below the 90% yield level). Since actual EC values at the root zone will depend on irrigation (and rainfall) applied, crop water requirements and drainage, it is always advisable to leave a margin so that salinity levels do not become a limiting factor at any given point in the crop cycle. Ayers and Wescot (1976) suggest LR values in the range 15-20%. This suggests that to avoid salinity problems, reduction in nitrate leaching should be achieved through improved fertilization practices.

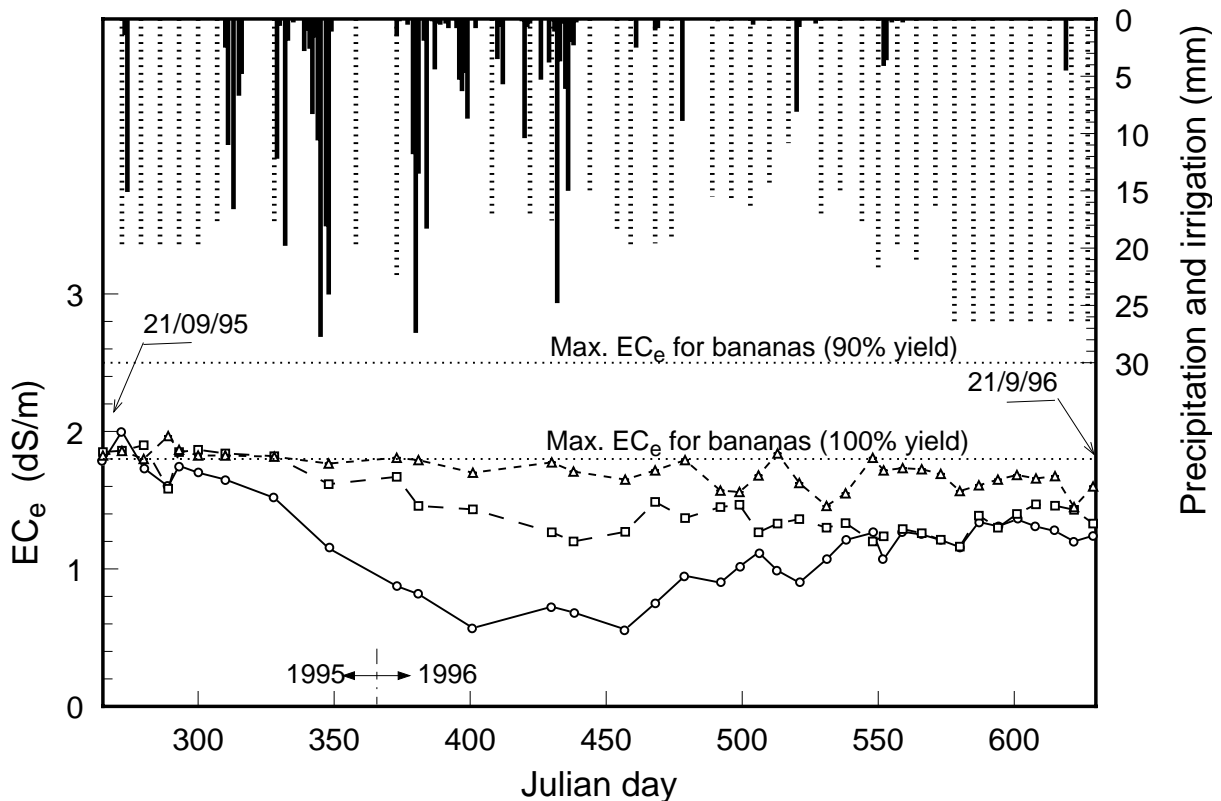


Figure 11. Salinity (soil extract  $EC_e$ , dS/m) variation in the soil profile for the experimental period.

As a comparison, nitrogen losses were also calculated combining drainage volumes with nitrogen soil concentration at 60 cm (Eq. (5)). Both methods yielded similar annual results. The amount determined by the drainage method results in 218 kg/ha per year, which is 16 kg/ha per year higher than the amount calculated with the balance method. However, monthly values estimated by the two methods are different (Figure 12). This discrepancy has been reported by other authors (Djurhuus and Jacobsen, 1995; Parker and van Genuchten, 1984), in terms of the dependency of soil water quantity sampled by each method. The soil balance method deals with the resident or volume -averaged concentration, whereas the

drainage method considers the flux concentration, i.e. mass of solute passing through a given cross section at an elementary time interval. Parker and van Genuchten (1984) showed that the concentrations obtained by each method are different, and thus the nitrate leaching estimates.

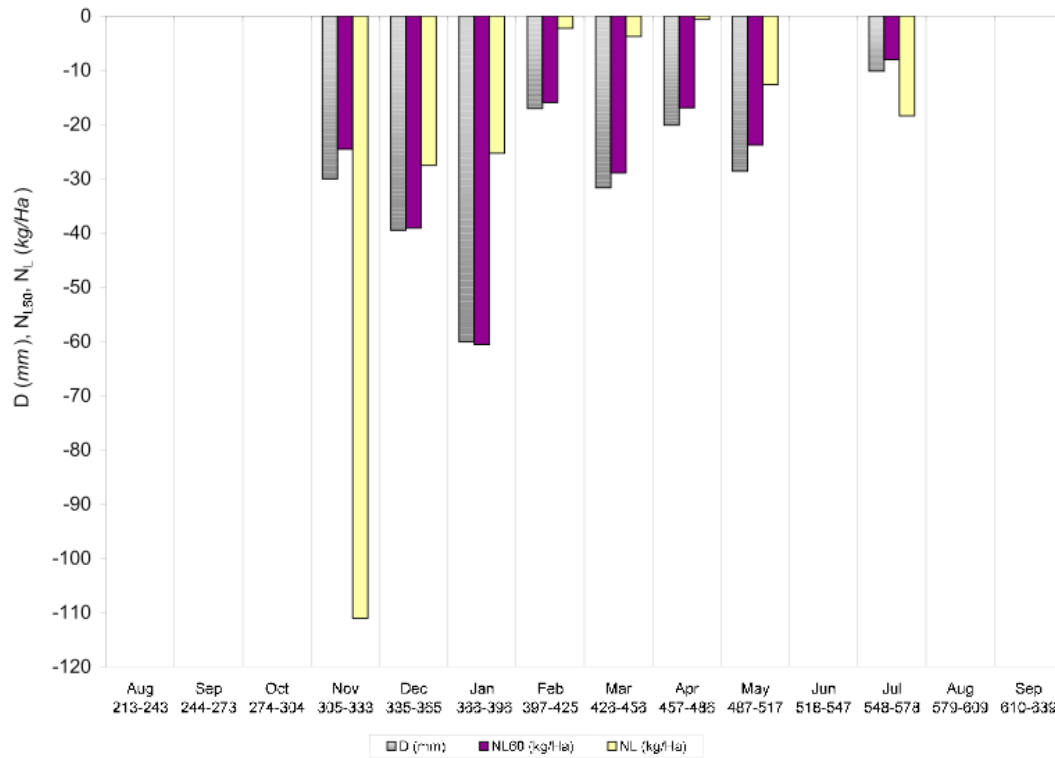


Figure 12. Nitrogen losses according to two methods: monthly balance and soil drainage at 60 cm.

The hydrogeological study (section 2.2) helps to understand N-NO<sub>3</sub> concentration data collected at the springs (Figure 13) and how the aquifer might be actually receiving the pollutants from the agricultural soil. Comparison of the nitrate concentrations found at the bottom of the soil profile (60 cm) with those found in the spring shows a dilution effect (from yearly mean concentration of 85 mg/l N-NO<sub>3</sub> to 49 mg/l) as the water moves through rock fractures in the non-soil section of the unsaturated zone. A nitrate dilution ratio of 0.60 can be calculated as concentration of the spring water samples over the concentration of the soil drainage (taken as the soil water concentration at the lower soil interface, i.e. 60 cm) (Figure 13). This is not in agreement with the 0.25 ratio established in the isotopic study using water samples (irrigation, spring and well water) from one sampling date. This partial isotopic result, though interesting, does not take into account: i) temporal variability; ii) the regional scale effect implicit in the spring water sample collected, iii) and the time of travel from the bottom of the soil profile down to the spring through the unsaturated fractured volcanic

material. There is no immediate extrapolation of this result to the simple nitrate dilution ratio calculated above. The concentration at the spring is an aggregation of the leaching contributions from the different farms and crops in the surrounding area, affected by the delay caused by the travel time of the contaminant in its way to the outlet, and partial mixing with groundwater interflow. To illustrate this point a screening for agrochemicals was performed on the spring water samples collected (Muñoz-Carpena et al., 1996a). The study revealed a herbicide used in other horticultural crops in the area (metribuzine) which had never been applied in the 42 ha banana plantation.

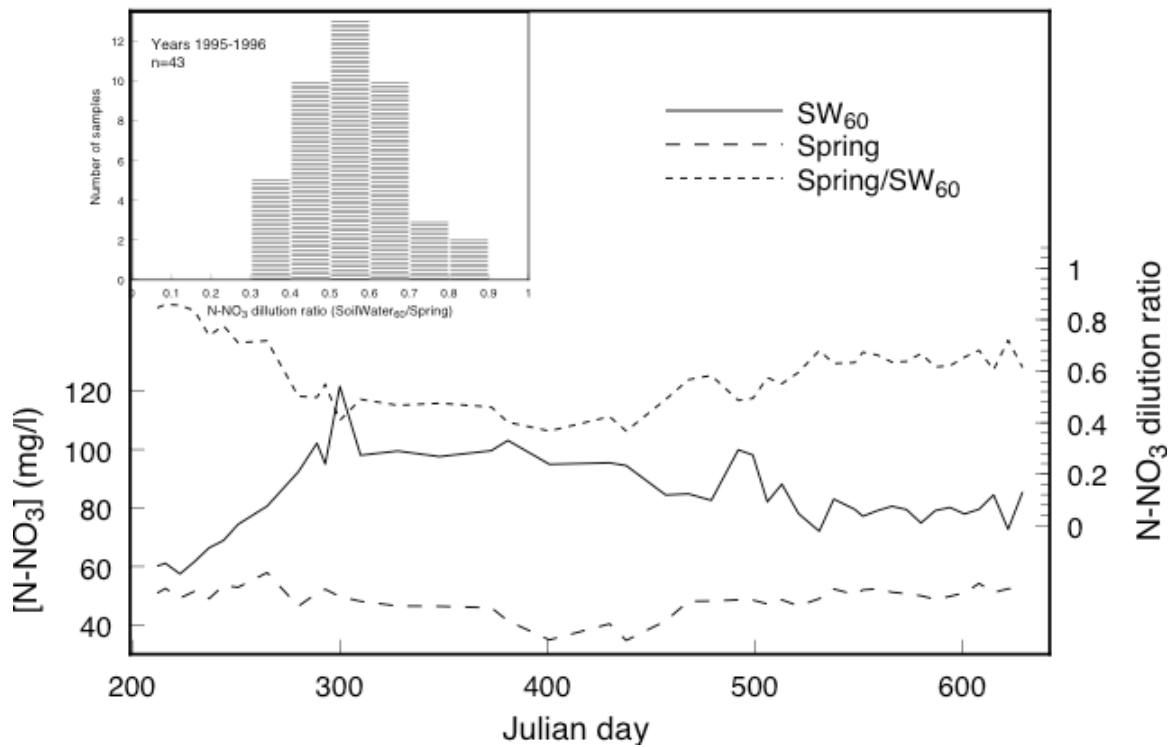


Figure 13. Dilution effect after leaching from the soil down to the lower springs in the sea side cliff.

#### 4. Conclusions

Bananas in the Canary Islands must be grown with the aid of irrigation to cover monthly water deficits in excess of 130 mm. Among the diverse crops produced in the Islands, banana is the major consumer of water. Since water is a very scarce resource, not only in terms of quantity but also in quality, pollution from agricultural lands threatens the sustainability not only of that crop, but of others in the Islands.

The study conducted herein shows that over 48-52% of the total nitrogen applied (202-218 kg/ha N) is not used by the plant but rather lost into the aquifer from a banana crop with

sprinkler fertigation system. Such losses are concentrated in periods when fertigation or rainfall is intensive. Since due to salt-leaching requirements total water drainage should not be significantly reduced, fertilizer practices (amount, timing and application technique) must be revised in order to control aquifer pollution.

#### *Acknowledgments*

The authors wish to thank the staff from the following institutions: *Dirección General de Aguas* (Water Commission) and *Servicio de Protección de los Vegetales* (Crop Protection Service) of the Government of the Canary Islands; *Servicio de Extensión Agraria - Cabildo de Tenerife* (Agricultural Extension Service); and CATESA. The work has been funded with grants from the European Union (Project EV5V-CT-93-0322) and National R&D Plan of Spain - INIA (Project SC95-059).

#### **5. References**

- AGRIMAC S.L.1995. Caracterización de los regadíos de la Isla Baja. Internal Report (unpublished).
- Alberts, E.E., R.E. Burwell and G.E. Schumann. 1977. Soil nitrate-nitrogen determined by coring and solution extraction techniques. *Soil Sci. Soc. of Am. Proc.*, 41:90-92.
- Ayers, R.S. and D.W. Westcot. 1976. *Agricultural Water Quality. Irrigation and Drainage no. 26.* FAO:Rome.
- Barbee, G.C. and K.W. Brown. 1986. Comparison between suction and free-drainage soil solution samplers. *Soil Science*, 141:149-154.
- Bernhard C., y C.Schenck. 1986. Utilisation de Bougies Poreuses pour Extraire la Solution du Sol dans Le Ried Central de L'ill en Alsace. *Bulletin du Groupe Francais de Humidite Neutronique*, 20:73-85.
- Briggs, L.J. and A.G. McCall. 1904. An artificial root for inducing capillary movement of soil moisture. *Science*, 20:566-569.
- [CIAGC] Consejo Insular de Aguas. 1995. *Las Aguas del 2000- Plan Hidrológico Insular de Gran Canaria.* Cabildo Insular de Gran Canaria: Las Palmas.
- [COAP] Consejería de Agricultura y Pesca. 1995. *Resumen de datos estadísticos agrícolas y ganaderos.* Gobierno de Canarias: Santa Cruz.

- [DGA-SPH] Dirección General de Aguas y Servicio de Planificación Hidráulica. 1993. PHI-Plan Hidrológico Insular de Tenerife. Cabildo de Tenerife: Santa Cruz.
- Djurhuus, J. and O.H. Jacobsen. 1995. Comparison of ceramic suction cups and KCl extraction for the determination of nitrate in soil. *European J. of Soil Sci.*, 46(3):387-395.
- Gros, A. 1976. *Abonos. Guía práctica de la fertilización*. Madrid: Ediciones Mundi-Prensa.
- Hansen E.A. and A.R. Harris .1975. Validity of soil-water samples collected with porous ceramic cups. *Soil Sci. Soc. Proc.* 39:528-536.
- Ingenieros Asociados de Tenerife, S.L. 1983. Evaluación de sistemas de riego en la isla de Tenerife. Internal Report (unpublished).
- Israeli, Y., E. Lahav and N. Nameri. 1986. The effect of salinity and sodium adsorption ratio in the irrigation water, on growth and productivity of bananas under drip irrigation conditions. *Fruits*, 41(5):297-302.
- Klute, A. (ed). 1986. *Methods of Soil Analysis. Part 1. Physical and Mineralogical Methods*. 2nd. Ed. Agronomy monograph no.9. Madison:ASA-SSSA.
- McCuen, R. H., W. J. Rawls and D. L. Brakensiek. 1981. Statistical Analysis of the Brooks and Corey and the Green-Ampt parameters across soil textures. *Water Resour. Res.* 17(4):1005-1013.
- Muñoz-Carpena, R., A.R. Socorro, J. Beltrán, G. Gonzalez, N. Pérez. 1995. Evaluación de métodos de muestreo de la zona no saturada para algunos contaminantes agrícolas. In: *Avances en la Investigación de la Zona No Saturada*. p. 49-61. Scio. Pub. Gobierno Vasco: Vitoria.
- Muñoz-Carpena, R., M.C. Cabrera, F. Hernández, A.R. Socorro. 1996a. Development of Analytical and Sampling Methods for Priority Pesticides and Relevant Transformation Products in Aquifers. Final EU Project Report EV5V-CT93-0322. ICIA: (unpublished).
- Muñoz-Carpena, R., D. Fernández, G. González y P. Harris. 1996b. Diseño y evaluación de una estación micrometeorológica de bajo coste para el cálculo de la evapotranspiración de referencia. *Riegos y Drenajes XXI*, 88:17-25.
- Nagpal, N.K. 1982. Comparison among, and evaluation of, ceramic porous cup soil water samplers for nutrient transport studies. *Canadian J. of Soil Sci.*, 62:685-694.
- Parker, J.C. and M.Th. van Genuchten. 1984. Flux-averaged and volume averaged concentrations in continuum approaches to solute transport. *Water Resour. Res.*, 20:866-872.

- Penman, H.L. 1950a. Evaporation over the British Isles. Quarterly Journal of the Royal Meteorological Society, 96: 372-383. In: Brassington, R. 1998. Field Hydrogeology. Chichester: Wiley.
- Penman, H.L. 1950b. The water balance of the Stour catchment area. Journal of the Institution of Water Engineers, 4: 457-469. In: Brassington, R. 1998. Field Hydrogeology. Chichester: Wiley.
- Poncela, R. 1994. Estudio Hidrogeológico de la zona de Valle de Guerra (Tenerife, España) con énfasis en la Hidrogeología e hidrogeoquímica en el entorno de la Finca "Catesa-Las Cuevas" y zonas adyacentes (internal report). Dirección General de Agua: Las Palmas de Gran Canaria
- Rawls, W.J. and D.L. Brakensiek. 1983. A procedure to predict Green-Ampt infiltration parameters. Adv. in Infiltration, pp. 102-112. ASAE Pub. no. 11-83.
- Regalado C.M., R. Muñoz-Carpena, J. Alvarez-Benedí, A.R. Socorro and J.M. Hernández-Moreno. 2001. Field and laboratory setup to determine preferential flow in volcanic soils. In: Proc. 2nd Intl. Symposium on Preferential Flow. Hawaii, January 3-5, 2001. ASAE:St. Joseph.
- SYSCONSULT-AICASA. 1987. Estudio de los Consumos y Necesidades Hídricas Agrarias en las Islas Canarias. Plan Hidrológico del archipiélago Canario. 3 tomos (unpublished).
- Sánchez Padrón, M. 1985. Tecnología y desarrollo. El estudio de un caso: El riego por goteo en el cultivo de la platanera en Canarias. Tesis Doctoral. Universidad de La Laguna, Facultad de Ciencias Economicas.
- Shaffer, K.A., D.D. Fritton and D.E. Baker. 1979. Drainage water sampling in a wet, dual pore soil system. Journal of Env. Quality, 8:241-246.
- Smith, M. C. and D.L Thomas. 1990. Measurement of pesticide transport to shallow ground water. Transactions of the ASAE,33(5):1573-1582.
- Soil Survey Staff. 1978. Keys to Soil Taxonomy. US Dept. of Agr:Washington.
- Soto Ballesteros, M. 1990. Bananos, Cultivo y Comercialización. Costa Rica: Asociación Bananera Nacional.
- van Genuchten, M.Th. 1980. A closed form equation for predicting the hydraulic conductivity of unsaturated soils. Soil Sci. Soc. of Am. Jour., 44: 892-898.
- Wagner, G.H. 1962. Use of porous ceramic cups to sample soil water within the profile. Soil Science, 94:379- 386.

## **Capítulo 2**

### **Using inverse methods for estimating soil hydraulic properties from field data as an alternative to direct methods**

*Agricultural Water Management*, , (aceptado octubre, 2002)

## **Abstract**

Water and solute transport in the vadose zone greatly depends on the soil physical and chemical properties, which generally exhibit high variability. Additionally, the experimental determination of those properties in the field or laboratory is tedious, time consuming and involves considerable uncertainty for most practical applications. Recently, inverse modeling has been introduced to estimate effective properties in-situ by deducing them from e.g. a measured time series of soil water content. Inverse methods combine forward soil water flow models with appropriate optimization algorithms to find the best parameter set that minimizes an objective function. Global optimization methods are suitable for locating a global optimum for a given set of conditions (number of parameters, boundary conditions, etc.). In this paper we estimate the soil hydraulic properties of a sprinkler fertigated banana plot in the North of Tenerife (Canary Islands) in a direct and inverse way. For the inverse method, use was made of the measured time series of soil water content at three different depths. The forward model is the numerical solution of the Richards equation as implemented in the agro-environmental model WAVE. Two inverse methods are compared: the traditional “trial and error” method and an inverse method using a global search algorithm referred to as the Global Multilevel Coordinate Search combined sequentially with Nelder-Mead Simplex algorithm (GMCS-NMS). The global search is shown to be a relatively efficient procedure for estimating the soil hydraulic properties from measured soil water contents in the banana plantation. However, some ill-posedness problems are identified which should be solved by upgrading the quality of the experimental programs in irrigated banana plantations.

*Keywords:* Inverse modeling; Multilevel coordinate search; Bananas; Water flow; WAVE model; Canary Islands.

## 1. Introduction

The degradation of groundwater resources in the Canary Islands as a result of agricultural activities suggests the need to design strategies to reduce and control the environmental impact of agriculture. Bananas are the most important crop cultivated in the Archipelago and represent an extreme situation of intensive agriculture. Mean nitrate concentration values of groundwater found in the main agricultural valleys range within 9-11 mg/l N-NO<sub>3</sub> (40-50 mg/l NO<sub>3</sub>), in some areas exceeding 25 mg/l (110 mg/l NO<sub>3</sub>) (DGA-SPH, 1993).

In this context, numerical, physically based models for water and solute transport are useful tools for analyzing nitrogen leaching as a consequence of fertilizer practices. However, the use of such models is not an easy task, since they contain a large number of parameters that must be identified before the model can be applied to the considered specific situation. The success of predictions and associated uncertainties strongly depends on the identification of the parameters, which is clearly the most critical step in the modeling process.

Some of these parameters can be measured directly in the laboratory or in-situ. However, parameters determined from laboratory experiments might not be representative of field conditions. Furthermore, direct methods for the determination of soil hydraulic parameters require the experiments to reach several stages of steady-state conditions and restrictive initial and boundary conditions as well (van Dam et al., 1990). To overcome these problems indirect methods such as inverse modeling can be used to identify the basic flow and transport parameters. This procedure has the advantage that the results are based on a variable, which is observed at a larger time scale and under natural boundary conditions.

A popular inverse method is the manual calibration by a “trial and error” procedure of a soil water and flow model by comparing simulated values of a state variable (e.g. soil water content) with those experimentally measured. From a scientific point of view, the latter is a tricky method that should not be applied by model user. The main drawbacks of this method are that it is time consuming; and when several parameters are involved, it is difficult to judge in which direction these should be modified. It is also quite subjective, as the modeler does not know when to stop the calibration process. Finally, the uncertainty on the obtained parameters cannot be quantified in a rigorous way. Consequently, the “trial and error” calibration method cannot ensure that the best parameter set is found.

A more elaborated inverse method combines the numerical model with an algorithm for parameter estimation (e.g. Simunek et al., 1999). Basically the process searches for the best set of parameters in an iterative way, by varying the parameters and comparing the real response of the system measured during an experiment with the numerical solution given by the model. Indeed, the search should consist of finding the global minimum of an objective function defined by the error between measured and simulated values. The algorithm minimizes the objective function following its own particular strategy, e.g. by gradient based search. Within this framework, many different optimization algorithms have been developed to numerically solve inverse problems. Among others, we may consider Steepest Descendent Method, Newton's Method, Gauss Method, Levenberg-Marquardt Method, Simplex Method, Global Optimization Techniques, etc. (Hopmans and Simunek, 1999). Each of these methods has its own advantages and drawbacks, and the success of finding the global minimum depends generally on the presence of multiple local minima in the objective function. Recently Huyer and Neumaier (1999) have developed a global optimization algorithm (*Multilevel Coordinate Search*) that combines global search and local search capabilities with a multilevel approach that enhances the convergence to the smallest objective function value. In a soil physics context, Lambot et al., (2002) used the Global Multilevel Coordinate Search (GMCS) algorithm combined sequentially with the classical Nelder-Mead Simplex algorithm (Nelder and Mead, 1965) to determine subsurface hydraulic properties from a continuously observed soil water content time series obtained from a numerical one-dimensional infiltration-redistribution experiment. The efficiency of the algorithm in finding the global minimum of the objective function depends on the number of parameters to be optimized, the objective function topology, the parameterization of the algorithm, etc.

The success of an inverse parameter determination depends on how well the problem can be posed. Three aspects generally characterize the posedness: identifiability, stability and uniqueness. If more than one parameter set leads to the same model response, the parameters are unidentifiable. Instability means that small errors in the measured variable or in some fixed parameters may result in large changes of the optimized estimated parameters. In contrast to identifiability, uniqueness refers to the inverse relationship; if a given response leads to more than one set of parameters, the inverse solution is non-unique (Russo et al., 1991; Hopmans and Simunek, 1999). The posedness of an inverse method depends on the soil under investigation, the type and range of boundary conditions used, the model structure,

and the magnitude of the measurement errors of the input data (Russo et al., 1991; Durner et al., 1999).

The optimization techniques mentioned above are widely used in the context of fundamental soil physics research mostly limited to the estimation of soil hydraulic parameters for uniform soils on small, undisturbed soil columns (see e.g. Hopmans and Simunek, 1999; Zou et al., 2001). However, they may be considered as powerful engineering tools as they can be applied on field experimental data sets to derive parameters of the system under consideration. The first application of inverse modeling to field data was reported by Dane and Hruska (1983), who optimized van Genuchten's function parameters from drainage data.

In this framework, our study presents a comparison of the performance of two indirect methods for identifying the hydraulic parameters of a stratified soil profile of a banana plot: the traditional "trial and error" method and the inverse modeling method by using the multilevel coordinate search global optimization method. For this purpose the numerical model WAVE (Vanclooster et al., 1996) was used to simulate water fluxes in the stratified soil profile in a sprinkler fertigated banana plantation.

The main objectives of the study can be defined as follows:

- 1) To perform a thorough sensitivity analysis to identify the most sensible parameters on which the optimization will be focused. Indeed, it is well known that the efficiency of parameter calibration can clearly be enhanced if the efforts are concentrated on those parameters to which the model simulation results are most sensitive (Beven, 2001);
- 2) To compare the optimized parameter sets of the two above-discussed indirect methodologies and compare them with directly obtained parameter values;
- 3) To investigate the impact of the calibration methodology on the simulated water fluxes that leave the soil profile.

## 2. Materials and methods

### 2.1. Field experimental setup

The experiment was conducted in a 4800 m<sup>2</sup> banana field plot selected within an intensive agricultural area, the valley of Valle de Guerra, in the north of Tenerife (Canary Islands). The valley is enclosed by the Anaga Mountain on its NE side and is open to the Atlantic Ocean on its NW exposure, ending in a cliff 70 m high. Mean annual temperature in this area is 20 °C (minimum of 15 °C in winter), and annual precipitation and crop potential evapotranspiration are around 380 mm and 1000 mm, respectively. The experimental plot was chosen inside a 42 ha banana plantation (Las Cuevas) owned and operated by a private company. It was selected to represent the average conditions of the area (fertilization and cultural practices) at the time. The plantation, located on a fairly steep ground in the lower part of the valley, is terraced all the way down to the edge of the cliff 70 meters above sea level.

The bananas (*Musa acuminata*, cv “Dwarf Cavendish”) were grown in the open air and at a plant density of about 1800 plants/ha. The field was irrigated weekly with a sprinkler fertigation system.

As common practice in the Canary Islands, due to the steep slopes of the landscape, crops grow on “sorribas”, i.e. terraces built across the steep slopes with rock retaining walls, filled with soils imported from the high mountain areas where changes in humidity and temperature have allowed weathering of the volcanic material producing well developed soil. The experimental plot, on a “sorriba” built over 50 years ago, showed an averaged soil depth of 60 cm, with a range of 50 – 70 cm, below which a net contact with the fractured basaltic rock was found. The soil profile exhibits three different soil horizons (0 – 20; 20 – 50; 50 – 70 cm). Further details are described elsewhere (Muñoz-Carpena et al., 2002).

Soil water content was measured at 6 locations uniformly distributed within the field with covered double waveguides TDR probes. At each location, TDR probes were installed at three different depths, 15, 30 and 60 cm, each corresponding to approximately the middle of the three above-mentioned horizons. Between the 26<sup>th</sup> of July 1995 and the 30<sup>th</sup> of September of 1996, soil water content readings were taken on 286 dates resulting in a data set of more than 5000 measurements. A TDR calibration was performed using a packed soil column

(Ø16 x 20 cm), that was stepwise dried after saturation. During each step, weight and TDR measurements were taken. The relation between the dielectric constant and the soil water content (Figure 1) followed the commonly used Topp's Equation (Topp et al., 1980). Irrigation amounts were measured at the 6 locations with ground level raingauges. 6 different locations were chosen to account for spatial variability of both soil water content and irrigation, but in the following analyses, we only use the average values for the 6 locations, considered as representative for the whole experimental field. An automatic weather station was installed on-site (Muñoz-Carpena et al., 1996) to estimate reference evapotranspiration for the crop at intervals of 15 min (1 min data average).

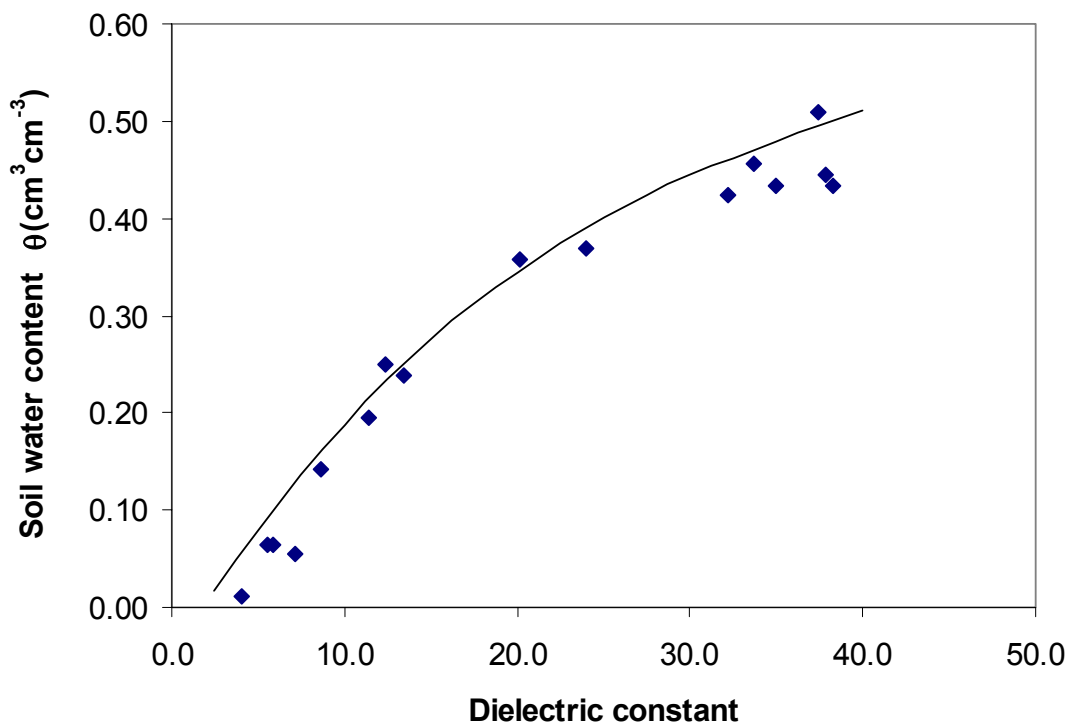


Figure 1. TDR calibration curve for the considered volcanic soil. Measured data (symbols) and Topp's Equation (line).

## 2.2. Model description

Developed at the Institute for Land and Water Management of the K.U. Leuven (Belgium), the WAVE model (Water and Agrochemicals in soil, crop and Vadose Environment) is a numerical, deterministic model for simulation of the vertical transport of energy (heat) and mass (water, non-reactive solutes, nitrogen species and pesticides) in the soil-plant-atmosphere-continuum. It can be applied to soil laboratory columns, field

lysimeters and to the field scale if transport is mainly vertical and if effective (1-D) parameters are used.

The WAVE model (Vancllooster et al., 1996) integrates several models developed earlier: SWATRE (Belmans et al., 1983), SWATNIT (Vereecken et al., 1990; 1991), the universal crop growth model SUCROS (van Keulen et al., 1982; Spitters et al., 1988) and subroutines for heat and nitrogen transport based on the LEACHN model (Wagenet and Hutson, 1989). The WAVE model is structured in five modules for determining respectively water transport, solute transport, heat balance, nitrogen transformations and crop growth. In this study, only the water transport module was used.

Water transport is modeled by solving a one-dimensional, isothermal Darcian flow equation in a variably, saturated, rigid porous medium, expressed by the following form of Richards equation:

$$C(h) \frac{\partial h}{\partial t} = \frac{\partial}{\partial z} \left[ K(h) \left[ \frac{\partial h}{\partial z} + 1 \right] \right] - \Gamma(z, h) \quad (1)$$

where  $C(h)$  is the soil water content capacity [ $L^{-1}$ ] equal to the slope of the soil moisture retention curve;  $z$  is the vertical distance from the soil surface [ $L$ ];  $t$  is the time [ $T$ ];  $K(h)$  is the soil hydraulic conductivity function [ $LT^{-1}$ ],  $h$  is the matric pressure head [ $L$ ] and  $\Gamma(z, h)$  is the sink term describing water uptake by plant roots. The latter accounts for root water uptake reduction due to water stress and is based on a factor, which reduces linearly the maximal root water uptake ( $S_{max}$  [ $L^3L^{-3}T^{-1}$ ]) according to four critical matric pressure head:  $h_0$ ,  $h_1$ ,  $h_2$ , and  $h_3$  [ $L$ ]. Under conditions wetter than  $h_0$ , water uptake ceases due to lack of oxygen in the root zone; below  $h_3$ , it stops due to drought stress, while between  $h_1$  and  $h_2$  water uptake is optimal and  $S_{max}$  is not reduced. Furthermore, the threshold matric pressure head below which water uptake decreases, depends on whether the atmospheric demand is low or high ( $h_{2l}$  and  $h_{2h}$ , respectively). On the other hand, the atmospheric demand is estimated by splitting the potential crop evapotranspiration into potential transpiration and evaporation using the Leaf Area Index ( $LAI$  [-]) as division parameter (Vancllooster et al., 1996).

The soil water retention function is given by (van Genuchten, 1980):

$$Se(h) = \frac{\theta(h) - \theta_r}{\theta_s - \theta_r} = \left[1 + \alpha|h|^n\right]^m \quad (2)$$

where  $Se$  is the effective saturation [-];  $\theta(h)$  is the soil water content [ $L^3L^{-3}$ ] at matric pressure head  $h$ ;  $\theta_s$  and  $\theta_r$  are the saturated and residual soil water content [ $L^3L^{-3}$ ], respectively;  $\alpha$  is the inverse of the air entry value of  $h$  [ $L^{-1}$ ];  $m$  and  $n$  are curve shape parameters. The former characterizes the asymmetry and is assumed to be  $m=1-1/n$ , while the latter is related to the slope of the curve (van Genuchten, 1980).

The hydraulic conductivity can be described in WAVE with several model equations. In this study the following expression for the unsaturated hydraulic conductivity function was chosen. It results when combining Eq. (2) with the pore-size distribution model of Mualem (1976).

$$K(Se) = K_s Se^\lambda \left[1 - (1 - Se^{-m})^m\right]^2 \quad (3)$$

where  $K(Se)$  and  $K_s$  are the unsaturated and saturated hydraulic conductivity [ $LT^{-1}$ ], respectively and  $\lambda$  is the pore connectivity parameter [-], which accounts for tortuosity and correlation between pore sizes (Durner et al., 1999).

In the vertical direction, the model considers the existence of heterogeneity in the form of horizons or layers within the soil profile. These layers are subdivided in space intervals called soil compartments. Halfway in each soil compartment, a node is identified for which the state variables are calculated using finite difference techniques, space implicit and time explicit.

To model less dynamic processes (crop growth) a fixed daily time step is used, while for strongly dynamic processes, such as water, solute and heat transport and solute transformations, a smaller variable time step can be chosen to limit mass balance errors induced by solving the flow equation. The model inputs are given on a daily basis and outputs can be obtained at daily intervals or higher (e.g. Muñoz-Carpena et al., 2001).

### 2.3. Direct estimation of model parameters

Concerning the high number of parameters required by the model, although there was the possibility to obtain them from the literature, it was decided to measure as many of them as possible. Thus, the effort spent on parameter determination was hoped to be regained in terms

of minimal calibration work. Model inputs and parameters used in this work and also the methodology applied for their determination is described in Muñoz-Carpena et al. (1999a; 1999b). Hydraulic properties were determined on undisturbed USDA 7,62 cm soil cores using Tempe cells and laboratory constant head permeameters (Klute, 1986). The undisturbed samples were taken at the 6 different locations and the 3 above-mentioned depths. Thus, average values for each depth were used. The soil moisture retention curves were then fitted (Table 1) to van Genuchten's water retention model (van Genuchten, 1980), which is available in WAVE. Table 1 shows also the saturated hydraulic values obtained with the constant head permeameters, and Mualem's pore connectivity parameter ( $\lambda$ ), which can be assumed equal to the most commonly accepted value of 0.5 (Mualem, 1976). The maximum root water uptake rate ( $S_{max}$ ) was considered constant within the root zone and was fixed at  $0.023 \text{ cm}^3 \text{ cm}^{-3} \text{ day}^{-1}$  (Vanclooster et al., 1996). In addition, the matric pressure head values, which characterize the root water uptake for bananas, were obtained from Simunek et al., (1998). The Leaf Area Index ( $LAI$ ) function and the crop coefficients ( $K_c$ ) were taken from (Muñoz-Carpena et al., 1999a; 1999b). The yearly evolution of both parameters,  $K_c$  and  $LAI$  is presented in Figure 2, where linear interpolation between values is considered.

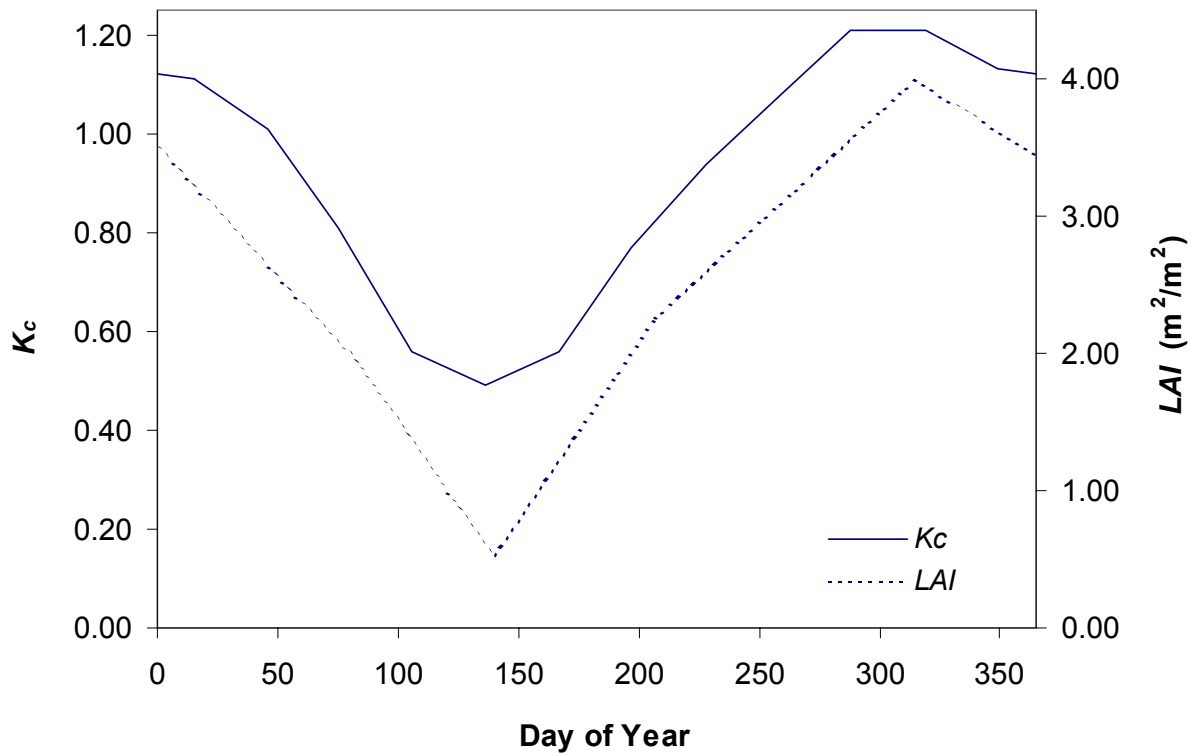


Figure 2.  $K_c$  and  $LAI$  functions used in the simulations.

Table 1  
Hydraulic parameters selected for the sensitivity analysis

Depth (cm)	van Genuchten parameters			$n$	$K_s$ (cm/day)	$\lambda$
	$\theta_s$ (cm <sup>3</sup> /cm <sup>3</sup> )	$\theta_r$ (cm <sup>3</sup> /cm <sup>3</sup> )	$\alpha$ (cm <sup>-1</sup> )			
15	0.549	0.322	0.278	1.377	311	0.5
30	0.520	0.315	0.220	1.406	201	0.5
60	0.495	0.250	0.189	1.292	199	0.5

#### 2.4. Sensitivity analysis

Model parameter estimation is an arduous task, which can be done efficiently if the parameters most influencing the model response are previously identified. For this purpose, a sensitivity analysis provides information about the sensitivity of the model to its parameters, i.e. it indicates those parameters whose variation has large effects on the model outputs. This analysis is usually based on coefficients, which express the proportion of variation ( $\partial q/\partial b_j$ ) in a model output variable ( $q$ ) relative to an infinitesimal change in a particular parameter ( $b_j$ ). According to Yeh (1986), sensitivity coefficients can be calculated with the “influence method” (finite differences). In an attempt to optimize van Genuchten’s hydraulic parameters from actual evapotranspiration and actual transpiration, Jhorar et al. (2002) used the root mean square error between reference and modeled values of cumulative actual transpiration as a sensitivity estimator. Furthermore, they varied the parameters over a particular range. However, as a common practice, the “influence method” is used and only a 1% parameter change is considered (Simunek and van Genuchten, 1996).

The final aim of the modeling analysis is to obtain good predictions of the flux at the bottom of the soil profile as this strongly influences the mass of nitrogen leaving the soil profile. Unfortunately, the flux at the bottom was not measured and time series of soil water content were the only available data for the model calibration. Hence, we performed two different sensitivity analyses. The first was carried out to check the sensitivity of soil water content to change in a range of soil and plant parameters. The selection of the soil and plant parameters was based on previous global sensitivity analysis done with the model (e.g. Diels 1994; Vanclooster et al. 1995). This analysis was done to identify the most sensitive parameters on which the calibration process should be focused. The second one was performed to check the sensitivity of the flux at the bottom of the soil profile, as it is ultimately the predictive variable of interest.

Sensitivity coefficients for soil water content were formulated with the “influence method” following Simunek and van Genuchten (1996). These coefficients were normalized

according to Simunek et al. (1999) to allow for comparison of sensitivities between different parameters, independent of their magnitudes (see Eq. (4)).

$$SC_{\theta}(z, t, b_j) = \Delta b_j \frac{\partial \theta(z, t, b_j)}{\partial b_j} \approx \left| 0.1 b_j \frac{\theta(\mathbf{b} + \Delta \mathbf{b} \cdot \mathbf{e}_j) - \theta(\mathbf{b})}{1.1 b_j - b_j} \right| = \left| \theta(\mathbf{b} + \Delta \mathbf{b} \cdot \mathbf{e}_j) - \theta(\mathbf{b}) \right| \quad (4)$$

where  $SC_{\theta}(z, t, b_j)$  represents the soil water content change at time  $t$  and depth  $z$ , due to a variation of the parameter  $b_j$ . The magnitude of variation was set here to 10% ( $\Delta \mathbf{b} \cdot \mathbf{e}_j = 0.10 b_j$ ) to avoid possible disturbances associated to the numerical solving process used for the simulation. Thereby,  $\mathbf{b}$  is the parameter vector, while  $\mathbf{e}_j$  is the  $j$ -th unit vector.

Table 1 shows the hydraulic parameters selected for the sensitivity analysis, while some of the crop parameters are presented in Figure 2. The hydraulic parameters considered include saturated and residual soil water contents ( $\theta_s$  and  $\theta_r$ ), inverse of the air entry value of the matric pressure head ( $\alpha$ ), van Genuchten's shape parameter  $n$ , Mualem's pore connectivity parameter ( $\lambda$ ) and saturated hydraulic conductivity ( $K_s$ ). As described before, the van Genuchten parameter values were estimated by fitting matric pressure head vs. soil water content data obtained with Tempe cells. The crop parameters chosen were leaf area index ( $LAI$ ), crop coefficient ( $K_c$ ) and maximum root water uptake rate ( $S_{max}$ ).

The sensitivity coefficients of each parameter were calculated for the whole simulation period (432 days) and for the three different depths at which soil water content was measured (15, 30 and 60 cm). Variation of hydraulic parameters was considered independently layer by layer. To compare the sensitivity coefficients among parameters, time-average coefficients were calculated according to the following expression (Inoue et al, 1998):

$$SC_{\theta}(z, b_j) = \frac{1}{t_{end} - t_0} \int_{t_0}^{t_{end}} SC_{\theta}(z, t, b_j) dt \quad \text{with } t_0 > t > t_{end} \quad (5)$$

In a similar way as in Eq. (4), the formulation of the sensitivity coefficients for the cumulative flux at the bottom of the soil profile will lead to:

$$SC_F(b_j) = \left| F(\mathbf{b} + \Delta \mathbf{b} \cdot \mathbf{e}_j) - F(\mathbf{b}) \right| \quad (6)$$

where  $SC_F(b_j)$  is the accumulated bottom flux change corresponding to a variation of the parameter  $b_j$  of the parameter set  $\mathbf{b}$  ( $\Delta \mathbf{b} \cdot \mathbf{e}_j = 0.10 b_j$ ).

## 2.5. Indirect parameter estimation

The calibration process was performed with only one part of the available data set in order to leave the rest for model validation. The period between the 1<sup>st</sup> of October 1995 and 31<sup>st</sup> of March 1996 was selected for the calibration as this period seems to contain useful information and explores a large range of soil water content conditions.

### 2.5.1 The “trial and error” procedure

The strategy used consisted of performing a first simulation run with the parameter sets obtained from direct measurements (Table 1 and Figure 2). The modeled soil water contents were then compared with the measured ones. Then we tuned progressively some parameters selected for calibration according to the sensitivity analysis, until an adequate fit was achieved. The goodness of the fit was based on the calculated root mean square error (RMSE) and the visual inspection of the time series of measured and simulated soil water contents. The simulated flux at the bottom of the profile was also considered.

### 2.5.2 The inverse modeling procedure

This technique consisted of calibrating selected parameters using an iterative process of three basic steps: i) parameter perturbation; ii) forward modeling and iii) objective function evaluations. For the third step the error between the forward simulation results and field measurements is considered as objective function. The optimal parameter set is the one, which produces the minimum objective function. To minimize the objective function, the forward model was combined with a global optimization algorithm. In this study the *Global Multilevel Coordinate Search*, GMCS, algorithm was used. The latter combines a global minimum search and local minima search with a multilevel approach (Huyer and Neumaier, 1999). Basically, using the GMCS, the parameter search space is split into smaller “boxes”. Each box is characterized by its midpoint, whose function value is known. A box can be split into smaller ones. As a rough measure of the numbers of times a box has been split, a level is assigned to each box. The fact that the algorithm starts with the boxes at the lowest levels (i.e. less split) constitutes the global part of the algorithm. The local part of the algorithm is characterized by the fact that at each level the box with the lowest function value is selected. The GMCS is a good alternative to other optimization algorithms: initial values of the parameters to be optimized are not needed and it is very robust, because it can deal with discontinuous nonlinear multimodal objective functions. To enhance the minimization of the

objective function the GMCS is combined sequentially with the Nelder-Mead Simplex algorithm (NMS) (Nelder and Mead, 1965). Indeed, the GMCS algorithm needs only to find an approximate solution, which is supposed to be in the basin of attraction of the global minimum. By using this solution as initial guess for the NMS, fast convergence towards the global minimum is ensured (Lambot et al., 2002).

Since the parameter calibration by inverse modeling can be considered as a nonlinear optimization problem and can be solved as a generalized least squares problem, we defined the objective function by:

$$OF(\mathbf{b}) = W \sum_{i=1}^N [\theta_{mea}(t_i) - \theta_{sim}(t_i, \mathbf{b})]^2 \quad (7)$$

where  $OF(\mathbf{b})$  [-] is the objective function of the parameter vector  $\mathbf{b}$ ;  $\theta_{mea}$  and  $\theta_{sim}$  [ $L^3L^{-3}$ ] are the measured and simulated soil water content, respectively;  $t$  is the time [T] and  $N$  is the number of measurements available. The normalizing coefficient,  $W$  is set equal to  $(Ns^2)^{-1}$ , where  $s$  denotes the standard deviation of the measurement data (Lambot et al., 2002).

Parameter uncertainty was estimated using linear regression analysis. Although restrictive and only approximately valid for nonlinear problems, it allows comparing confidence intervals between parameters (Hopmans and Simunek, 1999). This analysis implies the estimation of the parameter covariance matrix, which allows calculating both 95% parameter confidence intervals, based on Student's t-distribution, and parameter correlation matrix. Details of the formulation can be found elsewhere (Hopmans and Simunek, 1999; Lambot et al., 2002).

The selected parameters were first optimized, within the calibration period, layer by layer using only soil water content data of the corresponding layer ( $N = 125$ ). Next, all available soil water content measurements ( $N = 375$ ) in the profile were used, but again the parameters of each horizon were determined independently. Finally, due to the clear interactions between the layers, it was decided to optimize simultaneously the parameters of the three different horizons. Values of the flux at the bottom of the profile predicted by the model with the optimized parameters were also considered.

As mentioned above, the RMSE was used to evaluate the goodness of fit. Indeed, the RMSE is a useful single measure of the prediction capability of a model, since it indicates the precision with which the model estimates the value of the depended variable. The smaller the

RMSE, the better the simulated values fit the observed data (Eching and Hopmans, 1993). Accordingly to the notations described above, RMSE was calculated as follows:

$$RMSE = \sqrt{\frac{1}{N} \sum_{i=1}^N [\theta_{mea}(t_i) - \theta_{sim}(t_i, \mathbf{b})]^2} \quad (8)$$

### 2.6. Validation process

For the validation process, two periods were used: the first between the 26<sup>th</sup> of July and the 30<sup>th</sup> of September 1995 and the second between the 1<sup>st</sup> of April and 30<sup>th</sup> of September 1996. Three simulation runs were performed: first with the parameter set identified directly from the measurements; second with parameter set obtained by the trial and error method; and finally with the parameter sets obtained by the inverse procedure. The goodness of the fit was based on the RMSE and the visual inspection of simulated and observed soil water contents.

## 3. Results and discussion

Results of the sensitivity analysis for soil water content (Table 2 and Table 3), showed that soil water content, predicted by WAVE, was more sensitive to the hydraulic than to the crop parameters. These results are consistent with the findings of Musters et al. (2000) who applied inverse modeling to a forest ecosystem (pine stand) and Hupet et al. (2002) who analyzed parameter sensitivity of the WAVE model in a maize-cropped field. At any depth, sensitivity of the soil water content to  $\theta_s$ ,  $\theta_r$  and  $n$  parameters was high. The sensitivity coefficient of the saturated hydraulic conductivity ( $K_s$ ) was low, but still relatively significant. Among the hydraulic parameters, Mualem's pore connectivity parameter ( $\lambda$ ) presented the smallest coefficient. It is also worth mentioning that parameter change in one layer affected specially soil water content of the corresponding layer.

Concerning the flux at the bottom of the profile, the sensitivity coefficients (Table 4) showed that this model output variable was also most sensitive to  $\theta_s$  and  $n$ . However, it is interesting to note that it was very sensitive to the crop coefficient ( $K_c$ ) too, illustrating that the model sensitivity to a particular parameter depends on the objective function (output variable) considered. Vanclooster et al. (1995) presented similar results, but by contrast to

values in Table 4, they found WAVE to be relatively sensitive to  $K_s$ . This can be explained by the fact that they analyzed the sensitivity of the model for wet conditions. The next most sensitive parameters were  $\theta_r$  and  $LAI$ , while  $\lambda$  had the smallest coefficient.

Table 2

Average sensitivity coefficient (% Soil water content),  $SC_{\theta(z,b_j)}$ , for the hydraulic parameters corresponding to the variation of those of the first, second and third layer respectively

Depth	$\theta_s$	$\theta_r$	$n$	$\alpha$	$K_s$	$\lambda$
First layer (0 – 20 cm)						
15	$3.0 \cdot 10^{-3}$	$6.0 \cdot 10^{-4}$	$3.8 \cdot 10^{-3}$	$2.3 \cdot 10^{-4}$	$1.7 \cdot 10^{-4}$	$7.7 \cdot 10^{-5}$
30	$2.4 \cdot 10^{-4}$	$1.0 \cdot 10^{-4}$	$2.2 \cdot 10^{-4}$	$7.3 \cdot 10^{-5}$	$4.9 \cdot 10^{-5}$	$3.2 \cdot 10^{-5}$
60	$1.4 \cdot 10^{-4}$	$6.0 \cdot 10^{-5}$	$1.9 \cdot 10^{-4}$	$3.7 \cdot 10^{-5}$	$2.4 \cdot 10^{-5}$	$2.3 \cdot 10^{-5}$
Second layer (20 – 50 cm)						
15	$5.6 \cdot 10^{-5}$	$1.9 \cdot 10^{-5}$	$9.4 \cdot 10^{-5}$	$2.7 \cdot 10^{-4}$	$1.0 \cdot 10^{-4}$	$3.7 \cdot 10^{-5}$
30	$2.8 \cdot 10^{-3}$	$6.6 \cdot 10^{-4}$	$3.4 \cdot 10^{-3}$	$7.3 \cdot 10^{-5}$	$2.2 \cdot 10^{-4}$	$7.0 \cdot 10^{-5}$
60	$2.5 \cdot 10^{-4}$	$6.8 \cdot 10^{-5}$	$1.0 \cdot 10^{-4}$	$1.1 \cdot 10^{-5}$	$3.6 \cdot 10^{-5}$	$1.4 \cdot 10^{-5}$
Third layer (50 – 70 cm)						
15	$5.6 \cdot 10^{-5}$	$3.7 \cdot 10^{-6}$	$4.2 \cdot 10^{-5}$	$2.4 \cdot 10^{-5}$	$3.6 \cdot 10^{-5}$	$8.8 \cdot 10^{-6}$
30	$2.8 \cdot 10^{-3}$	$3.3 \cdot 10^{-6}$	$4.2 \cdot 10^{-5}$	$4.2 \cdot 10^{-5}$	$3.5 \cdot 10^{-5}$	$9.9 \cdot 10^{-6}$
60	$2.5 \cdot 10^{-4}$	$3.3 \cdot 10^{-4}$	$4.4 \cdot 10^{-3}$	$3.2 \cdot 10^{-5}$	$2.4 \cdot 10^{-4}$	$5.0 \cdot 10^{-5}$

Table 3

Average sensitivity coefficient (% Soil water content),  $SC_{\theta(z,b_j)}$ , for the crop parameters

Depth	$K_c$	$LAI$	$S_{max}$
15	$2.9 \cdot 10^{-5}$	$2.8 \cdot 10^{-5}$	$3.1 \cdot 10^{-6}$
30	$2.7 \cdot 10^{-5}$	$2.7 \cdot 10^{-5}$	$3.1 \cdot 10^{-6}$
60	$1.8 \cdot 10^{-5}$	$2.1 \cdot 10^{-5}$	$1.6 \cdot 10^{-6}$

Table 4

Sensitivity coefficient (mm),  $SC_F(b_j)$ , for the hydraulic and crop parameters

$n$	$K_c$	$\theta_s$	$LAI$	$\theta_r$	$\alpha$	$K_s$	$S_{max}$	$\lambda$
63.50	40.60	38.20	9.50	8.10	2.30	2.20	0.30	0.20

Consequently, the van Genuchten hydraulic parameters were selected for calibration based on soil water content data measured experimentally. Among these parameters,  $\theta_s$  has a clear physical significance and can rather be determined directly. Thus, the number of parameters for optimization was reduced to  $\theta_r$ ,  $\alpha$  and  $n$ .

The parameters estimated by the “trial and error” method are shown in Table 5. Soil water content simulations at 15, 30 and 60 cm depth corresponding to these parameters are presented in Figure 3. The simulated values approximate the measured values in the field rather well and the model responded satisfactorily to drought periods and rain and irrigation events. Simulations and measurements compared better during rain and irrigation periods

than during drought ones. The average coefficients of variation among sampling locations for each soil depth TDR reading were 24, 17 and 21%, respectively. The model prediction in the calibration period was better than in the validation one. During May of 1996 the simulation did not fit the field data, probably due to sampling errors, because there was no response of the measured values to the irrigation events during this period.

Table 5  
Calibrated hydraulic parameters with 95% confidence intervals (for inverse optimization only)

Depth (cm)	$\theta_r$ ( $cm^3/cm^3$ )	$\alpha$ ( $cm^{-1}$ )	$n$
Experimental determination			
15	0.322	0.278	1.377
30	0.315	0.220	1.406
60	0.250	0.189	1.292
“trial and error” method			
15	0.200	0.018	1.45
30	0.220	0.019	1.55
60	0.220	0.023	1.35
Inverse Optimization			
15	0.254 ±0.040	0.0191 ±0.007	2.653 ±0.893
30	0.256 ±0.038	0.0234 ±0.010	2.471 ±0.830
60	0.269 ±0.041	0.0565 ±0.024	1.643 ±0.270

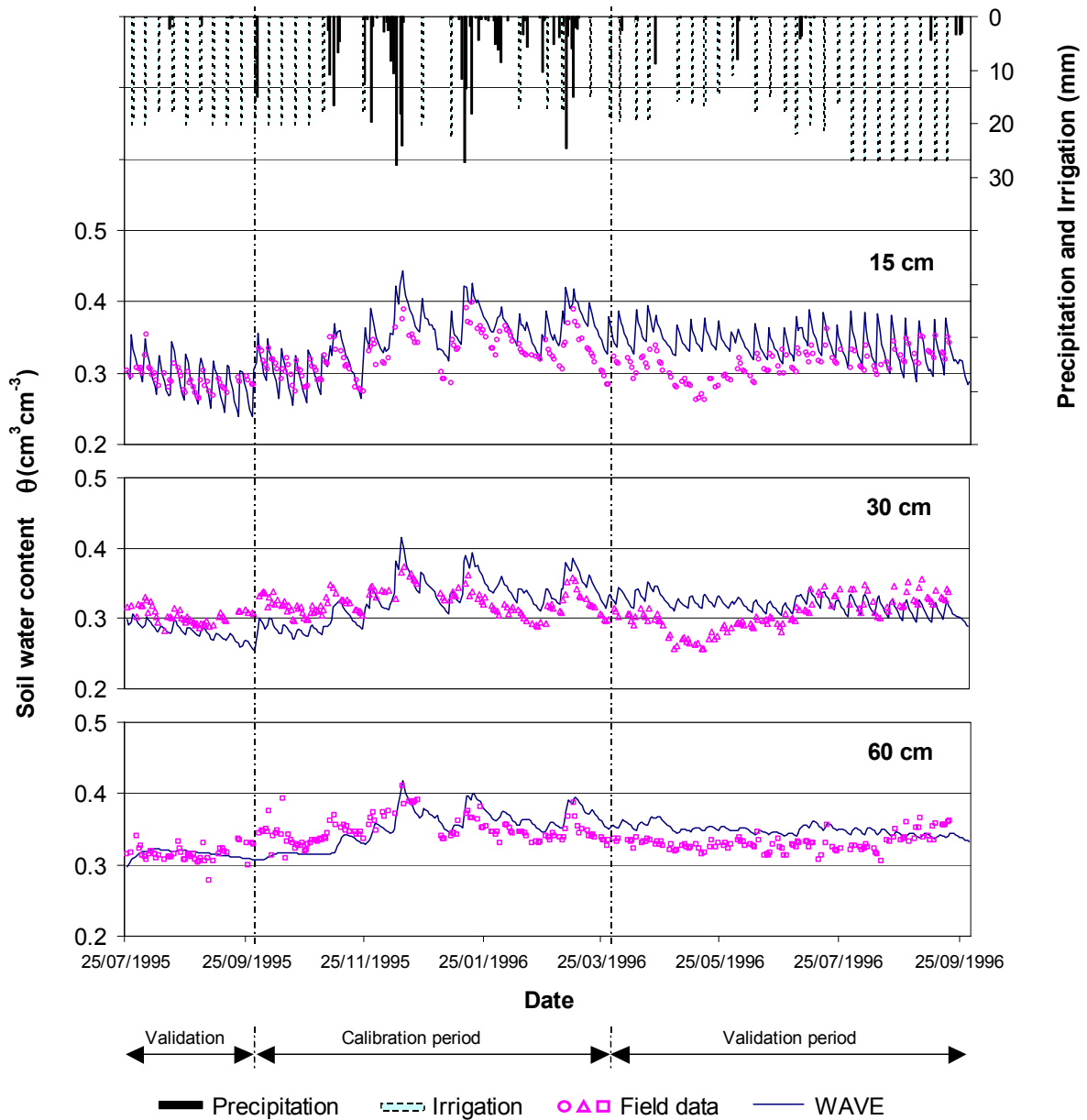


Figure 3. Soil water content simulation with parameters calibrated by the “trial and error” method. Measured data (symbols) and WAVE prediction (lines).

Concerning the inverse simulation methodology applied to this stratified soil profile, as the experimentally determined soil moisture retention curves at the three depths were not so different, an initial strategy was adopted. This strategy consisted of optimizing the three parameters,  $\theta_r$ ,  $\alpha$  and  $n$ , layer by layer and iteratively applying the inverse procedure on the different layers until the parameter values obtained were stable. However, this strategy failed due to the strong interactions between the three horizons. Hence, the inverse procedure was changed to determine the above-mentioned parameters of the three layers simultaneously, resulting in 9 parameters to optimize.

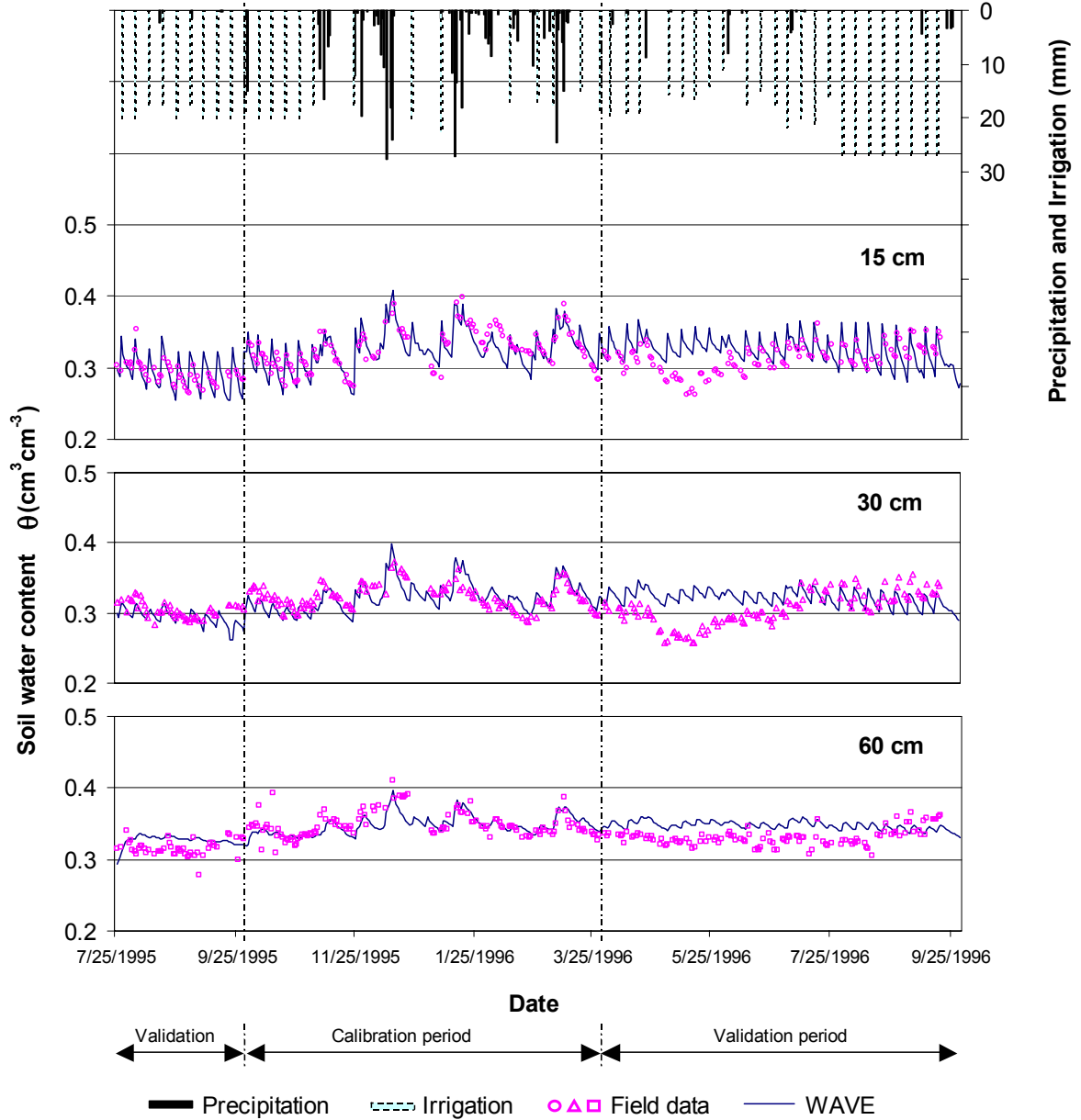


Figure 4. Soil water content simulation using the parameters of Table 5 estimated by inverse optimization. Measured data (symbols) and WAVE prediction (lines).

First, we started the inverse optimization procedure using broad parameter intervals, i.e.  $\theta_r[0.01-0.350]$ ;  $\alpha[0.005-0.300]$  and  $n[1.05-3.30]$ . No acceptable results were obtained, because the search space defined by those intervals was too large. Thereby, we decided to reduce the parameter intervals trying four new alternatives: *Inv.Opt.1*  $\{\theta_r[0.15-0.30]$ ;  $\alpha[0.050-0.200]$ ;  $n[1.05-2.00]\}$ ; *Inv.Opt.2*  $\{\theta_r[0.01-0.270]$ ;  $\alpha[0.005-0.050]$ ;  $n[1.10-3.00]\}$ ; *Inv.Opt.3*  $\{\theta_r[0.15-0.320]$ ;  $\alpha[0.005-0.050]$ ;  $n[1.10-3.3]\}$ ; *Inv.Opt.4*  $\{\theta_r[0.15-0.320]$ ;  $\alpha[0.010-0.070]$ ;  $n[1.10-3.30]\}$ . All of them, except *Inv.Opt.1*, yielded acceptable parameters according to RMSE and visual inspection of goodness of fit. Although different parameter

estimations were obtained, 95% confidence intervals of the optimized parameters overlapped for the distinct inverse simulations carried out. The best solution (corresponding *Inv.Opt.3*) is presented in Table 5. As can be seen in this table, the  $\alpha$  value for the third layer was outside of the *Inv.Opt.3*  $\alpha$  interval. This can be explained by the fact that the GMCS solution serves as initial guess to initialize the NMS algorithm. The latter performs an additional local search without limitations of iterations and parameter space, which may force the optimal value to be out of the predefined interval. Each inverse optimization included 4095 iterations and took around 2 hours using a PC Pentium4 at 1.4GHz.

Figure 4 shows the soil water content simulation at the three depths for the optimized parameters presented in Table 5. Like in Figure 3, predictions in the calibration period were more successful than in the validation one. Graphical comparison between model predictions with the parameters estimated by the “trial and error” method (Figure 3) and between those resulting from the set of parameters optimized in each inverse simulation procedure (Figure 4 and others not included), showed that inverse optimization yielded better results than the “trial and error” method. RMSEs for the calibration, validation and whole period (Table 6) confirmed the conclusions obtained from the visual inspection above-mentioned.

Table 6  
Root mean square errors (RMSEs) and predictions of flux at the bottom of the profile

Estimation method	RMSE			Cum. bottom flux ( <i>mm</i> )		
	Calibration	Validation	Whole	Calibration	Validation	Whole
Experimental determination	0.0417	0.0490	0.0447	511.7	339.7	851.4
“trial and error” method	0.0288	0.0341	0.0319	163.6	56.9	220.5
Inverse Optimization	0.0175	0.0305	0.0257	246.1	178.1	424.2

Concerning model predictions for the flux at the bottom of the profile, there were little differences between the values obtained for each inverse simulation procedure carried out (ranging between 410.4–429.2 mm). Table 6 shows the simulated bottom flux values for the three periods using the parameter sets of Table 5. Extremely large differences were observed when comparing the three estimation methods. The direct estimation of parameters yielded very large amount of water leaving the soil profile, while the value obtained from the “trial and error” method was much smaller. Furthermore, it is interesting that small RMSE differences (0.0319 vs. 0.0257) had a large effect on the cumulative bottom flux (220.5 vs. 424.2 *mm*). This illustrates that even with an acceptable model calibration uncertainties in flux predictions could be extremely large.

Consequently, although the “trial and error” method is more flexible and popular in modeling water balances in agricultural soils, it has some disadvantages: i) it is more time consuming; ii) it is difficult to know in which directions the parameters should be tuned (particularly if they interact among each other); iii) the result depends on the initial values; iv) it is a subjective process; v) it does not assure to find the best solution; and vi) it does not allow the parameter uncertainty to be quantified objectively. Moreover, from a scientific point of view it is not an appropriate method.

On the contrary, the use of the inverse optimization algorithm makes the calibration process faster, because it does not depend on initial values and within the search space (defined by the given parameter intervals) it does not test all the possible combinations, just those sets with more likelihood to be the solution. This technique is less subjective and due to its working procedure, it is more efficient in finding the best solution. However, its flexibility depends on the number of parameters to optimize, which is limited by convergence problems.

As illustrated in this study, the inverse optimization method is a promising parameter estimation procedure, but it requires the inverse problem to be well-posed. Our situation suffers from ill-posedness, since 9 parameters were estimated simultaneously. In addition, the optimization algorithm was shown by Huyer and Neumaier (1999) and Lambot et al. (2002) to be effective when no more than 4 parameters were identified. Figure 5 shows the different soil moisture retention curves corresponding to the distinct sets of parameters calibrated by the “trial and error” methodology and by some of the inverse simulations performed, as well as those determined by the direct approach (Table 5). From this figure, we can see that the algorithm was not able to find the global solution. Coefficients of correlations between several estimated parameters were high. This means that different parameter combinations can equally well describe the experimental measurements. On the other hand, the soil water content input data used for the optimization might not contain enough information for a unique identification of the hydraulic parameters. Thus, an increase in the number of optimized parameters entails the need for further measurements of different types (Hopmans and Simunek, 1999), such as tensiometric and/or outflow data. Yet, it must also be taken into account that additional data require more time and make the experimental setup more difficult (Zou et al., 2001). Moreover, it must be considered that, as shown by Carrera and Neuman (1986), when input data are subject to measurement errors, the convergence of the minimization algorithm at several points in the parameter space may be very slow due to instability. Inverse optimization techniques should be complemented with direct methods,

especially when over-parameterized models are used. Indeed, Russo et al. (1991), analyzing infiltration events to determine soil hydraulic properties by inverse simulation, concluded that the use of prior information of the model parameters reduces the degree of ill-posedness of the inverse problem and might lead to a stable and unique solution, even when the input data are associated with considerable measurement errors.

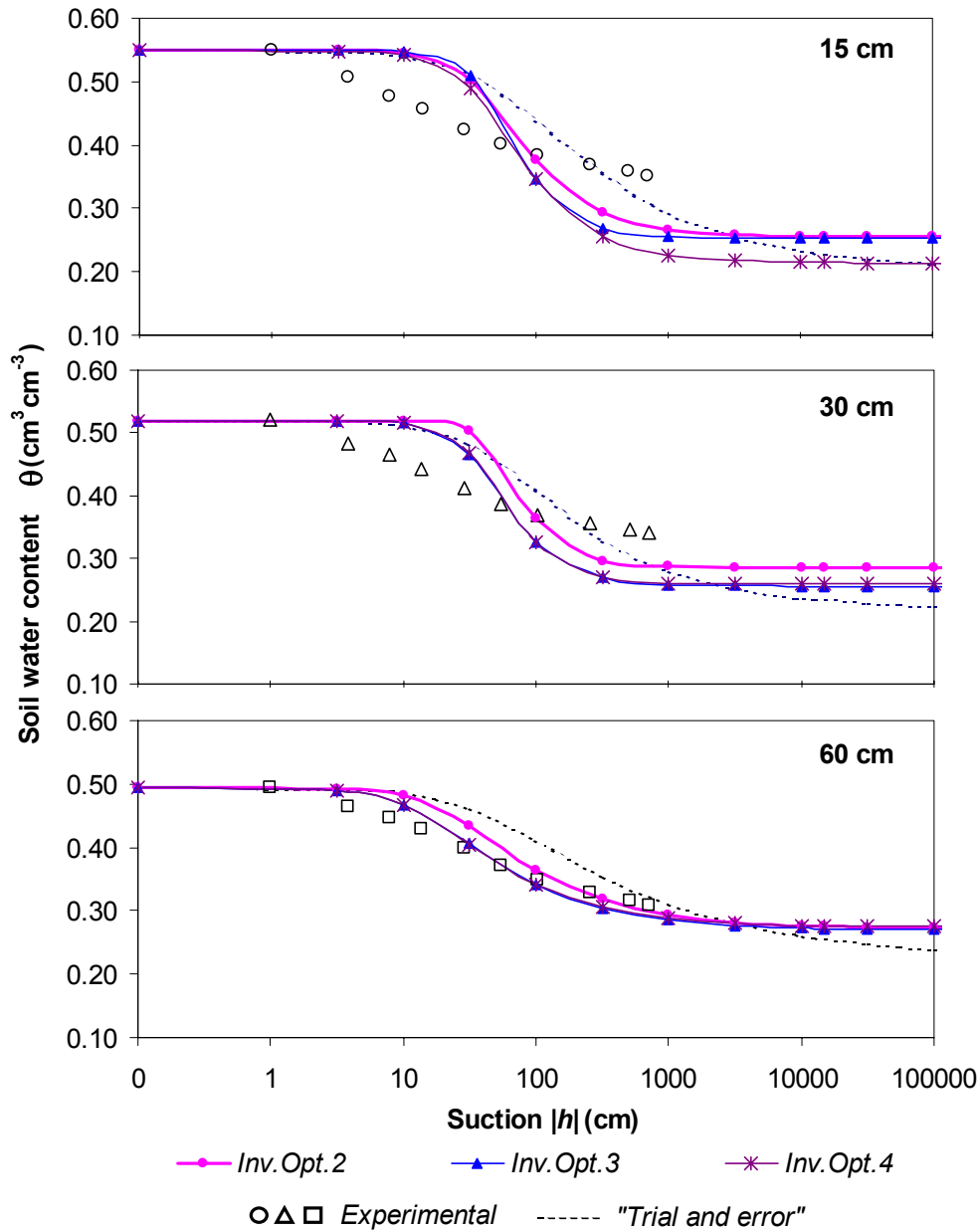


Figure 5. Soil moisture retention curves for the different parameter estimation methods. Measured data (symbols) and obtained from calibration (lines).

In addition, it should be taken into account that, although laboratory determinations are more precise and in general more convenient than field measurements, the use of soil properties determined in small cores is questionable (Russo et al., 1991). In this work there is

a considerable deviation between the directly determined and inversely estimated soil moisture retention curves in particular for the top soil layer. This may be explained by the fact that the soil structural phenomena, which generally drives soil water flow at the field scale, are poorly represented at the core scale on which soil retention curves are directly determined.

#### **4. Conclusions**

The use of the WAVE model applied to a sprinkler fertigated banana plantation in the North of Tenerife (Canary Islands) showed that using laboratory-determined soil hydraulic properties to simulate the field water balance at field scale in a stratified soil profile can produce inaccurate results. Although there are many other uncertainties (e.g. semi-empirical crop parameters, spatial variability within the field, determination of irrigation amounts, representation of a 3-D situation with a 1-D model), it is generally well accepted that some of the soil parameters experimentally determined should be further calibrated with an observed data set.

The study also pointed out the issues related to the “trial and error” calibration procedure, which, besides being a tricky and non-scientific method, it is not really objective (certainly not for a cropped three-layered soil) and it can lead to relatively poor fit of the measured data, even if time is not a limiting factor. An alternative method is the use of an optimization algorithm, like GMCS-NMS that, combined with the numerical model, results in a relatively efficient parameter estimation technique. However, under certain boundary conditions of the inverse problem, it may yield different solutions, that lead to the same response for the model variable used in the calibration process (i.e. soil water content), but with different results for other variables such as the cumulative bottom flux. This clearly illustrates the problem of ill-posedness, which, in this study, can be partially explained due to a large number of parameters to optimize and to errors or insufficient information in the measured input data set used for calibration. Nevertheless, ill-posedness is an intrinsic problem of parametric models suggesting the necessity of additional experimental data to identify the more realistic optimized solution.

*Acknowledgments*

The authors want to thank K.L. Campbell and W.D. Graham for their helpful comments during the internal review process prior to submission to the journal. This work was financed with funds of the INIA-Plan Nacional de I+D Agrario (Proyectos I+D INIA SC95-059 and SC99-024-C2) and Consejería de Educación Cultura y Deportes del Gobierno de Canarias. This research was supported by the Florida Agricultural Experiment Station, and approved for publication as Journal Series No. R-08630.

## 5. References

- Belmans, C., Wesseling J.G., Feddes, R.A., 1983. Simulation model of a water balance of a cropped soil: SWATRE. *J. Hydrol.* 63, 271-286.
- Beven, K.J., 2001. *Rainfall-Runoff Modelling-The Primer*. Wiley, Chichester.
- Carrera, J., Neuman, S.P., 1986. Estimation of aquifer parameters under transient and steady state conditions. 2. Uniqueness, stability and solution algorithms. *Water Resour. Res.* 22, 211-227.
- Dane, J.H., Hruska, S., 1983. In-situ determination of soil hydraulic properties during drainage. *Soil Sci. Soc. Am. J.* 47, 619-624.
- Diels J., 1994. A validation procedure accounting for model input uncertainty applied to the SWATRER model. Ph.D thesis, KU Leuven, Belgium, pp. 173.
- Dirección General de Aguas y Servicio de Planificación Hidráulica (DGA-SPH), 1993. PHI-Plan Hidrológico Insular de Tenerife. Cabildo de Tenerife: Santa Cruz.
- Durner, W., Schultze, B., Zurmühl, T., 1999. State-of-the-Art in inverse modeling of inflow/outflow experiments. In M. Th. van Genuchten, F.J. Leij and L. Wu (eds) *Proc. Int. Workshop, Characterization and Measurement of the Hydraulic Properties of Unsaturated Porous Media*: 713-724. University of California, Riverside, C.A.
- Eching, S.O., Hopmans, J.W., 1993. Optimization of hydraulic functions from transient outflow and soil water pressure data. *Soil Sci. Soc. Am. J.* 57, 1167-1175.
- Hopmans, J.W., Simunek, J., 1999. Review of inverse estimation of soil hydraulic properties. In M. Th. van Genuchten, F.J. Leij and L. Wu (eds) *Proc. Int. Workshop, Characterization and Measurement of the Hydraulic Properties of Unsaturated Porous Media*, 713-724. University of California, Riverside, C.A.

- Hupet, F., Lambot, S., Javaux, M., Vanclooster, M., 2002. On the identification of macroscopic root water uptake parameters from soil moisture observations. *Water Resources Research (in press)*.
- Huyer, W., Neumaier, A., 1999. Global optimization by multilevel coordinate search. *J. Global Optimization* 14, 331-355.
- Inoue, M., Simunek, J., Hopmans, J.W., Clausnitzer, V., 1998. In situ estimation of soil hydraulic functions using a multistep soil-water extraction technique. *Water Resour. Res.* 34(5), 1035-1050.
- Jhorar, R.K., Bastiaanssen, W.G.M., Feddes, R.A., van Dam, J.C., 2002. Inversely estimating soil hydraulic functions using evapotranspiration fluxes. *J. Hydrol.* 258: 198-213.
- Klute, A. (ed). 1986. *Methods of Soil Analysis. Part 1. Physical and Mineralogical Methods.* 2nd. Ed. Agronomy monograph no.9. Madison: ASA-SSSA.
- Lambot, S., Javaux, M., Hupet, F., Vanclooster, M., 2002. A Global Multilevel Coordinate Search procedure for estimating the unsaturated soil hydraulic properties. *Water Resources Research (in press)*.
- Mualem, Y., 1976. A new model for predicting the hydraulic conductivity of unsaturated porous media. *Water Resour. Res.* 12, 513-522.
- Muñoz-Carpena, R., Fernández, D., González, G., Harris, P., 1996. Diseño y evaluación de una estación micrometeorológica de bajo coste para el cálculo de la evapotranspiración de referencia. *Riegos y Drenajes XXI* 88, 17-25.
- Muñoz-Carpena, R., Parsons, J.E., Ducheyne, S., 1999a. Simulación con el modelo numérico WAVE del transporte de agua y nitrógeno a través de la zona no saturada en un cultivo de platanera. En: R. Muñoz-Carpena, A. Ritter, C. Tascón (eds.). *Estudios en la Zona no Saturada del Suelo*, 163-168.
- Muñoz-Carpena, R., Parsons, J.E., Ducheyne, S., 1999b. Banana water quality modeling with WAVE. Paper of ASAE no. 992217. ASAE: St. Joseph. 1999.
- Muñoz-Carpena, R., Vanclooster, M., Villacé-Reyes, E., 2001. Evaluation of the WAVE model. In: J.E. Parsons; D.L. Thomas and R.L. Huffman (eds.) *Agricultural Non-Point Source Water Quality Models: Their use and Application.* Southern Cooperative Series Bull. No. 398. ISBN: 1-58161-398-9.
- Muñoz-Carpena, R., Ritter, A., Socorro, A.R., Pérez, N., 2002. Nitrogen evolution and fate in a Canary Islands (Spain) sprinkler fertigated banana plot. *Agric. Water Manage.* 52, 93-117.

- Musters, P.A.D., Bouten, W., Verstraten, J.M., 2000. Potentials and limitations of modelling the vertical distributions of root water uptake of an Austrian pine forest on a sandy soil. *Hydrol. Proc.* 14, 103-115.
- Nelder, J. A. and R. Mead, 1965. A Simplex Method for Function Minimization. *Computer Journal* 7, 308 - 313.
- Russo, D., Bresler, E., Shani, U., Parker, J.C., 1991. Analyses of infiltration events in relation to determining soil hydraulic properties by inverse problem methodology. *Water Resour. Res.* 27(6), 1361-1373.
- Simunek, J., van Genuchten, M.Th., 1996. Estimating unsaturated soil hydraulic properties from tension disc infiltrometer data by numerical inversion. *Water Resour. Res.* 32(9), 2683-2696.
- Simunek, J., Huang, K., Sejna, M., van Genuchten, M.Th., 1998. The HYDRUS-1D software package for simulating the one-dimensional movement of water, heat, and multiple solutes in variably-saturated media. Version 1.0. IGWMC-TPS-70, International Ground Water Modelling Center, Colorado School of Mines Golden, CO.
- Simunek, J., Wendroth, O., van Genuchten, M.Th., 1999. Soil hydraulic properties from laboratory evaporation experiments by parameter estimation. In M. Th. van Genuchten, F.J. Leij and L. Wu (eds) *Proc. Int. Workshop, Characterization and Measurement of the Hydraulic Properties of Unsaturated Porous Media*, 713-724. University of California, Riverside, C.A.
- Spitters, C.J.T., Van Keulen, H., Van Kraalingen, D.W.G., 1988. A simple but universal crop growth simulation model, SUCRO87. En: R. Rabbinge, H. Van Laar and S. Ward (eds). *Simulation and systems management in crop protection. Simulation Monographs*, PUDOC, Wageningen, The Netherlands.
- Topp, G.C., Davis, J.L., Annan, A.P., 1980. Electromagnetic determination of soil water content: measurement in coaxial transmission lines. *Water Resour. Res.* 16, 574-582.
- van Dam, J.C., Stricker, J.N.M., Droogers, P., 1990. From one-step to multistep determination of soil hydraulic functions by outflow experiments. *Dep. of Hydrol., Soil Phys., and Hydraul. Rep.*, Wageningen Agric. Univ., Wageningen, The Netherlands.
- van Genuchten, M.Th., 1980. A closed-form equation for predicting the hydraulic conductivity of soil. *Soil Sci. Soc. Am. J.* 44, 892-898.
- Vanclooster, M., Viaene, P., Diels, J., Feyen, J., 1995. A deterministic evaluation analysis applied to an integrated soil-crop model. *Ecological Modelling* 81, 183-195.

- Vanclooster, M., P. Viaene, K. Christiaens, Ducheyne, S., 1996. WAVE : a mathematical model for simulating water and agrochemicals in the soil and vadose environment, Reference and user's manual (release 2.1), Institute for Land and Water Management, Katholieke Universiteit Leuven, Leuven, Belgium.
- Van Keulen, H., Penning, F.W.T., de Vries, J., Drees, E.M., 1982. A summary model for crop growth. In: F.W.T. Penning de Vries and H.H. van Laar (eds.). Simulation of crop growth and crop production. PUDOC, Wageningen, The Netherlands, 87-98.
- Vereecken, H., Vanclooster, M., Swerts, M., 1990. A simulation model for the estimation of nitrogen leaching with regional applicability. In: R. Merckx and H. Vereecken (eds.). Fertilization and the environment. Leuven Academic Press, Belgium, 250-263.
- Vereecken, H., Vanclooster, M., Swerts, M., Diels, J., 1991. Simulating water and nitrogen behaviour in soil cropped with winter wheat. *Fertilizer Research* 27, 233-243.
- Wagenet, R., Hutson, J., 1989. LEACHM, a process-based model of water and solute movement, transformations, plant uptake and chemical reactions in the unsaturated zone. Centre for Environ. Research., Cornell University, Ithaca, N.Y., pp. 147.
- Yeh, W.W.-G., 1986. Review of parameter identification procedures in groundwater hydrology: The inverse problem. *Water Resour. Res.* 22(2), 96-108.
- Zou, Z.-Y., Young, M.H., Li, Z., Wierenga, P.J., 2001. Estimation of depth averaged unsaturated soil hydraulic properties from infiltration experiments. *J. Hydrol.* 242, 26-42.

## **Capítulo 3**

### **Analysis of alternative measurement strategies for the inverse optimization of the hydraulic properties of a volcanic soil**

*Journal of Hydrology*, (enviado octubre, 2002)

## Abstract

In this paper, the suitability of alternative measuring strategies for identifying the flow parameters from transient flow experiments in an undisturbed volcanic soil column is analyzed. Alternative measurement strategies are defined by combining observed data from different hydraulic state variables with a variable depth resolution. The state variables considered are soil water content ( $\theta$ ), matric pressure head ( $h$ ), and the water flux at the bottom of the soil column ( $q$ ). For  $\theta$  and  $h$  a maximum measurement depth frequency of seven observation depths per profile was used. A first outflow experiment allows making an initial direct estimate of the flow parameters for the four soil horizons in the column. From this initial experiment, the hydraulic parameters selected for inverse estimation are reduced to the saturated water content, the van Genuchten's  $n$  suction curve shape parameter and the saturated hydraulic conductivity. The performance of the inverse analysis is measured by means of a factorial evaluation index, encompassing a measure of the goodness of fit and parameter uncertainty. Results show that the best measurement strategies for inverse analysis are those combining  $\theta$  with either  $h$  or  $q$ . Although inverse modeling using data from all the state variables considered ( $\theta$ ,  $h$  and  $q$ ) give the best results, monitoring of  $\theta$  in combination with either  $h$  or  $q$  proves to be sufficient, even when only four observation depths are considered.

*Keywords:* Canary Islands; Inverse modeling; Multilevel coordinate search; Parameter estimation; Volcanic soils; WAVE model.

## 1. Introduction

Computer models of soil water and solute transport are nowadays widely used for assessing the impact of agricultural activities on groundwater resources and for designing best management practices (BMPs) to reduce these impacts. This is the case in the Canary Islands (Spain), where appropriate agricultural and water management is needed for reducing the impacts of the intensive subtropical horticulture on the groundwater resources.

The success of modeling soil flow and transport processes heavily depends on the quality of the model parameters that are used to describe the soil's hydraulic behavior. There are several direct field and laboratory methods that allow determining the soil hydraulic properties. However, they are relatively tedious, time-consuming, expensive, and involve considerable uncertainty for practical applications (Russo et al., 1991; Abbaspour et al., 1999). An alternative approach is to obtain the flow properties by using "indirect methods", where the parameters are treated as unknowns and are estimated based on a certain system response (i.e. a measurable variable) (Russo et al., 1991). In this context, curve fitting may be considered as the simplest way to estimate parameters indirectly (Vrugt et al., 2001). A more complex and increasingly attractive form of parameter estimation is inverse modeling. With this latter method, parameters are optimized by minimizing a suitable objective function that expresses the discrepancy between the output of the numerical model and the measurement of a certain hydraulic state variable (matric pressure head, soil water content, flow rates, etc.) (Si and Kachanoski, 2000). For this approach the numerical flow model is coupled with a global optimization algorithm. Among such algorithms, the GMCS-NMS algorithm (Global Multilevel Coordinate Search-Nelder Mead Simplex), described by Huyer and Neumaier (1999) and Lambot et al. (2002), is a powerful algorithm.

Inverse optimization has several advantages over the traditional direct methods (Si and Kachanoski, 2000; Zou et al., 2001): i) it provides effective parameters in the range of envisaged model applications; ii) it allows for relatively simple experimental design, as few restrictions are imposed upon the experimental conditions; iii) it allows to determine simultaneously water retention and hydraulic conductivity functions; and iv) it can handle data from transient flow experiments, which are inherently faster than steady-state experiments. Disadvantage of the method is the ill-posedness of many inverse problems. As stated by several authors (Beven, 1996; Carrera and Neuman, 1986; Russo et al., 1991), the

well-posedness of the inverse problem depends upon three aspects: parameter identifiability, solution uniqueness and solution stability or robustness. If more than one parameter set lead to the same model response, the parameters are unidentifiable and the solution is non-unique. Stability means that small errors in the response data should not yield large changes in the estimated parameters.

Many authors (Dane and Hruska, 1983; Kool et al., 1985; Ritter et al., 2002) experienced difficulties to achieve the unique solution when using inverse optimization to estimate soil hydraulic properties. To overcome the non-uniqueness problem several recommendations have been suggested such as modifying the experimental boundary conditions (e.g. multistep instead of one-step outflow experiments (Eching and Hopmans, 1993)); constraining the parameter space by introducing prior parameter information (Abbaspour et al., 1999; Russo et al., 1991); reducing the experimental errors (Kool et al., 1985); improving the efficiency and robustness of the inversion algorithm (Kool et al., 1987); or introducing additional measurements of one or more state variables (Eching and Hopmans, 1993; Kool and Parker, 1988).

The efficiency of this latter strategy will depend on the quality of the information contained in the new data (Vrugt et al., 2001). The usefulness of additional measurements depends on its sensitivity to the hydraulic parameters, the independence of the existing measurements, and the measurement error (Si and Kachanoski, 2000). In such a context, the effectiveness of different measurement strategies for the inverse estimation of soil hydraulic properties could be analyzed in detail. This is an important issue, since some variables are easier to measure than others and are thus more suitable for estimation by inversion (Abbaspour et al., 1999). Moreover, when designing an experiment, efforts and costs should be minimized. Decisions on sampling methods and variables should be based on quantitative and objective information rather than on intuition.

In this paper, the suitability of alternative measuring strategies for identifying the flow parameters from transient flow experiments in an undisturbed volcanic soil column is analyzed. The adopted method of analysis can be used at the experimental design stage using synthetic data obtained from a simulation run with reference parameters or for the estimation of flow parameters from real 'observed' data. Alternative measurement strategies combining different state variables at different sampling locations are considered. To facilitate the evaluation of the alternative strategies, we introduce a factorial evaluation index that

integrates goodness of fit and parameter uncertainty. The analysis deals with the estimation of the soil hydraulic parameters from outflow experiments performed on a large undisturbed volcanic soil column. Matric pressure head, soil water content, and/or bottom flux data are introduced in the inversion problem. The parameters were inversely estimated using the water flow module of the WAVE model coupled with the Global Multilevel Coordinate Search combined sequentially with Nelder-Mead Simplex algorithm (GMCS-NMS).

## 2. Materials and methods

### 2.1. The forward numerical model

To describe the flow across the initially unsaturated monolith, the one-dimensional computer code WAVE (Vanclooster et al., 1996) was used. The quality of the numerical solution of this model was recently successfully tested in a numerical flow modeling benchmark exercise (Vanderborght et al., 2002). WAVE simulates transient flow by numerically solving a one-dimensional, isothermal Darcian flow equation in a variably saturated, rigid porous medium, using the mass-conservative scheme of Richards equation proposed by Celia et al. (1990):

$$C(h) \frac{\partial h}{\partial t} = \frac{\partial}{\partial z} \left[ K(h) \left[ \frac{\partial h}{\partial z} + 1 \right] \right] \quad (1)$$

where  $C(h)$  is the soil water content capacity [ $L^{-1}$ ];  $z$  is the vertical distance from the soil surface [ $L$ ];  $t$  is the time [ $T$ ];  $K(h)$  is the hydraulic conductivity [ $LT^{-1}$ ] and  $h$  is the matric pressure head [ $L$ ].

The soil moisture retention curve is assumed to be of the form described by van Genuchten (1980):

$$Se(h) = \frac{\theta(h) - \theta_r}{\theta_s - \theta_r} = \left[ 1 + \alpha |h|^n \right]^{-m} \quad (2)$$

where  $Se$  is the effective saturation [-];  $\theta(h)$  is the soil water content [ $L^3L^{-3}$ ] at matric pressure head  $h$ ;  $\theta_s$  and  $\theta_r$  are the saturated and residual soil water content [ $L^3L^{-3}$ ], respectively;  $\alpha$  is the inverse of the air entry value of  $h$  [ $L^{-1}$ ];  $m$  and  $n$  are curve shape parameters. The  $m$  characterizes the asymmetry, while the  $n$  is related to the slope of the

curve (Vanclooster et al., 1996). Combining Eq. (2) with the pore-size distribution model of Mualem (1976) and using the constraint  $m=1-1/n$ , yields an expression for the unsaturated hydraulic conductivity function (van Genuchten, 1980):

$$K(Se) = K_s Se^\lambda \left[ 1 - (1 - Se^{-m})^m \right]^2 \quad (3)$$

where  $K(Se)$  and  $K_s$  are the unsaturated and saturated hydraulic conductivity [ $LT^{-1}$ ], respectively and  $\lambda$  is the pore connectivity parameter [-], which accounts for tortuosity and correlation between pore sizes (Durner et al., 1999).

## 2.2. Inverse optimization procedure

### 2.2.1 Formulation of the inverse optimization problem

The inverse parameter estimation is formulated here as a nonlinear optimization problem, where the model soil hydraulic parameters are optimized by minimizing a suitable objective function based on the deviations between observed and predicted system response variables (Hopmans and Simunek, 1999). The optimization process includes three basic steps repeated until some predefined convergence criteria are satisfied. These steps are: i) parameter perturbation; ii) forward modeling and iii) objective function evaluations. In addition, an analysis of uncertainty is also performed. The formulation of the objective function can be derived from the maximum likelihood theory, that leads to the generalized least squares problem when measurement errors follow a multivariable normal distribution with zero mean and known variance-covariance matrix:

$$OF(\mathbf{b}) = \mathbf{e}^T \mathbf{V}^{-1} \mathbf{e} \quad (4)$$

where  $OF(\mathbf{b})$  [-] is the objective function of the parameter vector  $\mathbf{b}$ ;  $\mathbf{V}$  is the error covariance matrix, so that  $\mathbf{V}^{-1}$  denotes the weighting matrix. The residual vector is equal to  $\mathbf{e} = (\mathbf{q}^* - \mathbf{q})$ , and  $\mathbf{q}^* = \mathbf{q}^*(z, t)$  and  $\mathbf{q} = \mathbf{q}(z, t, \mathbf{b})$  are vectors containing the observed and the simulated data, respectively, at time  $t$ , and depth  $z$ . When residuals are independent and normally distributed with different variances for the different data types,  $\mathbf{V}$  reduces to a diagonal matrix leading to a weighted least squares problem (Carrera and Neuman, 1986; Hopmans and Simunek, 1999), where the objective function ( $OF$ ) takes the form:

$$OF(\mathbf{b}) = \sum_{j=1}^{n_m} \left\{ W_j \sum_{z=1}^{n_z} \sum_{i=1}^{n_j} w_{i,j} [Y_j^*(z, t_i) - Y_j(z, t_i, \mathbf{b})]^2 \right\} \quad (5)$$

where  $j$  represents the different sets of observation type (here matric pressure head, soil water content and bottom flux);  $n_j$  is the number of measurements within a particular set of type  $j$ ;  $Y_j^*(z, t_i)$  are measurements of type  $j$  at time  $t_i$  and depth  $z$ ;  $Y_j(z, t_i, \mathbf{b})$  are the corresponding model predictions using the parameter vector  $\mathbf{b}$ . The  $n_m$  and  $n_z$  denote the number of different measurement types and observation depths, respectively, while  $W_j$  and  $w_{i,j}$  are weighting factors associated with observation type and individual measurements, respectively (Vrugt et al., 2001). The  $W_j$  factor accounts for the differences between observation types due to different magnitudes and numbers ( $n_j$ ), and is equal to  $(n_j s_j^2)^{-1}$ , where  $s_j$  denotes the standard deviation of  $j$ -type observations (Vrugt et al., 2001).

### 2.2.2 Global optimization algorithm

To minimize the objective function, the WAVE model was coupled with the *Global Multilevel Coordinate Search*, GMCS algorithm (Huyer and Neumaier, 1999). This algorithm combines global and local search capabilities with a multilevel approach. The GMCS is a good alternative to other existing optimization algorithms. It can deal with objective functions with complex topography, does not require powerful computing resources and initial values of the parameters to be optimized are not needed. In addition, for problems with finite bound constraints (parameter search space), the convergence is guaranteed if the objective function is continuous in the neighborhood of the global minimum. To refine the minimization of the objective function the GMCS is combined sequentially with the Nelder-Mead Simplex (NMS) algorithm (Nelder and Mead, 1965). Further details about application of GMCS-NMS to inverse modeling of soil hydraulic properties are given in Lambot et al. (2002) and Ritter et al. (2002).

The code that couples the GMCS-NMS algorithm with the WAVE model requires specific input files for each inverse optimization procedure, making multiple inverse simulations a tedious task. We modified the code for this study by adding several routines that allow for quicker and more flexible inverse procedures when combining different hydraulic variables and observation depths. Furthermore, the new code saves the results in appropriate files depending on the combination of measurement types and observation depths chosen. The format of these files was designed to allow for direct import of results into spreadsheets. In

addition, the modified system can be easily set up to run automatically inverse simulations in batch mode.

### 2.2.3 Quantification of parameter uncertainty

Uncertainty associated with parameter estimated by inverse modeling is an essential aspect. The quantification of the parameter uncertainty for non-linear models is built upon the following assumptions: i) convergence to the global minimum; ii) zero model error; and iii) independent and normally distributed residuals (measurement errors) (Hopmans and Simunek, 1999). For nonlinear fitting models, knowledge of the true distributions of the optimized parameters is required. The latter can be obtained using the Monte Carlo method. However, since this is usually a very time consuming task, linear regression analysis is often performed to approximate parameter confidence intervals for the nonlinear problem nearby the optimum. In this case, the objective function in the parameter space must be quasi-linear within the confidence interval region.

Although this approach is restrictive and only approximately valid for nonlinear problems, it allows comparing confidence intervals between parameters, indicating which of them need to be measured or estimated independently (Hopmans and Simunek, 1999).

Considering the previous assumptions, parameter uncertainty can be determined on the basis of the parameter variance-covariance matrix, which can be estimated from the variance of the residuals  $e$  (Eq. (4)) and the Jacobian matrix (Kool and Parker, 1988). By using this estimation of the covariance matrix, 95% parameter confidence intervals based on Student's t-distribution can be determined. Furthermore, the correlation matrix can be calculated from the covariance matrix. Details of this formulation can be found elsewhere (Hopmans and Simunek, 1999; Kool and Parker, 1988; Lambot et al., 2002). It must be taken into account that high correlation coefficients between estimated parameters might lead to non-uniqueness of the solution and overestimation of the parameter uncertainty. Indeed, a change of one parameter may be balanced by a change of the correlated parameter. Thus, correlated parameters cannot be independently determined by the inverse method (Zurmühl and Durner, 1998).

### 2.2.4 Sampling strategies for the inverse procedure

We refer here to the term “strategy” to denote a certain combination of measured data to be used for the inverse optimization of parameters. Each strategy implies a particular formulation of the objective function according to the number and type of observations chosen. Thus, when considering only distinct types of measurements, seven different objective functions (Eq. (5)) can be formulated by combining three hydraulic variables: ( $h$ ), ( $\theta$ ), ( $q$ ), ( $h\theta$ ), ( $hq$ ), ( $\theta q$ ) and ( $h\theta q$ ); where  $h$ ,  $\theta$  and  $q$ , represent matric pressure head, soil water content and bottom flux, respectively. On the other hand, using these combinations, more strategies can be obtained by taking into consideration different numbers of observation depths. Further in this paper, we will use the notation  $(var)_L$  to identify the strategies; where  $var$  represents the combinations of hydraulic variables and  $L$  the number of observation depths.

The performance of several sampling strategies for the inverse optimization of hydraulic parameters was analyzed. First, considering that the readings from all observation depths are available, we performed inverse modeling independently for each of the seven objective functions mentioned above. Secondly, once we evaluated which of those strategies were more appropriate, these were further tested by reducing the number of observation depths. Thereby, we verified if the same solution of the inverse problem was achieved with less observations points, i.e. lower experimental cost.

The performance of the inversion procedure was evaluated first using the approximate 95% confidence interval ( $CI_{95}$ ) and goodness of fit. Parameter identifiability was analyzed by considering the overlap and length of  $CI_{95}$  (Durner et al., 1999). The shorter the length of the  $CI_{95}$ , the more suitable is the strategy to find the solution of the inverse problem.

The model’s goodness of fit is usually quantified by using the average of the squared deviations between observed and simulated data. Thus, the commonly used statistic is the mean square error ( $MSE$ ) or the root mean square error ( $RMSE$ ). The smaller their value, the better the model predictions fit the observed data (Eching and Hopmans, 1993). However, to allow for a comparison between results of different observation types, non-dimensional statistics are required (Wilson, 2001). The normalized  $MSE$  per range of observed values ( $nMSE$ ) expresses the proportion of the variance about the 1:1 line compared to the variance of the observed data ( $\sigma_o^2$ ). It is calculated as follows:

$$nMSE_j = \frac{MSE_j}{\sigma_{o_j}^2} = \frac{\sum_{i=1}^{n_j} [Y_j^*(z, t_i) - Y_j(z, t_i, \mathbf{b})]^2}{\sum_{i=1}^{n_j} [Y_j^*(z, t_i) - \bar{Y}_j^*]^2} \quad (6)$$

Thereby, for each strategy and considering the whole profile, a  $nMSE$  corresponding to the three observation types (matric pressure head, soil water content and bottom flux) were calculated.

A factorial evaluation index ( $FEI$ ) was proposed to combine the above-mentioned criteria, and make comparisons between strategies easier. The  $FEI$  takes into account that model performance is better when  $nMSE$  and parameter uncertainty are small. Non-dimensional  $CI_{95}$  lengths relative to the mean value were considered for each  $k$ -parameter and are denoted herein as  $(L_{95})_k$ .

To evaluate the alternative strategies, we considered that the contribution of both criteria to the index is multiplicative, so that geometric means of components may be used (Limpert et al., 2001). Therefore, we calculated the  $FEI$  as follows:

$$FEI = C \left[ \prod_{k=1}^{n_k} (L_{95})_k \right]^{-\frac{1}{n_k}} \left[ \prod_{j=1}^{n_m} nMSE_j \right]^{-\frac{1}{n_m}} = C \frac{1}{(L_{95})_{GM} nMSE_{GM}} \quad (7)$$

where the subscript  $GM$  denotes the geometric mean among the  $j$ -type hydraulic variables considered ( $n_m=3$ , for  $\theta$ ,  $h$  and  $q$ ) or among the  $k$ -parameters ( $n_k= 8$ , as described below). In addition, the  $FEI$  includes a scaling constant,  $C$ , to avoid too large index values. In our case, we fixed a value of  $C= 10^{-3}$ , to ensure that the calculated values were within the range 0-1. Following  $FEI$ 's definition, appropriate measurement strategies will be characterised by a high  $FEI$ .

Finally, to determine whether alternative measurement strategies perform statistically different, significance tests were made on the  $nMSE$ 's (Steel et al., 1997).

### 2.3. Experimental set-up

A large monolith of undisturbed volcanic soil (sandy-clay-loam texture) was taken from a banana (*Musa accuminata* cv. 'Giant Cavendish') field in Tenerife (Canary Islands, Spain). The plantation was under a shadehouse and drip irrigated.

Agriculture in the Canary Islands is carried out on terraced areas containing soil transported from the higher parts of the Islands, where weathering conditions allow for well-developed soils. Terraces are built by distributing a 70-90 cm thick layer of soil upon a drainage layer of fractured basaltic rock. The resulting soil profiles are relatively homogeneous.

To reduce the effect of preferential flow along the walls during the outflow experiments, large cylinders with big diameters are recommended (Schneider and Howell, 1991). A device was developed to extract large undisturbed soil columns in stainless steel cylinders ( $\varnothing 45$  cm x 85 cm x 0.4 cm thickness), based on an oil hydraulic press, which applied up to 66 kN pressure on a steel plate. The insertion plate was supported by a metallic structure that was anchored to the soil. The monolith was then brought to the laboratory, where it was instrumented with 21 TDR probes (3 waveguides  $\varnothing 0.3 \times 20$  cm and 2.5 cm separation) and seven digital tensiometers (tensiometric tube with porous ceramic and a pressure transducer) (Figure 1), inserted at seven observation depths (denoted as A, B, C, D, E, F and G). At each depth, three TDR probes were inserted at  $120^\circ$  from each other. A collector, equipped with a pressure transducer, was used to measure the volume of water coming out from the base of the monolith during each experiment (bottom flux). All devices were multiplexed and connected to a PC. Monitoring the hydraulic variables was possible using a custom-made software (developed at S.I.D.TA-Valladolid, Spain).

A small rainfall-simulator was constructed to apply water uniformly at the top of the column using a 550 x 550 x 32 mm plexi-glass box equipped with 310 hypodermic needles ( $\varnothing 0.3$  mm spaced 25 mm apart). Water was pumped to the rainfall-simulator from a main container. On the bottom of the monolith, a constant-head boundary condition was imposed by using a 5 cm saturated sand bed (73  $\mu\text{m}$ ), connected to a constant-level reservoir through a water-hose (Figure 1).

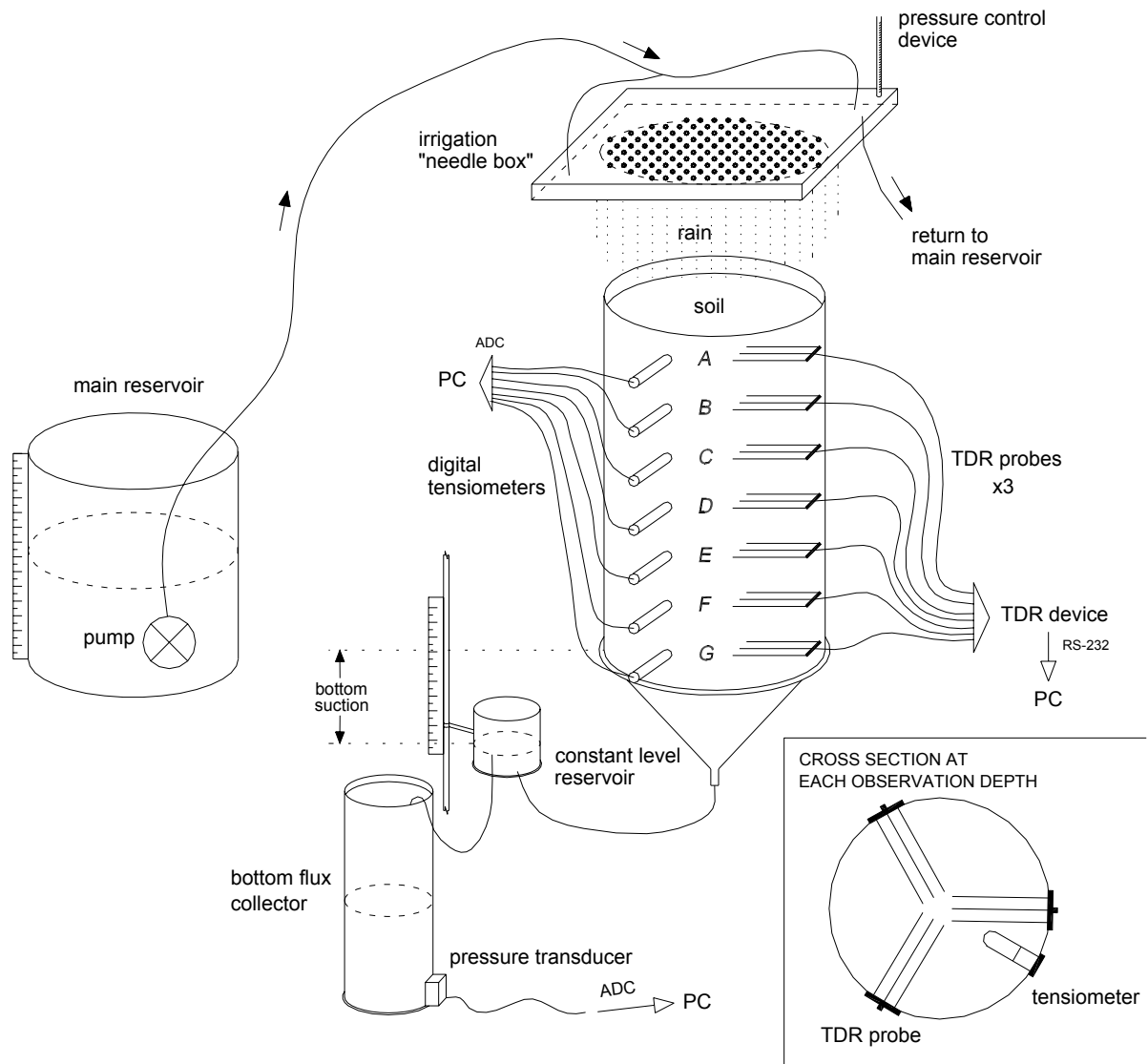


Figure 1. Experimental set-up for outflow experiments in the volcanic soil monolith.

#### 2.4. Outflow experiments

The laboratory experimental set-up allowed performing outflow experiments on an undisturbed soil column with controlled boundary conditions while monitoring different hydraulic variables. The top boundary condition consisted of irrigation applied homogeneously with the rainfall-simulator at the surface of the soil. To avoid soil dispersion, a 0.005 M  $\text{CaSO}_4$  (Klute and Dirksen, 1986) solution was used. To simplify we will refer to the latter as water. The bottom boundary was set at 10 cm, suction close to the average field values expected at that depth (Muñoz-Carpena, 1999).

Throughout each outflow experiment, matric pressure head, soil water content and bottom flux were recorded at 15 minutes increments and then averaged at 1 hour intervals. Averaging

in time was possible, because it did not imply strong curve smoothing. However, for some soils subjected to particular boundary conditions, this may not be the case. The sensor measurement error for the three variables was estimated from their calibration in less than  $\pm 1\%$ .

The soil water content was estimated using a specific TDR-calibration for the same soil used in this study (Regalado et al., 2002). Soil water content at each time and depth was obtained by averaging the values measured with the three TDR probes at each of the seven depths.

A first outflow experiment was performed to obtain information about the water retention in the soil profile. Starting from near saturation conditions, the monolith was continuously irrigated at different flow rates. The flux was reduced in four steps (5 mm/h during 94 hours; 2,7 mm/h during 32 hours; 1 mm/h during 41 hours, and 0.2 mm/h during 72 hours). Afterwards, irrigation was stopped and measurements continued until the soil profile reached hydraulic equilibrium (271 hours). By using distinct flow rates it was possible to monitor the hydraulic variables at different moisture conditions. Plotting soil water content versus matric pressure head data provided information about the water retention curve at the observation depths. Furthermore, these data, fitted to van Genuchten's curve with the RETC code (van Genuchten et al., 1991), provided an initial guess of the hydraulic parameters in the optimization process.

A second multi-step outflow experiment was carried out to obtain data for the inverse optimization of the hydraulic parameters. Four equal 5-liter irrigations were applied at a rate of approximately 5.25 mm/h. Each one took around 6 hours, while the time between irrigations was 18, 65 and 18 hours.

Data corresponding to the first two irrigations of the second outflow experiment were used for calibration, while the rest of the data set served for validation.

### **3. Results and discussion**

Water retention data at each soil depth obtained from the first outflow experiment was helpful to select the parameters to be optimized by inverse modeling with the second experiment. The first experiment suggested heterogeneities in the soil profile, where four

horizons (H1–H4) with different water retention can be identified (Figure 2). Table 1 shows van Genuchten parameters for those horizons.

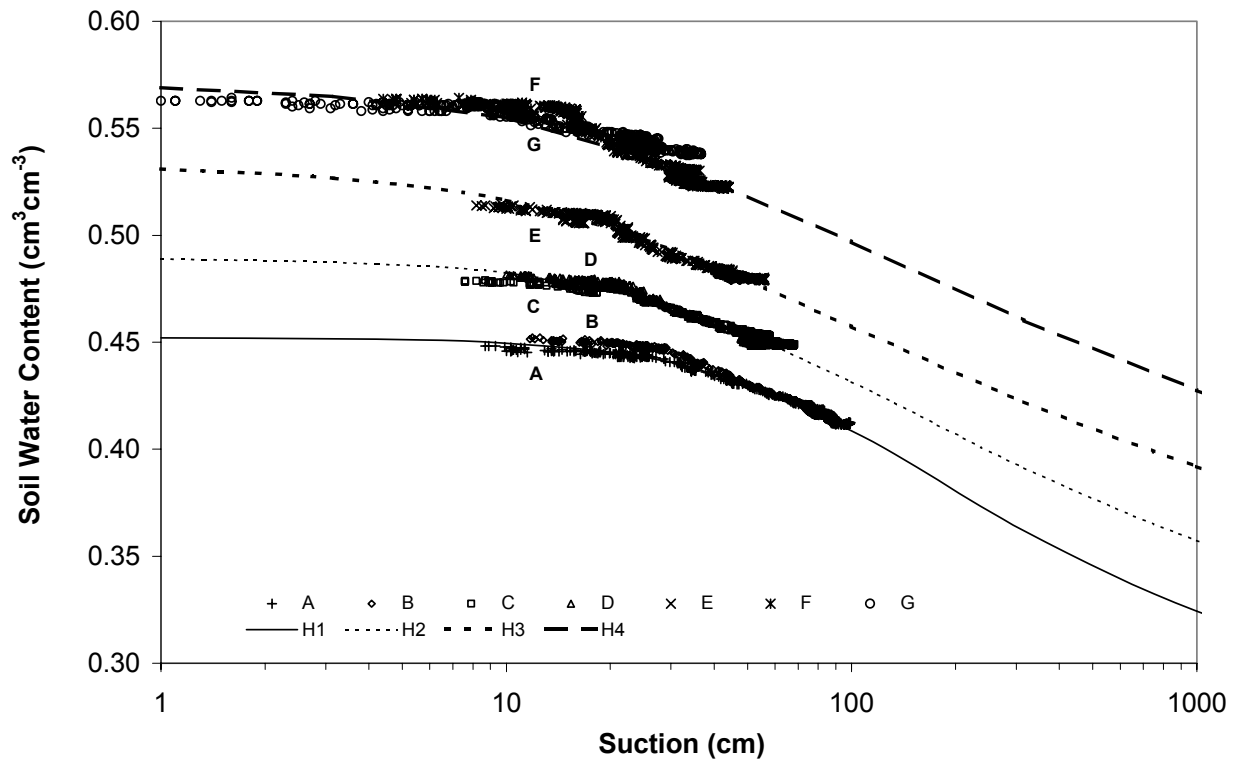


Figure 2. Soil moisture retention curves observed in the monolith. Measured data (symbols) and fitted van Genuchten curves (lines).

Table 1  
Initial values of van Genuchten soil moisture curve parameters based on first outflow experiment (Figure 2)

Horizon	Observation depths	Depth (cm)	$\theta_s$ ( $cm^3/cm^3$ )	$\theta_r$ ( $cm^3/cm^3$ )	$\alpha$ ( $cm^{-1}$ )	$n$	$R^2$
H1	A,B	0-25.5	0.452	0.268	0.0120	1.473	0.9856
H2	C,D	25.5-45.0	0.489	0.268	0.0223	1.290	0.9631
H3	E	45.0-54.0	0.531	0.268	0.0489	1.193	0.9714
H4	F,G	54.0-72.0	0.569	0.268	0.0454	1.166	0.7667

The soil comes from a terraced banana field, where it has sustained continuous cultivation for the last 20 years. Changes in the water holding capacity can be attributed to organic matter incorporation to the soil (Vereecken et al., 1989), soil degradation due to saline water irrigation (Armas-Espinel et al., 2002), and surface compaction processes, which affect porosity (Dorel et al., 2000).

A small experimental range of soil water content and matric pressure head was obtained and used for the inverse method. Although small, these ranges match those observed in the drip-irrigated banana plantation in this soil during normal conditions (Muñoz-Carpena,

1999). Therefore, under this high frequency irrigation technique, hydraulic properties near saturation are most important (Durner et al., 1999).

Inverse optimization of all van Genuchten's parameters with the suggested algorithms is impractical when working with four distinct horizons, since the number of parameters that describe the hydraulic functions increased four-fold up to 24 parameters (i.e.  $\theta_s$ ,  $\theta_r$ ,  $\alpha$ ,  $n$ ,  $K_s$  and  $\lambda$  for each of the four horizons). To reduce the number of parameters to be optimized,  $\lambda=0.5$  was assumed (Mualem, 1976). The large variability associated with  $K_s$  (Warrick and Nielsen, 1980) suggests its estimation by inverse modeling. In addition to  $K_s$ , the other parameters to optimize by the inverse procedure were based on a sensitivity analysis. Thereby, the sensitivity of the three model outputs (water content, matric pressure head and bottom flux) to the parameters of Table 1 was evaluated by calculating relative sensitivity coefficients according to Yeh (1986) and Haan et al. (1982). In addition, time-averaged coefficients were obtained following Inoue et al. (1998). Results showed that soil water content was mainly sensitive to the four saturated water contents, while matric pressure head was more sensitive to the four  $n$  shape parameters. The bottom flux was also sensitive to these parameters. Finally, we averaged the sensitivity coefficients among the three state variables (Figure 3). From Figure 3 we chose  $\theta_{s1}$ ,  $\theta_{s2}$ ,  $n_3$ , and  $n_4$  for optimization. Thus, a total of 8 parameters were selected. Intervals delimiting the parameter search space for GMCS were set at [0.40–0.65] for  $\theta_s$  ( $\text{cm}^3\text{cm}^{-3}$ ) (according to Figure 2); [1.05–1.60] for  $n$  (according to the range that corresponds to USDA soil fine textures reported by Carsel and Parrish, 1988); and [1.0–40.0] for  $K_s$  (cm/h) (according to field measurements reported in Muñoz-Carpena, 1999). The other fixed hydraulic parameters needed in the model were set to the values of Table 1. For the same experimental plot,  $\theta_r$  values at several depths were reported by Muñoz-Carpena et al. (1999) and at 15 cm by Armas-Espinel et al. (2002); the values at 15, 30 and 60 cm ranged between 0.219 and 0.330, showing no significant differences (at level 0.05), thus  $\theta_r$  was fixed to the average value (0.268).

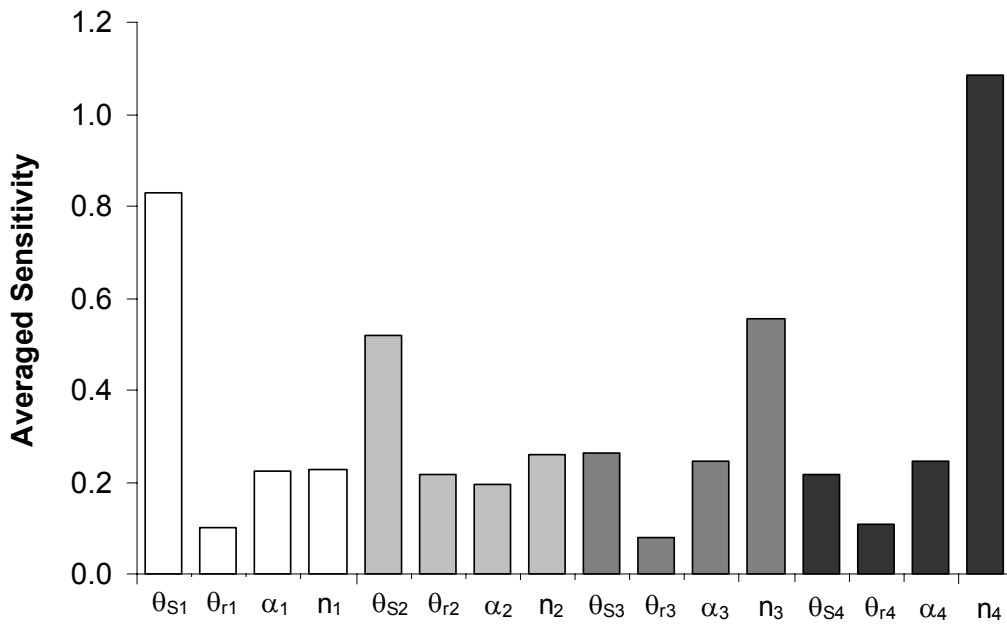


Figure 3. Averaged sensitivity for the van Genuchten parameters of Table 2.

Figure 4 presents the uncertainty ( $CI_{95}$ ) associated with the estimated parameters when considering strategies based on all the seven observation depths available,  $(var)_7$ . In general, combinations of two or three hydraulic variables, i.e.  $(h\theta)_7$ ,  $(hq)_7$ ,  $(\theta q)_7$  and  $(h\theta q)_7$ , improved the identifiability (i.e. short lengths and overlapping of  $CI_{95}$ ) of  $\theta_{s1}$ ,  $\theta_{s2}$ ,  $n_3$  and  $n_4$ . In the case of  $K_s$ , identifiability was not so good, particularly for  $K_{s3}$  and  $K_{s4}$ . Uncertainty of  $K_s$  estimations by inverse modeling was also reported by Durner et al. (1999) and Zurmühl and Durner (1998). They explained it based on the low sensitivity of the hydraulic conductivity function near saturation for any outflow/inflow experiment. The best strategy,  $(h\theta q)_7$ , yielded  $\theta_{s1}=46.6\pm0.2\%$ ,  $\theta_{s2}=49.4\pm0.3\%$ ,  $n_3=1.273\pm0.013$ ,  $n_4=1.156\pm0.010$ ,  $K_{s1}= 3.33\pm0.63$  cm/h,  $K_{s2}= 12.00\pm2.76$  cm/h,  $K_{s3}= 23.76\pm5.66$  cm/h and  $K_{s4}= 16.17\pm1.21$  cm/h.

Moreover, the correlation matrix for each strategy (not shown) showed high ( $>0.5$ ) negative correlation between some parameters for  $(h)_7$ ,  $(\theta)_7$ ,  $(hq)_7$ ,  $(q)_7$  and  $(\theta q)_7$ .

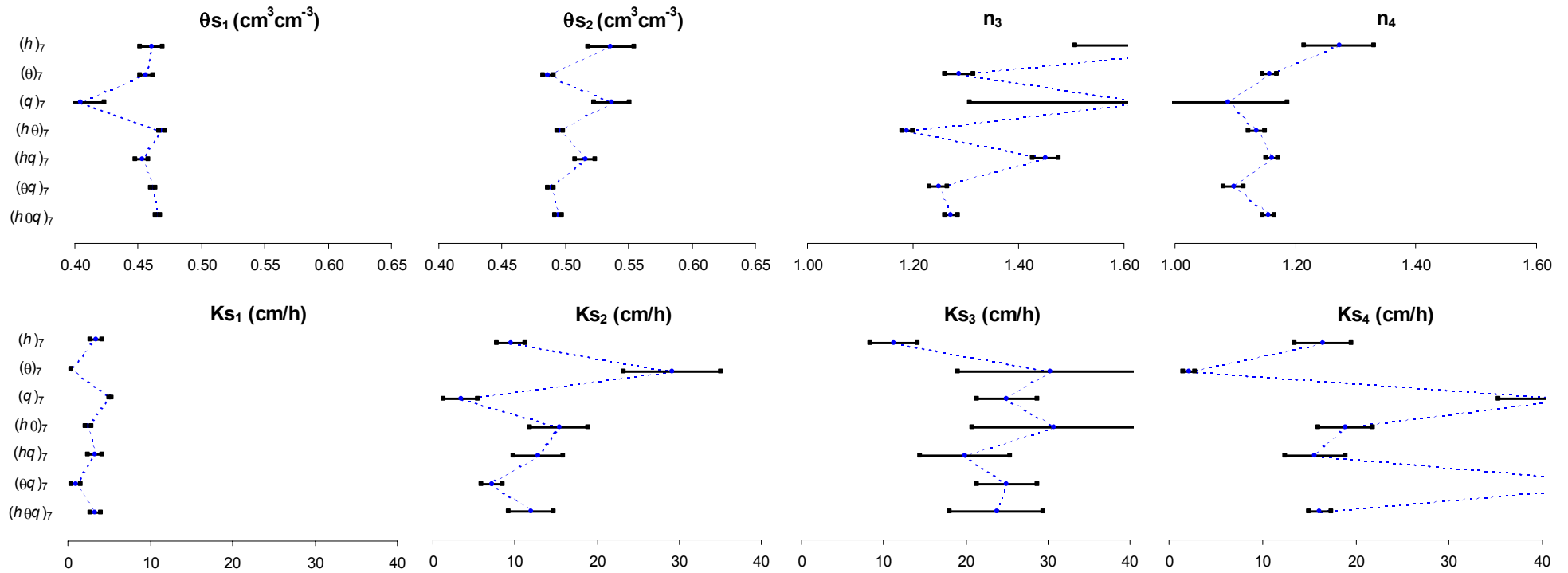


Figure 4. Uncertainty interval overlapping for the different estimated parameters, according to the distinct strategies based on 7 observation depths. Solid lines with symbols represent  $CI_{95}$ 's, while the dotted lines connect mean values.

Calculated *FEI* values (Figure 5) show strategies  $(h\theta q)_7$ ,  $(\theta q)_7$ , and  $(h\theta)_7$  to be the best (highest index, respectively). As expected, including all information available in the objective function, i.e.  $(h\theta q)_7$ , leads to best results. From these results we concluded, the adequacy of using soil water content data combined with other hydraulic variables (e.g. matric pressure head or bottom flux).

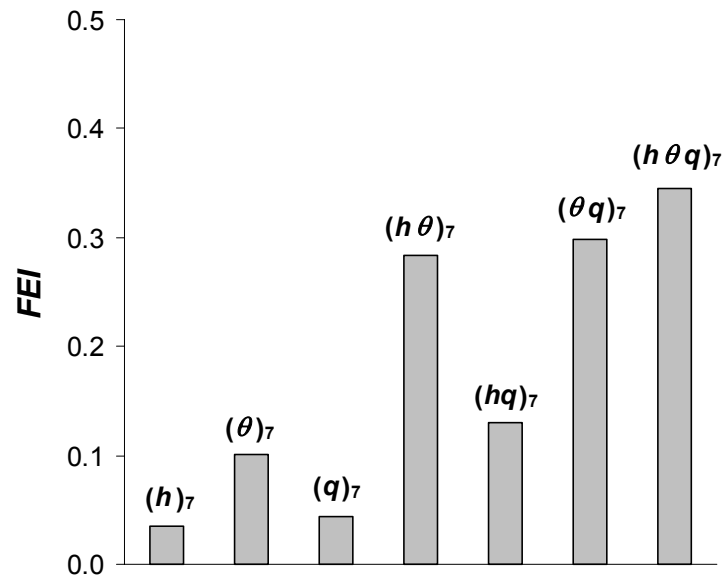


Figure 5. Comparison of strategies  $(var)_7$  based on the proposed *FEI*.

The evaluation of the strategies was also complemented by visual inspection of simulated versus observed data. From the seven strategies only the three above-mentioned show a satisfactory fit. As an example, Figures 6–8 show model performance using  $(h\theta)_7$  for soil water content and matric pressure head at the seven monitoring depths, and for bottom flux as well. From these figures, we concluded that model predictions were generally satisfactory. In addition, agreement between observed and predicted data for the three hydraulic variables is presented in Figure 9.

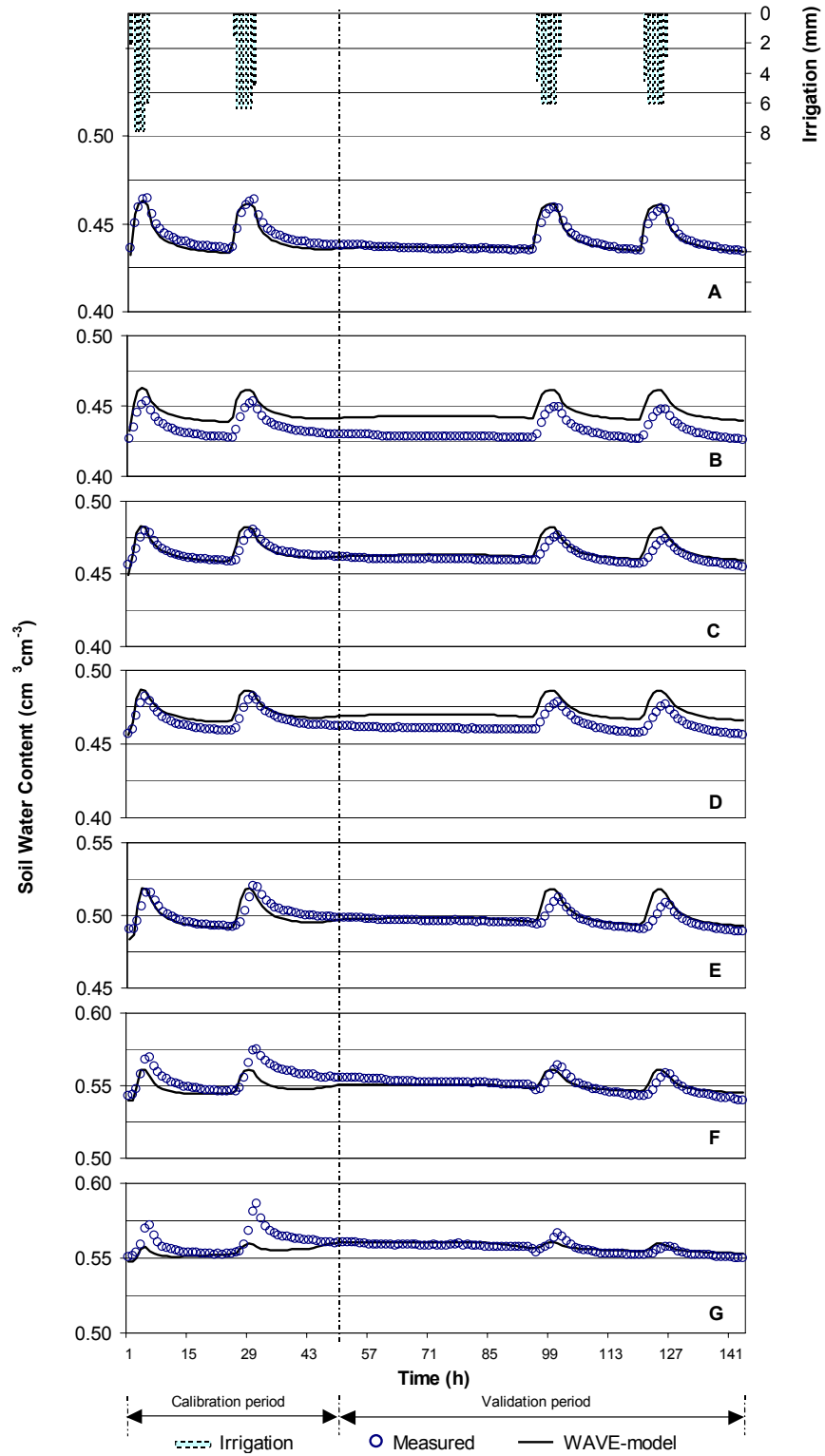


Figure 6. WAVE model fit to soil water content data corresponding to  $(h\theta q)_7$ .

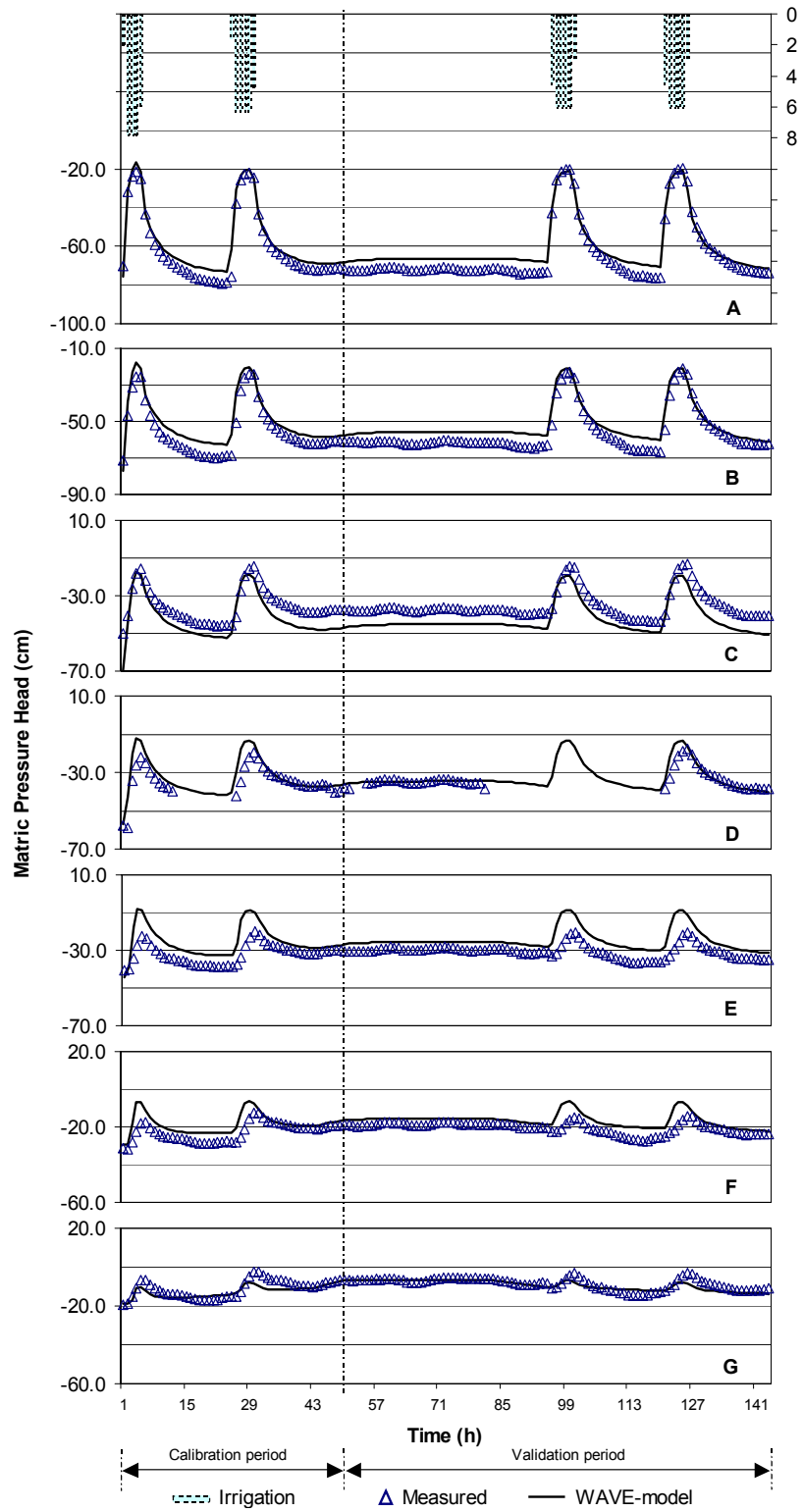


Figure 7. WAVE model fit to matric pressure head data corresponding to  $(h\theta)_7$ .

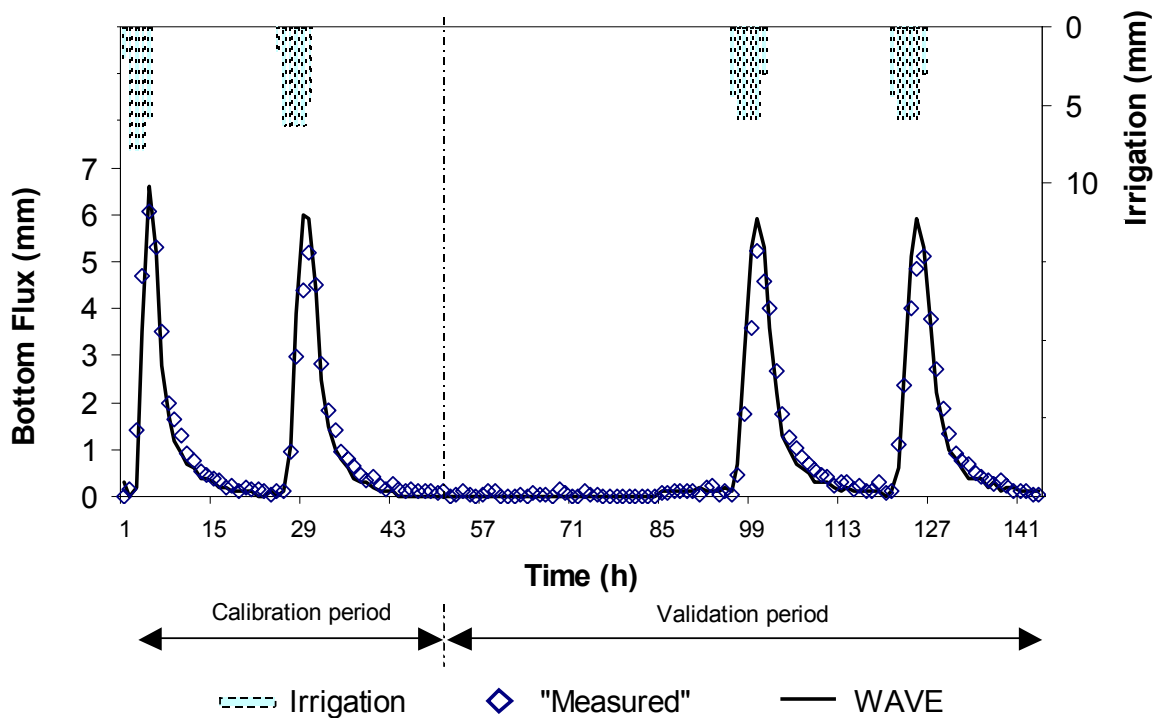


Figure 8. WAVE model fit to bottom flux data corresponding to  $(h\theta q)_7$ .

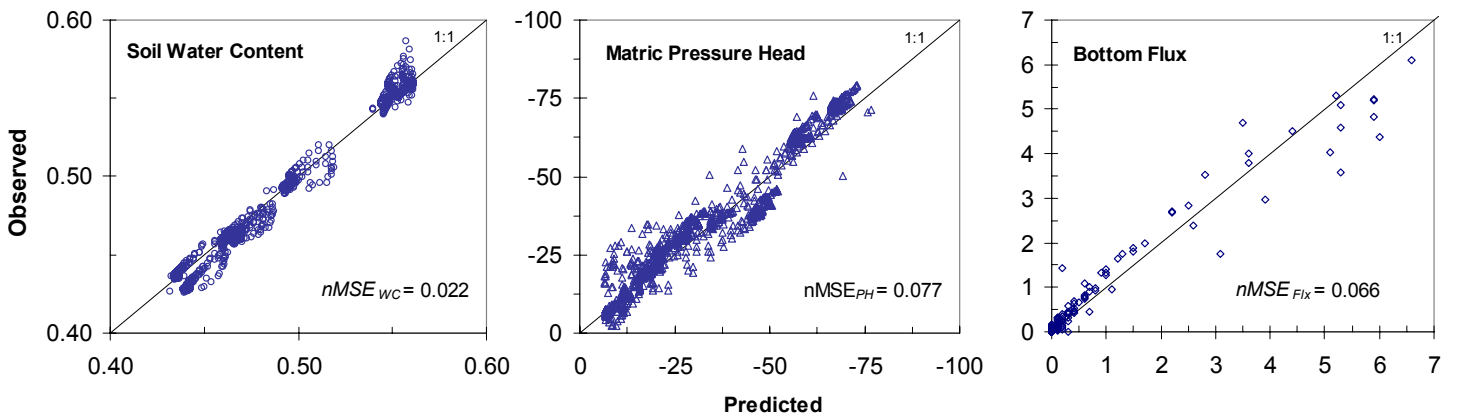


Figure 9. Goodness of fit between observed and simulated values with  $(h\theta q)_7$ .

Keeping in mind that we are interested in finding a suitable strategy (i.e. best results with lower costs), we tested if those strategies were statistically different. No significant differences (at level 0.05) were found between the  $nMSE$ 's corresponding to  $(h\theta)_7$ ,  $(\theta q)_7$  and  $(h\theta q)_7$ .

Based on our previous results, we used the best alternatives  $[(h\theta)_L, (\theta q)_L$  and  $(h\theta q)_L]$  to test if reducing the number of measurement points (depths) would lead to acceptable results. First, we chose four observation depths (one per horizon) trying two different combinations of them:  $(var)_4'$  {ACEG} and  $(var)_4''$  {BDEF}. Second, combinations of three depths were considered:  $(var)_3'$  {ADG},  $(var)_3''$  {AEG} and  $(var)_3'''$  {BCF}.

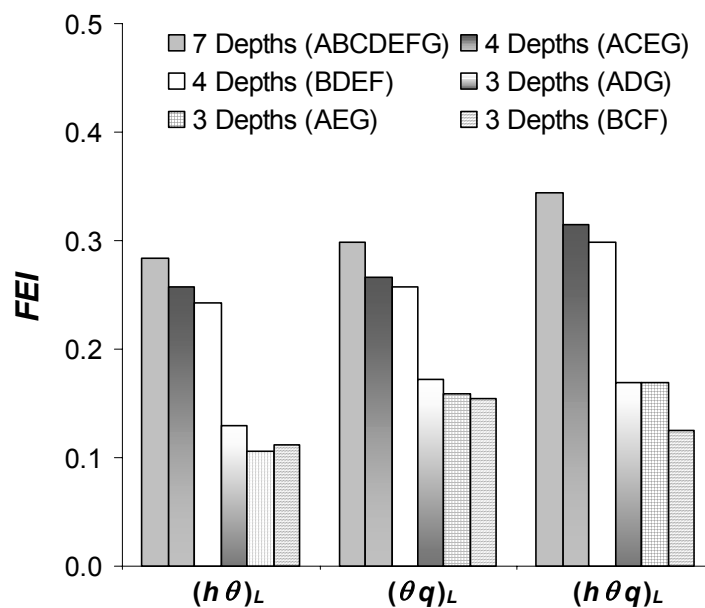


Figure 10. Comparison of strategies  $(h\theta)_L$ ,  $(\theta q)_L$  and  $(h\theta q)_L$  based on the proposed FEI.

Parameter uncertainty (not shown) associated with  $\theta_{s1}$ ,  $\theta_{s2}$ ,  $n_3$  and  $n_4$  was similar to that found using all depths,  $(var)_7$ . However, it increased for  $K_s$ , specially when using three depths,  $(var)_3$ . On the other hand, by reducing the number of observation depths, high correlation between some parameters arises, particularly with the  $K_s$ . Finally the  $FEI$  values (Figure 10) for the six combinations and the three alternatives were considered. First,  $(var)_3$  implied an important reduction of efficiency. Therefore, strategies with less observation depths are supposed to yield also reduced efficiency. Second, when using four observation depths,  $(var)_4'$  and  $(var)_4''$ , a decrease in the calculated  $FEI$  was observed, too. However, no significant differences (at level 0,05) were found between  $(var)_7$  and  $(var)_4$ . The estimated parameters obtained with each strategy are presented in Table 2.

Table 2  
Estimated soil hydraulic parameters and  $CI_{95}$  for all strategies

Strategy	$\theta_{s1}$	$\theta_{s2}$	$n_3$	$n_4$	$K_{S1}$	$K_{S2}$	$K_{S3}$	$K_{S4}$
ABCDEFG								
$(h)_7$	0.461±0.009	0.536±0.018	1.839±0.331	1.273±0.058	3.44±0.76	9.52±1.73	11.22±2.90	16.49±3.06
$(\theta)_7$	0.456±0.005	0.486±0.004	1.287±0.027	1.158±0.012	0.44±0.03	29.19±5.89	30.34±11.24	2.18±0.60
$(q)_7$	0.405±0.019	0.536±0.014	1.641±0.333	1.088±0.100	5.20±0.19	3.43±2.09	25.00±3.68	43.11±7.76
$(h\theta)_7$	0.469±0.002	0.496±0.002	1.190±0.010	1.136±0.013	2.50±0.40	15.40±3.55	30.81±10.04	18.92±2.95
$(hq)_7$	0.453±0.005	0.516±0.028	1.452±0.025	1.161±0.010	3.33±0.89	12.92±3.03	19.96±5.49	15.65±3.22
$(\theta q)_7$	0.462±0.002	0.489±0.002	1.249±0.016	1.097±0.017	1.02±0.53	7.23±1.29	25.04±3.67	49.98±5.77
$(h\theta q)_7$	0.466±0.002	0.494±0.003	1.273±0.013	1.156±0.010	3.33±0.63	12.00±2.76	23.76±5.66	16.17±1.21
ACEG								
$(h\theta)_4'$	0.471±0.003	0.494±0.003	1.185±0.016	1.111±0.012	4.30±0.59	6.45±1.17	27.17±5.29	23.61±3.87
$(\theta q)_4'$	0.466±0.002	0.492±0.003	1.211±0.012	1.122±0.010	1.96±1.32	12.17±8.18	22.08±1.11	27.95±1.44
$(h\theta q)_4'$	0.468±0.003	0.494±0.003	1.210±0.013	1.139±0.011	3.55±0.23	9.78±2.46	25.23±6.38	22.23±1.19
BDEF								
$(h\theta)_4''$	0.467±0.003	0.497±0.003	1.163±0.017	1.103±0.013	1.41±0.27	11.96±1.80	27.05±4.67	22.49±1.59
$(\theta q)_4''$	0.455±0.002	0.491±0.002	1.223±0.012	1.109±0.011	1.01±0.22	2.55±1.04	18.70±3.96	25.45±3.26
$(h\theta q)_4''$	0.467±0.003	0.497±0.004	1.223±0.015	1.160±0.012	1.02±0.33	10.82±3.22	25.37±1.08	27.34±2.82
ADG								
$(h\theta)_3'$	0.474±0.002	0.492±0.002	1.483±0.034	1.124±0.013	5.52±3.45	16.93±4.68	39.95±11.93	12.01±6.82
$(\theta q)_3'$	0.469±0.002	0.480±0.002	1.673±0.045	1.094±0.035	1.90±0.82	19.23±8.31	22.94±1.26	36.30±10.33
$(h\theta q)_3'$	0.471±0.002	0.492±0.002	1.405±0.027	1.094±0.035	2.55±0.86	22.47±7.84	25.11±4.59	35.59±9.34
AEG								
$(h\theta)_3''$	0.472±0.002	0.501±0.011	1.177±0.015	1.135±0.018	2.45±1.45	6.93±4.02	40.81±13.17	16.02±6.35
$(\theta q)_3''$	0.469±0.003	0.475±0.014	1.204±0.013	1.101±0.013	1.00±0.32	8.87±5.20	22.93±1.59	34.64±7.81
$(h\theta q)_3''$	0.471±0.003	0.500±0.011	1.215±0.012	1.117±0.010	2.21±1.08	9.37±6.84	25.13±2.12	43.76±15.63
BCF								
$(h\theta)_3'''$	0.463±0.004	0.497±0.004	1.576±0.027	1.099±0.018	3.59±1.40	25.54±7.59	11.93±6.36	43.83±9.87
$(\theta q)_3'''$	0.459±0.002	0.498±0.002	1.664±0.038	1.078±0.014	2.60±1.19	11.32±5.15	28.95±6.35	40.56±16.42
$(h\theta q)_3'''$	0.461±0.003	0.501±0.004	1.535±0.031	1.134±0.011	3.73±1.40	25.78±9.61	8.39±8.22	18.31±6.35

Based on all this, measuring at only four depths (one per horizon) would be sufficient if soil water content data and either matric pressure head or bottom flux are used. From a practical point of view (lower cost, simplicity), using soil water content and suction readings at only four depths, i.e.  $(h\theta)_4$ , is desirable. In this context, despite the higher cost of using suction readings (digital tensiometers) when compared to monitoring bottom flux, they have the added benefit of providing information about the soil water retention curve. In addition, bottom flux measurements are in most cases impractical in a field situation, so  $h$  and  $\theta$  (tensiometers and TDR) would be preferred.

#### 4. Conclusions

The suitability of alternative soil water flow monitoring strategies for the inverse estimation of the soil hydraulic parameters of a volcanic soil is analyzed. Inverse modeling is performed by coupling the GMCS-NMS algorithm to the flow module of the WAVE model. Use is made of experimental data collected during two outflow experiments conducted in a large undisturbed soil column. The results from the first experiment show the existence of four well-defined soil horizons with different water retention curves. Using these results and a sensitivity analysis, the hydraulic parameters selected for inverse modeling are reduced to 8 (saturated water content,  $\theta_s$ , in the first two horizons, curve shape parameter,  $n$ , in the two others horizons, and saturated hydraulic conductivity,  $K_s$  of each horizon). Inverse optimization of these properties is successful using different monitoring strategies. The alternative strategies are based on the consideration of different hydraulic state variables and observation depths for the formulation of the objective function. Furthermore, by defining an integrated index to account for different evaluation criteria, the best strategies are easily identified. We may conclude that strategies based on the measurement of a combination of the hydraulic state variables reduce the uncertainty associated with  $\theta_s$  and  $n$ . However, in general, estimated  $K_s$  show uncertainty that might be large in some cases due to the low sensitivity of the hydraulic conductivity function near saturation.

Although inverse modeling using simultaneously soil water content ( $\theta$ ), matric pressure head ( $h$ ), and bottom flux ( $q$ ) data give the best results, monitoring of  $\theta$  in combination with either  $h$  or  $q$  proofs to be sufficient, even if only four observation depths are considered. It must be noticed that, despite the higher cost of using suction readings (digital tensiometers) when compared to the monitoring of the bottom flux, they have the added benefit of providing direct information about the soil water retention curve. Thereby, if low cost bottom flux measurements are chosen, additional methods or surveys (e.g. profile description) might be needed to obtain prior information for the inverse procedure.

Using synthetic data, based on estimated reference parameters, the procedure presented here can serve as a general method for assessing, at the experimental design stage, appropriate strategies to estimate the soil hydraulic parameters by inverse modeling. Since decisions about the type and number of observations required for inverse optimization are usually based on intuition, the procedure applied in this study represents an objective way to base such decisions on quantitative information.

### *Acknowledgments*

Authors want to thank J. Álvarez-Benedí (S.I.D.T.A., Valladolid) for developing the data acquisition software used, and Martin Morawietz (University Friburg) during the preparation of the experimental set-up. This work was financed with funds of the INIA-Plan Nacional de I+D Agrario (Proyecto I+D SC99-024-C2) and Consejería de Educación Cultura y Deportes del Gobierno de Canarias. This research was supported by the Florida Agricultural Experiment Station, and approved for publication as Journal Series No. R-\_\_.

### **5. References**

- Abbaspour, K.C., Sonnleitner, M.A., Schulin, R., 1999. Uncertainty in estimation of soil hydraulic parameters by inverse modeling: example lysimeter experiments. *Soil Sci. Soc. Am. J.* 63: 501-509.
- Armas-Espinel, S., Hernández-Moreno, J.M., Muñoz-Carpena, R., Regalado, C.M., 2002. Physical properties of “sorriba” cultivated volcanic soils from Tenerife in relation to diagnostic Andic parameters. *Geoderma (in press)*.
- Beven, K.J., 1996. Equifinality and uncertainty in geomorphological modelling. In B. L. R. a. C. E. Thorn, editor. 27 th Binghamton Symposium in Geomorphology. John Wiley & Sons Ltd.
- Carrera, J., Neuman, S.P., 1986. Estimation of aquifer parameters under transient and steady state conditions. 2. Uniqueness, stability and solution algorithms. *Water Resour. Res.* 22: 211-227.
- Carsel, R.F., Parrish, R.S., 1988. Developing joint probability distributions of soil water retention characteristics. *Water Res. Resear.* 24(5): 775-769.
- Celia, M.A., Bouloutas, E.T., Zarba, R.L., 1990. A general mass-conservative numerical solution for the unsaturated flow equation. *Water Resour. Res.* 26: 1483-1496.
- Dane, J.H., Hruska, S., 1983. In-situ determination of soil hydraulic properties during drainage. *Soil Sci. Soc. Am. J.* 47: 619-624.
- Dorel, M., Roger-Estrate, J., Manichon, H., Devaux, B., 2000. Porosity and soil water properties of Caribbean volcanic ash soils. *Soil Use & Management*, 16: 133-145.
- Durner, W., Schultze, B., Zurmühl, T., 1999. State-of-the-Art in inverse modeling of inflow/outflow experiments. In M. Th. van Genuchten, F.J. Leij and L. Wu (eds) *Proc. Int.*

- Workshop, Characterization and Measurement of the Hydraulic Properties of Unsaturated Porous Media: 713-724. University of California, Riverside, C.A.
- Eching, S.O., Hopmans, J.W., 1993. Optimization of hydraulic functions from transient outflow and soil water pressure data. *Soil Sci. Soc. Am. J.* 57: 1167-1175.
- Haan, C.T., Johnson, H.P., Brakensiek, D.L., 1982. *Hydrologic Modeling of Small Watersheds*. ASAE Monograph 5. St. Joseph: ASAE.
- Hopmans, J.W., Simunek, J., 1999. Review of inverse estimation of soil hydraulic properties. In M. Th. van Genuchten, F.J. Leij and L. Wu (eds) *Proc. Int. Workshop, Characterization and Measurement of the Hydraulic Properties of Unsaturated Porous Media: 713-724*. University of California, Riverside, C.A.
- Huyer, W., Neumaier, A., 1999. Global optimization by multilevel coordinate search. *J. Global Optimization* 14: 331-355.
- Inoue, M., Simunek, J., Hopmans, J.W., Clausnitzer, V., 1998. In situ estimation of soil hydraulic functions using a multistep soil-water extraction technique. *Water Resour. Res.* 34(5): 1035-1050.
- Klute, A., Dirksen, C., 1986. Hydraulic conductivity and diffusivity: Laboratory Methods. In: A. Klute (ed.) *Methods of Soil Analysis Part 1*. Agronomy no. 9 ASA-SSSA: Madison.
- Kool, J.B., Parker, J.C., van Genuchten, M.Th., 1985. Determining soil hydraulic properties from one-step outflow experiments by parameter identification: I. Theory and numerical studies. *Soil Sci. Soc. Am. J.* 49: 1348-1354.
- Kool, J.B., Parker, J.C., M.Th. van Genuchten, 1987. Parameter estimation for unsaturated flow and transport models – A review. *J. Hydrol.* 91: 255-293.
- Kool, J. B., Parker, J.C., 1988. Analysis of the inverse problem for transient unsaturated flow, *Water Resour. Res.* 24: 817-830.
- Lambot, S., Javaux, M., Hupet, F., Vanclooster, M., 2002. A Global Multilevel Coordinate Search procedure for estimating the unsaturated soil hydraulic properties. *Water Resour. Res.* (*in press*).
- Limpert, E., Stahel, W.A., Abbt M., 2001. Log-normal distributions across the sciences: keys and clues. *Bioscience* 51(5): 341-352.
- Muñoz-Carpena, R., 1999. Estudio de la Integración a Diferentes Escalas del Transporte de Aguas y Solutos en Suelos –IDEASS. Annual Project Report: SC99-024-C2-1 (In Spanish). INIA, Madrid.

- Mualem, Y., 1976. A new model for predicting the hydraulic conductivity of unsaturated porous media. *Water Resour. Res.* 12: 513-522.
- Nelder, J. A., Mead, R., 1965. A Simplex Method for Function Minimization. *Computer Journal* 7: 308-313.
- Regalado, C. M., Muñoz-Carpena, R., Socorro, A. R., Hernández-Moreno, J.M., 2002. Time domain reflectometry models as a tool to understand the dielectric response of volcanic soils, *Geoderma (in press)*.
- Ritter, A., Hupet, F., Muñoz-Carpena, R., Lambot, S., Vanclooster, M., 2002. Using inverse methods for estimating soil hydraulic properties from field data as an alternative to direct methods. *Agric. Water Manage. (in press)*.
- Russo, D., Bresler, E., Shani, U., Parker, J.C., 1991. Analyses of infiltration events in relation to determining soil hydraulic properties by inverse problem methodology. *Water Resour. Res.* 27(6): 1361-1373.
- Schneider, A.D., Howell, T.A., 1991. Large, monolithic, weighing lysimeters. En: R.G. Allen et al. (eds). *Lysimeters for evapotranspiration and environmental measurements. Proceedings of the International Symposium on Lysimetry.* ASCE: 37-45.
- Si, B.C., Kachanoski, R.G., 2000. Estimating soil hydraulic properties during constant flux infiltration: inverse procedures. *Soil Sci. Soc. Am. J.* 64: 439-449.
- Steel, R.G.D., Torrie, J.H., Dickey, D.A., 1997. *Principles and procedures of statistics: a biometrical approach.* McGraw-Hill. New York, pp. 666.
- van Genuchten, M.Th., 1980. A closed-form equation for predicting the hydraulic conductivity of soil. *Soil Sci. Soc. Am. J.* 44: 892-898.
- van Genuchten, M.Th., Leij, F.J., Yates, S.R., 1991. The RETC code for quantifying the hydraulic functions of unsaturated soils. U.S. Salinity Laboratory, CA, pp. 85.
- Vanclooster, M., Viaene, P., Christiaens, K., Ducheyne, S., 1996. WAVE : a mathematical model for simulating water and agrochemicals in the soil and vadose environment, Reference and user's manual (release 2.1), Institute for Land and Water Management, Katholieke Universiteit Leuven, Leuven, Belgium.
- Vanderborght J., Kasteel, R., Ciocanaru, M., Herbst, M., Vereecken, H., Javaux, M., Vanclooster, M., 2002. Analytical solutions of non-linear flow and transport equations to test numerical models for simulating flow and transport in unsaturated soils. G. Marinoschi (Ed.), *Proceedings of the First Workshop on Mathematical Modelling of*

- Environmental Problems, Bucharest, Romania, June 2002. Publishing House of the Romanian Academy (Editura Academiei Romane).
- Vereecken, H., Maes, J., Feyen, J., Darius, P., 1989. Estimating the soil moisture retention characteristic from texture, bulk density and carbon content. *Soil Sci.* 148(6): 389-403.
- Vrugt, J.A., Bouten, W., Weerts, A.H., 2001. Information content of data for identifying soil hydraulic parameters from outflow experiments. *Soil Sci. Soc. Am. J.* 65: 19-27.
- Warrick, A.W., Nielsen, D.R., 1980. Spatial variability of soil physical properties in the field. In: *Applications of Soil Physics*. D. Hillel (ed.). Academic Press, New York, pp. 319-344.
- Wilson, B.N., 2001. Evaluation of hydrologic models using statistical methods. ASAE Paper 01-012207, Presented at 2001 ASAE Annual International Meeting, St. Joseph, MI.
- Yeh, W.W.-G., 1986. Review of parameter identification procedures in groundwater hydrology: The inverse problem. *Water Resour. Res.* 22: 95-108.
- Zou, Z.-Y., Young, M.H., Li, Z., Wierenga, P.J., 2001. Estimation of depth averaged unsaturated soil hydraulic properties from infiltration experiments. *J. Hydrol.* 242: 26-42.
- Zurmühl, T., Durner, W., 1998. Determination of parameters for bimodal hydraulic functions by inverse modeling. *Soil Sci. Soc. Am. J.* 62: 874-880.

## **Capítulo 4**

### **Characterization of solute transport properties in an agricultural volcanic soil using TDR and inverse modeling**

*Vadose Zone Journal* (enviado octubre, 2002)

## **Abstract**

Volcanic soils have particular properties, which might influence solute transport. The use of TDR to monitor bromide breakthrough curves during a miscible displacement experiment in a large column containing undisturbed volcanic soil is presented. The soil solute transport parameters were estimated by using inverse optimization techniques. In general, no differences were found between the CDE and MIM transport approaches. Under the high soil moisture regime considered, bromide was found to move in the undisturbed soil column mainly by convection. Dispersion and non-equilibrium transport were only observed at the bottom of the monolith. Early solute breakthrough suggests possible preferential flow effects. Thereby, the risk of groundwater contamination by agrochemicals applied in this soil is expected to increase in this type of soils.

*Keywords:* Canary Islands; Inverse modeling; Multilevel coordinate search; Parameter estimation; Volcanic soils; WAVE model.

## 1. Introduction

The intensive use of agrochemicals has led to groundwater contamination in many areas of the world. This is a continuing problem requiring the minimization of leaching losses from agricultural fields. In addition to potential pollution, these losses imply a reduction in the efficiency of the soil-applied chemicals. The transport of such substances in the soil depends however on many factors such as type of soil, irrigation, rainfall, tillage, chemical management practices, etc. (Lee et al., 2001). In that context, numerical leaching models considering those factors (once field tested) are useful tools to understand the movement of solutes in the soil and evaluate the potential contamination of agricultural practices on particular agro-scenarios. However, application of these models requires the estimation of many parameters, which cannot be measured directly in some cases (Jacques et al., 2002). Moreover, when considering layered soil profiles, the number of parameters to estimate increases.

Several approaches for description of the complex movement of solutes in the vadose zone have been proposed (Biggar and Nielsen, 1967; Coats and Smith, 1964; Jury, 1982; van Genuchten and Wierenga, 1976), and depending on the type of soil, the scale and the flow rate considered, some approaches are more suitable than others (Vanderborght et al., 2000).

Taking all this into consideration, methodologies for an efficient estimation of solute transport model parameters are demanded. An increasingly used procedure is inverse modeling, where parameters are identified based on the minimization of an objective function containing the differences between simulated and measured data (Hopmans and Simunek, 1999). For this purpose a global optimization algorithm needs to be coupled with the simulation model. Several classical optimization algorithms are available (Hopmans and Simunek, 1999), and new ones have been developed recently (Huyer and Neumaier, 1999). However, application of inverse simulation implies some difficulties that need to be overcome. These limitations are related to parameter identifiability, non-uniqueness of the solution and robustness of the algorithm.

While inverse optimization of soil hydraulic parameters is widespread, calibration of solute transport properties by this method is not so common. Indeed, inverse modeling requires a detailed (in time and/or space) and reliable data set (Jacques et al. 2002), however, obtaining detailed and reliable solute breakthrough curve data is often difficult (Risler et al.,

1996) because traditional techniques for solute concentration measurements are not suitable, soil coring is destructive, and solution extractors are usually inappropriate for obtaining high quality data (Roth et al., 1990).

Miscible displacement experiments are suitable for the calibration of solute leaching models, since they provide information about processes such as preferential flow, hydrodynamic dispersion, ion exchange and adsorption phenomena for solute transport under various flow rates and soil water content conditions (Ersahin et al., 2002). Usually, they involve the application of a tracer pulse in the soil surface, followed by measuring the solute flux and/or resident concentrations. For such experiments, time domain reflectometry (TDR) is becoming an increasingly used technique to measure soil water content and concentrations of conservative, saline solutes. It is a non-destructive and economic method (Kim et al., 1998; Vanclooster et al., 1993; 1995) and enables continuous readings at different depths in the soil of water content and solute concentrations (Vanclooster et al., 1995). The use of TDR for characterizing solute transport in the soil has been reported by many authors in both laboratory (Ersahin et al., 2002; Heimovaara et al., 1993; Kim et al., 1998; Lee et al., 2001; Mallants et al., 1994; Muñoz-Carpena et al., 2003; Persson, 1997; Risler et al., 1996; Vanclooster et al., 1993; 1995; Vanderborght et al., 2000; Vogeler et al., 1996) and field studies (Jacques et al., 1998; Kachanoski et al., 1992; Rudolph et al., 1996).

Volcanic soils are only present in 0.84% of the terrestrial surface. However, they are very important because they are amongst the most productive soils. In the Canary Islands these soils are crucial because 90% of the main crops (bananas and tomatoes) grow in them. These soils exhibit special properties due to the strong aggregation of particles, high concentration of Fe-oxihydroxides, and the presence of allophanic clays with large surface area and water affinity. The structure of these allophanic clays can be envisaged as hollow spherules so that the soil matrix is assumed to be divided into two regions: an intra-aggregate immobile region, where only diffusion controlled exchange of solutes between the inter-aggregate mobile region occurs. In this mobile phase, only convective-dispersive solute transport takes place. Evidence of the presence of mobile and immobile regions in the soil of this study were reported by Regalado et al. (2002) and Muñoz-Carpena et al. (2003).

In this paper we study the characteristics of solute transport in an agricultural volcanic soil from a miscible displacement experiment using a bromide (KBr) pulse. Solute volume-averaged resident concentrations were measured with TDR at different depths. Transport

properties were estimated by inverse modeling with the numerical model WAVE (Vanclooster et al., 1996) coupled with the global optimization algorithm, Multilevel Coordinate Search (Huyer and Neumaier, 1999). Two solute transport approaches were considered separately, the classical convection-dispersion equation (CDE) (Biggar and Nielsen, 1967) and the mobile-immobile model (MIM) (Coats and Smith, 1964; van Genuchten and Wierenga, 1976).

## 2. Materials and methods

### 2.1. Experimental set-up

The solute transport study was conducted on an undisturbed volcanic soil that was taken from a banana (*Musa accuminata* cv. ‘Giant Cavendish’) field in Tenerife (Canary Islands, Spain). The plantation was under a shadehouse and drip irrigated. The soil presents well-defined andic characteristics together with strong natural micro-aggregation that translate to large water retention, porosity and saturated hydraulic conductivity. In fact, the soil can be classified as an Andisol (USDA Soil Taxonomy) (Regalado et al., 2002). In a previous study, Ritter et al. (2003) reported in the same monolith four horizons with different water retention behavior and estimated the soil hydraulic properties of each horizon by inverse modeling (Table 1).

Table 1  
Hydraulic parameters for the undisturbed volcanic soil column

Horizon	Observation depths	Thickness (cm)	$\theta_s$ ( $cm^3/cm^3$ )	$\theta_r$ ( $cm^3/cm^3$ )	$\alpha$ ( $cm^{-1}$ )	$n$	$K_s$ (cm/h)
H1	A,B	0-25.5	0.466	0.268	0.0120	1.473	3.33
H2	C,D	25.5-45.0	0.494	0.268	0.0223	1.290	12.00
H3	E	45.0-54.0	0.531	0.268	0.0489	1.273	23.76
H4	F,G	54.0-72.0	0.569	0.268	0.0454	1.156	16.17

A custom-made device was used to insert a stainless steel cylinder ( $\varnothing 45$  cm x 85 cm x 0.4 cm thickness) into the soil to extract a column of undisturbed soil. Once inserted into the soil, the cylinder was isolated by excavating around it. During transportation, the top and the bottom of the soil column were covered with appropriate caps. Figure 1 presents a scheme of the laboratory experimental set-up. The soil monolith was equipped with 21 TDR probes (3 waveguides  $\varnothing 0.3 \times 20$  cm, and 2.5 cm separation) for measuring soil water content and solute concentration at seven depths (denoted as A, B, C, D, E, F and G). They were located at 10

cm apart on the vertical direction starting from the top. At each depth, 3 TDR probes were inserted at 120° from each other to increase the sampling region and ensure the detection of the solute plume and obtaining effective 1-D concentrations by averaging. All probes were multiplexed and connected to a TRASE TDR device (Soilmoisture, Inc.). At the same 7 depths, two solution extractors were inserted in the monolith. A suction of 60 cbar was applied to the 14 extractors to sample the soil solution at certain time intervals. Temperature was monitored with a thermistor inserted in the soil.

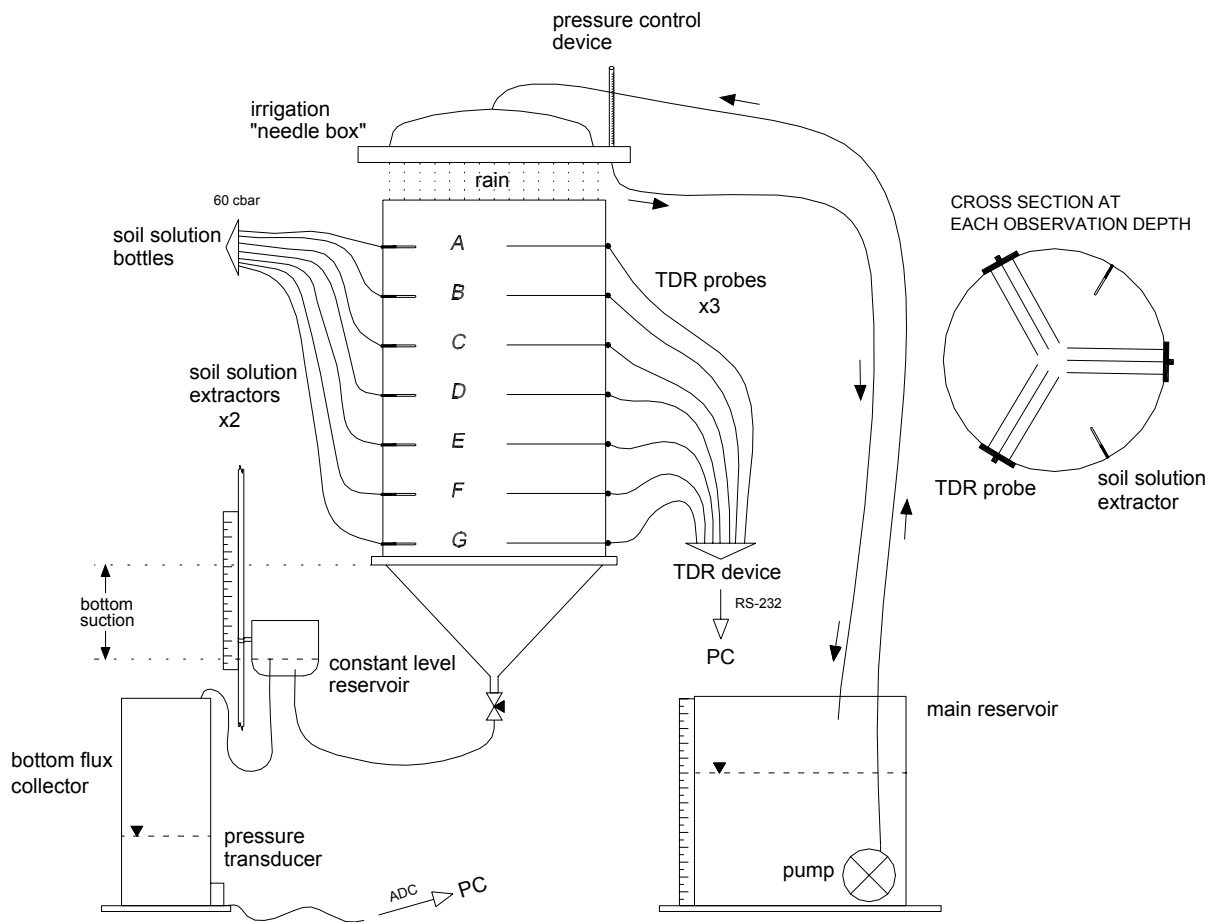


Figure 1. Experimental set-up for transport experiments in the volcanic soil monolith.

The soil monolith was placed onto a 5 cm saturated sand bed (73  $\mu\text{m}$ ), which was connected to a constant-level reservoir through a water-hose. Thus, by setting the reservoir at a distance in the vertical direction from the bottom of the column, a constant suction head was applied. Irrigation was applied on the top with a small-rainfall simulator that was constructed using a 550 x 550 x 32 mm plexi-glass box equipped with 310 hypodermic

needles ( $\varnothing 0.3$  mm spaced 2.5 cm apart) glued through the bottom. The solution was pumped to the rainfall-simulator from a main container. A collector, equipped with a pressure transducer, was used to measure the volume of water coming out from the base of the monolith during each experiment.

A custom-made software (developed at S.I.D.TA-Valladolid, Spain) was used to perform readings automatically.

## 2.2. Miscible displacement experiments

Before starting the experiment, the monolith was irrigated with a background solution. This was a solution of 0.005 M  $\text{CaSO}_4$  (Klute and Dirksen, 1986) to avoid soil dispersion. Afterwards, approximately one pore volume of tracer solution of 0.016 M KBr was applied at a flow rate of 1.8 mm/h during 250 h and the solution changed to the background solution for an additional 710 h.

Resident concentrations at the seven observation depths were estimated from TDR measurements. This approach is based on the assumption that the soil bulk electrical conductivity ( $EC_a$ ) and the electrical conductivity of the soil solution ( $EC_w$ ) are linearly related for a constant water content and salinity levels between 1–50 dS/m (Rhoades et al., 1976; 1989; Ward et al., 1994). Furthermore, assuming a linear relationship between the electrical conductivity and concentration of the soil solution, the relative concentration at any depth and time, can be described by:

$$c(z,t) = \frac{C(z,t) - C_i}{C_o - C_i} = \frac{EC_w(z,t) - EC_{w,i}}{EC_{w,o} - EC_{w,i}} \quad (1)$$

where  $c(z,t)$  and  $C(z,t)$  are the relative and absolute concentration at depth  $z$  and time  $t$ , respectively; and subscripts  $o$  and  $i$  denote input and initial concentrations, respectively. Muñoz-Carpena et al. (2003) found that, according to the equation proposed by Rhoades et al. (1976),  $EC_w$  can be best estimated in this volcanic soil from soil water content ( $\theta$ ) and  $EC_a$  measurements:

$$EC_w = \frac{EC_a - EC_s}{a\theta^2 + b\theta} \quad (2)$$

where  $EC_s$  is the apparent electrical conductivity of the soil solid phase, which usually is considered constant for each soil;  $a$  and  $b$  are fitted parameters. Both  $EC_a$  and  $\theta$  can be measured with TDR. For this soil, Muñoz-Carpena et al. (2003) obtained  $a= 1.876$ ,  $b= -0.512$  and  $EC_s= 0.112$  dS/m.

According to Nadler et al. (1991),  $EC_a$  (dS/m) is related to the impedance of electromagnetic wave moving through the soil as follows:

$$EC_a = \frac{K_{cc}}{Z - Z_{cable}} f_t \quad (3)$$

where  $K_{cc}$  is the cell constant of the TDR probe ( $m^{-1}$ );  $Z$  is the soil bulk impedance ( $\Omega$ );  $Z_{cable}$  is the impedance ( $\Omega$ ) due to cable, connectors, multiplexer and TDR device;  $f_t$  is a temperature correction factor ( $f_t=1$  at 25 °C). Performance of the application of the method in this soil is given in Muñoz-Carpena et al. (2003).

The  $K_{cc}$  and  $Z_{cable}$  (for 50  $\Omega$  coaxial cable) of each TDR probe were obtained by immersing them in different KBr solutions of known concentration (Heimovaara et al., 1995) ranging from 0.5 – 4.0 dS/m. The background electrical conductivity  $EC_{w,i}$  at concentration  $C_i$ , was obtained from the initial conditions before the tracer application. On the other hand, since the solute pulse applied was long enough, the  $EC_{w,o}$  at concentration  $C_o$ , was estimated from the TDR readings corresponding to the maximum (saturation) of the breakthrough curve (Mallants et al., 1994; 1996).

### 2.3. The forward numerical model

In this study we used the mechanistic-deterministic WAVE model (Vanclooster et al., 1996). This code simulates the one-dimensional transport of solute and water in the vadose zone. Transient flow is described with the one-dimensional, isothermal Darcian flow equation in a variably, saturated, rigid porous medium, using the mass-conservative scheme of Richards equation proposed by Celia et al. (1990). The soil moisture retention curve is assumed to be of the form given by van Genuchten (1980), while the unsaturated hydraulic conductivity function is simulated with the van Genuchten-Mualem model (Mualem, 1976; van Genuchten, 1980).

Considering equilibrium (i.e. homogeneity and perfect solute mixing), the solute transport of a non-sorbing, non-reactive solute in a one-dimensional flow system reduces to the convection-dispersion equation (CDE):

$$\frac{\partial(\theta C)}{\partial t} = \frac{\partial}{\partial z} \left( \theta D \frac{\partial C}{\partial z} \right) - \frac{\partial(v\theta C)}{\partial z} \quad (4)$$

where  $C$  is the soil solute concentration [ $\text{ML}^{-3}$ ];  $\theta$  is the soil water content [ $\text{L}^3\text{L}^{-3}$ ];  $t$  is the time [T];  $z$  is the vertical distance from the soil surface [L];  $D$  is the apparent dispersion coefficient [ $\text{L}^2\text{T}^{-1}$ ] and  $v$  the average pore water velocity [ $\text{LT}^{-1}$ ].  $D$  accounts for both the chemical diffusion and the hydrodynamic dispersion coefficients (Wagenet and Hutson, 1989):

$$D = \frac{0.01D_o e^{10\theta}}{\theta} + \lambda v \quad (5)$$

where  $D_o$  is the chemical diffusion coefficient of the considered solute in pure water [ $\text{L}^2\text{T}^{-1}$ ] and  $\lambda$  is the hydrodynamic dispersivity [L], which is a material constant independent of flow rate.

Breakthrough curves could present asymmetry or tailing, which cannot be described using the CDE. Thereby an alternative two-domain model was proposed (Coats and Smith, 1964; van Genuchten and Wierenga, 1976). This model, also known as the mobile-immobile model (MIM) considered the soil water content divided into two regions. Convective-dispersive transport is only assumed in the mobile water domain. The water in the immobile region is not available for convective solute transport, but acts like a source or sink of solute for the mobile one. The solute exchange between both regions is diffusion controlled and described by a first-order rate exchange process. The MIM for transient water flow and for a non-sorbing, non-reactive solute is written as follows (Vanclouster et al., 1996):

$$\frac{\partial(\theta_m C_m)}{\partial t} = \frac{\partial}{\partial z} \left( \theta_m D_m \frac{\partial C_m}{\partial z} \right) - \frac{\partial(v\theta_m C_m)}{\partial z} + \omega(C_m - C_{im}) \quad (6)$$

$$\frac{\partial(\theta_{im} C_{im})}{\partial t} = -\omega(C_m - C_{im}) \quad (7)$$

where Eq. (6) describes the solute transport in the mobile region and Eq. (7) in the immobile domain. The subscripts  $m$  and  $im$  indicate the mobile and immobile soil regions [ $ML^{-3}$ ], respectively.  $D_m$  is the dispersion coefficient in the mobile phase [ $L^2T^{-1}$ ] and  $\omega$  is the mass-transfer coefficient, which controls the exchange between both regions [ $T^{-1}$ ].

#### 2.4. Formulation of the inverse optimization problem

The estimation of parameters by inverse modeling involves the minimization of a suitable objective function, that expresses the differences between observed and predicted values of one or more system response variables (Hopmans and Simunek, 1999). This method requires the coupling of a forward simulation model and an algorithm for global minimum search. The optimization procedure is based on three steps that include: i) parameter perturbation; ii) forward modeling and iii) objective function evaluation. These steps are repeated until certain predefined criteria are fulfilled. The minimization of the objective function is a non-linear problem that can be formulated as a generalized least squares problem when it is assumed that measurement errors follow a multivariable normal distribution with zero mean and known variance-covariance matrix. In general, the error covariance matrix is unknown a priori and further assumptions are needed. Thus, when the differences between observed and predicted values (residuals) are independent and the observation types considered have difference variances, it leads to a weighted least squares problem (Carrera and Neuman, 1986; Hopmans and Simunek, 1999) and the objective function is formulated as follows:

$$OF(\mathbf{b}) = \sum_{z=1}^{n_z} \sum_{i=1}^n w_i [Y^*(z, t_i) - Y(z, t_i, \mathbf{b})]^2 \quad (8)$$

where  $Y^*(z, t_i)$  are measurements of resident concentration at time  $t_i$  and depth  $z$ ;  $Y(z, t_i, \mathbf{b})$  are the corresponding model predictions using the parameter vector  $\mathbf{b}$ ;  $n$  is the number of measurements for each depth and  $n_z$  denote the number observation depths;  $w_{i,j}$  is a weighting factor associated with individual measurements (Vrugt et al., 2001).

To account for the uncertainty associated with the estimated parameters we used linear regression analysis, which, although restrictive and only approximately valid for non-linear problems, it provides some information about parameter confidence intervals. This analysis involves the estimation of the parameter variance-covariance matrix, which is used to calculate 95% parameter confidence intervals, based on Student's t-distribution, and the parameter correlation matrix. The variance-covariance matrix is estimated from the Jacobian

matrix, whose elements are obtained by forward difference approximation with 1% parameter variation. Details of the formulation can be found elsewhere (Hopmans and Simunek, 1999; Lambot et al., 2002).

The global optimization algorithm, GMCS, proposed by (Huyer and Neumaier, 1999) was used here to minimize the objective function. Previous studies (Lambot et al., 2002, Ritter et al., 2002; 2003) showed that the GMCS combined sequentially with the Nelder-Mead-Simplex (NMS) algorithm (Nelder and Mead, 1965) was a useful tool for the estimation of the soil hydraulic parameters. The code used in this study was the one developed by Lambot et al. (2002) and later modified by Ritter et al. (2003). In addition, for the optimization of the solute transport parameters we further changed this code to couple the GMCS-NMS algorithm with the solute transport module of the numerical WAVE model.

The goodness of fit of the simulation performed with the optimized parameters was evaluated with the normalized mean squared error (*nMSE*) (Wilson, 2001) and visual inspection of observed and predicted breakthrough curves. The normalized *MSE* per range of observed values (*nMSE*) expresses the proportion of the variance about the 1:1 line compared to the variance of the observed data ( $\sigma_o^2$ ) and is calculated as follows:

$$nMSE = \frac{MSE}{\sigma_o^2} = \frac{\sum_{i=1}^n [Y^*(z, t_i) - Y(z, t_i, \mathbf{b})]^2}{\sum_{i=1}^n [Y^*(z, t_i) - \bar{Y}^*]^2} \quad (9)$$

Fixing the chemical diffusion coefficient ( $D_o$ ) of bromide to 1.797 cm<sup>2</sup>/day (Lide, 1998), we considered first the CDE approach and performed inverse optimization of the hydrodynamic dispersivity ( $\lambda$ ) for the seven observation depths in the monolith. The parameter search interval was set to [0 – 100 mm]. Secondly, we used the MIM approach. Since the dispersivity is viewed as material constant (Jacques et al., 2002), to reduce the number of parameters to optimize, the dispersivities in the monolith were set equal to the values obtained with the CDE approach. Moreover, considering that the mass-transfer coefficient ( $\omega$ ) depends on the flux conditions rather than on soil properties (Álvarez-Benedí et al., 1999), we assumed the same  $\omega$  for the whole profile. Thereby,  $\theta_m$  for the seven depths and  $\omega$  were estimated by inverse modeling. The search intervals were set at [0 – 1] for  $\theta_m$  and [0 – 1 h<sup>-1</sup>] for  $\omega$ .

### 3. Results and discussion

The use of the TDR technique to monitor the bromide transport in this volcanic soil was successful. As an example, Figure 2 shows for the middle depth in the monolith, the breakthrough curves measured with TDR (three probes) and those obtained from the solution extractors.

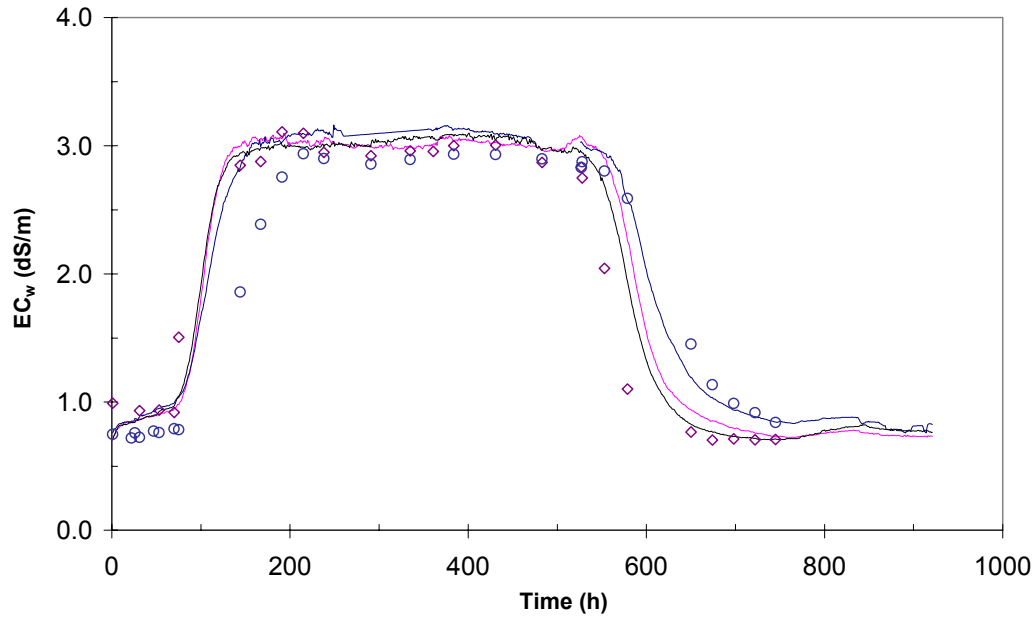


Figure 2. Breakthrough curves (BTC) observed at the middle of the monolith with TDR (lines) and with solution extractors (symbols).

These results confirm the applicability of TDR to estimate in this volcanic soil the electrical conductivity of the soil solution quickly and nondestructively. Furthermore, using Nadler et al. (1991) approach together with a calibrated Rhoades et al. (1976) model may be a good choice.

Figure 3 presents the breakthrough (BTC) curves obtained from TDR readings at the seven observation depths. It is clearly seen how the solute front displaces at each observation depth. At the flow rate applied, the solute pulse is immediately detected at the first depth. However it needs around 8 days to reach the bottom of the monolith.

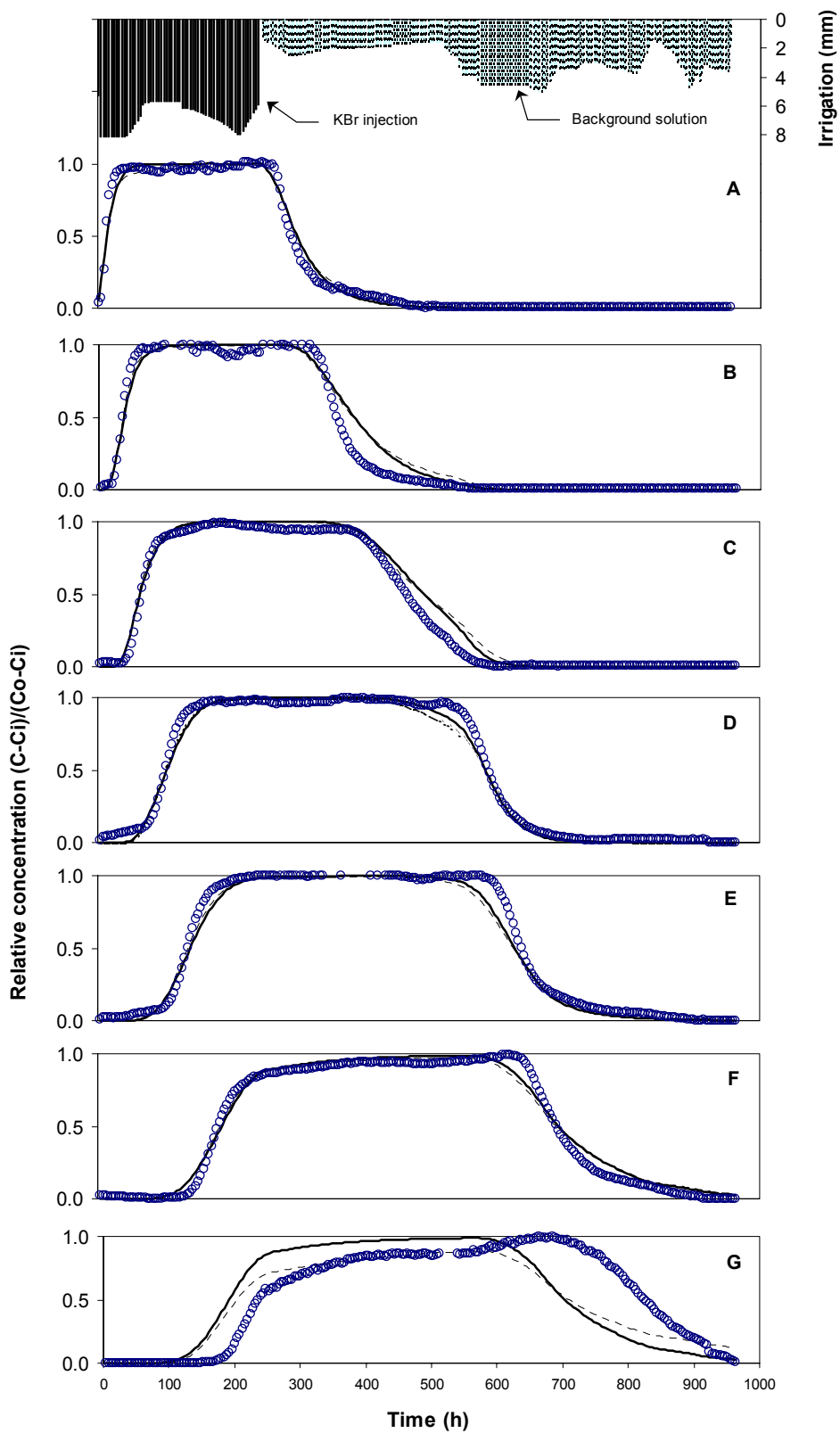


Figure 3. Average breakthrough curves (BTC) at the seven observation depths. BTC obtained from TDR (symbols) and BTC simulated by the WAVE model with CDE (bold lines) and with MIM (dashed lines).

Symmetrical BTCs are observed at depths A, B, D and E, suggesting equilibrium solute transport. On the other hand, asymmetrical curves indicate the presence of some type of non-equilibrium transport process (Mallants et al., 1994). Moreover, except for depths F and G, BTCs at the other depths show early appearance, which suggests that convective transport is the main process. The slow solute pulse arrival at depth G indicates strong non-equilibrium conditions.

Characterization of transport can be further investigated with the parameters estimated by inverse modeling (Table 2). Results using the CDE approach indicate low dispersivity values for the first five depths. A large  $\lambda$  was obtained for the depth G. Because of the large uncertainty associated with these parameters, only qualitative information can be obtained from them. Especially for depths B and C, confidence intervals cannot be calculated, because for a 1% parameter change, no variation in the model output is obtained. This illustrates a problem of parameter identifiability. Thus, more than one combination of dispersivities for the seven observation depths will lead to the same model response.

Table 2  
Inverse simulation results using CDE and MIM

Depth	A	B	C	D	E	F	G
CDE							
$\lambda$ (mm)	4.29±2.15	0.92±~	2.04±~	2.07±14.64	5.91±4.93	10.58±6.95	100±737.48
$nMSE$	0.0080	0.0284	0.0212	0.0095	0.0176	0.0166	0.4803
MIM							
$\theta_m/\theta$	0.919±0.023	1.000±0.000	0.996±0.000	1.000±0.000	0.999±0.000	0.951±0.033	0.760±0.055
$\omega$ (h <sup>-1</sup> )				3.6·10 <sup>-4</sup> ±2.1·10 <sup>-4</sup>			
$nMSE$	0.0073	0.0296	0.0252	0.0135	0.0215	0.0185	0.3064

Using the parameters of Table 2, the model describes satisfactorily the breakthrough curves at all depths, except at depth G. This is deduced from the calculated  $nMSE$  (Table 2) and from the visual inspection of simulated and observed BTCs (Figure 3). In general, model predictions for the ascendant part of the curves are better than for the descendant ones. The lag observed in the measured data at depth G, which causes model predictions to deteriorate, may be explained by some unexpected reactive behavior of Br<sup>-</sup>. A possible explanation could be based on the high Al and Fe oxyhydroxides contents in this volcanic soil (Muñoz-Carpena et al., 2003). Br<sup>-</sup> adsorption may occur since these oxyhydroxides exhibit increasing positive surface charge below the pH of its zero point of charge (Brooks et al., 1998). Thus leading to

a retardation in the breakthrough of the  $\text{Br}^-$  pulse. However, no explanation is found to support the fact that this effect is only observed at the bottom of the monolith.

When using the MIM approach, no significant improvement is achieved. The estimated  $\theta_m/\theta$  (Table 2) indicate that for the first six observation depths, all the pore space contributes to the convective transport process. Comparison between the calculated  $nMSE$  for both approaches shows that basically only at depth G the MIM is preferred (0.4803 vs 0.3064). Considering the whole profile, this implies a small decrease in  $nMSE$  from 0.0640 to 0.0481.

Figure 3 shows also model predictions using the MIM. For the first six depths, they are similar to those obtained with the CDE. At depth G, although the lag above-mentioned, the model matches the upper part of the BTC. Thus, at the bottom of the soil column non-equilibrium transport is expected.

From all these results it can be concluded that solute transport in this volcanic soil is mainly by convection. In addition, the early appearance observed in the BTCs suggests the presence of macropores and preferential flow (Nielsen and Biggar, 1962). This might be in contradiction with the solute transport properties expected in volcanic soils with high allophanic clays content. In these soils water is predominantly held in capillaries and micropores (immobile water) rather than in external clay surfaces (mobile/free water) (Rousseaux and Warkentin, 1976). However, although the volumetric fraction of free water is small (<20%), at high water contents ( $\theta > 30\%$  in this soil), there is a transition where larger pore spaces between micro-aggregates are filled with mobile water (Regalado et al., 2002), and this fraction starts to dominate the transport of solutes. This upper range of moisture in these soils is typically the most relevant in agricultural and contaminant transport scenarios. On the other hand, bromide transfer diffusion between mobile and immobile region may be reduced by coatings on the interface of these regions. Clayey and silty coatings are a widespread phenomenon particularly in illuvial horizons. Thereby, the clay or silt films that coat pore surfaces in structured soils may affect ion diffusion and significantly influence preferential solute transport (Köhne et al., 2002).

Consequently, agricultural practices in these soils would have more potential for contamination of groundwater resources.

#### **4. Conclusions**

Monitoring of bromide transport along a volcanic soil profile during a miscible displacement experiment using TDR probes at seven observation depths was successful. Transport properties were estimated by inverse optimization with the WAVE model and the GMCS-NMS algorithm. Both approaches for describing the movement of a non-sorbing, non-reactive solute in the soil, the classical CDE and the MIM, were used. Under the high soil moisture regime considered, bromide was found to move in the undisturbed soil column mainly by convection processes. Dispersion and non-equilibrium transport were only observed at the bottom of the monolith. At this depth a delay in the breakthrough curve was observed, so that the model could not describe solute dynamic well. This phenomenon could not be sufficiently explained. Results suggested that preferential flow might be present. Thereby the pollution potential of agrochemicals applied at the soil surface might be large.

#### *Acknowledgments*

Authors want to thank J. Álvarez-Benedí (S.I.D.T.A., Valladolid) for developing the data acquisition software used, and Martin Morawietz (University Friburg) during the preparation of the experimental set-up. This work was financed with funds of the INIA-Plan Nacional de I+D Agrario (Proyecto I+D SC99-024-C2) and Consejería de Educación Cultura y Deportes del Gobierno de Canarias. This research was supported by the Florida Agricultural Experiment Station, and approved for publication as Journal Series No. R-\_\_.

#### **5. References**

- Álvarez-Benedí, J., Isla, T., Cartón, A., Bolado, S., 1999. Efecto de la velocidad de flujo en los parámetros de transporte de solutos (In Spanish). In: Muñoz-Carpena, M., Ritter, A., Tascón, C. (eds.). Estudios de la Zona no Saturada del Suelo. Instituto Canario de Investigaciones Agrarias. Valle Guerra, Tenerife.
- Biggar, J.W., Nielsen, D.R., 1967. Miscible displacement and leaching phenomenon. *Agronomy* 12: 254-274.
- Brooks, S.C., Taylor, D.L., Jardine, P.M., 1998. Thermodynamics of bromide exchange on ferrihydrite: Implications for bromide transport. *Soil Sci. Soc. Am. J.* 62:1275–1279

- Carrera, J., Neuman, S.P., 1986. Estimation of aquifer parameters under transient and steady state conditions. 2. Uniqueness, stability and solution algorithms. *Water Resour. Res.* 22: 211-227.
- Celia, M.A., Bouloutas, E.T., Zarba, R.L., 1990. A general mass-conservative numerical solution for the unsaturated flow equation. *Water Resour. Res.* 26: 1483-1496.
- Coats, B.E., Smith, B.D., 1964. Dead-end pore volume dispersion in porous media. *SPE J.* 4: 73-84.
- Ersahin, S., Papendick, R.I., Smith, J.L., Keller, C.K., Manoranjan, V.S., 2002. Macropore transport of bromide as influenced by soil structure differences. *Geoderma* 108: 207-223.
- Heimovaara, T.J., Focke, A.G., Bouten, W., Verstraten, J.M., 1995. Assessing temporal variations in soil water composition with time domain reflectometry. *Soil Sci. Soc. Am. J.* 59, 689-698.
- Hopmans, J.W., Simunek, J., 1999. Review of inverse estimation of soil hydraulic properties. In M. Th. van Genuchten, F.J. Leij and L. Wu (eds) *Proc. Int. Workshop, Characterization and Measurement of the Hydraulic Properties of Unsaturated Porous Media*: 713-724. University of California, Riverside, C.A.
- Huyer, W., Neumaier, A., 1999. Global optimization by multilevel coordinate search. *J. Global Optimization* 14: 331-355.
- Jacques, D., Kim, D.J., Diels, J., Vanderborght, J., Vereecken, H., Feyen, J., 1998. Analysis of steady state chloride transport through two heterogenous field soils. *Water Resour. Res.* 34, 2539-2550.
- Jacques, D., Simunek, J., Timmerman, A., Feyen, J., 2002. Calibration of Richards' and convection-dispersion equations to field-scale water flow and solute transport under rainfall conditions. *J. Hydrol.* 259: 15-31.
- Jury, W.A., 1982. Simulation of solute transport using a transfer function model. *Water Resour. Res.* 18: 363-368.
- Kachanoski, R.G., Pringle, E.A., Ward, A.L., 1992. Field measurement of solute travel times using time domain reflectometry. *Soil Sci. Soc. Am. J.* 56: 47-52.
- Kim, D.J., Vanclooster, M., Feyen, J., Vereecken, H., 1998. Simple linear model for calibration of time domain reflectometry measurements on solute concentrations. *Soil Sci. Soc. Am. J.* 62: 83-89.
- Klute, A., Dirksen, C., 1986. Hydraulic conductivity and diffusivity: Laboratory Methods. In: A. Klute (ed.) *Methods of Soil Analysis Part 1*. Agronomy no. 9 ASA-SSSA: Madison.

- Köhne, J.M., Gerke, H.H., Köhne, S., 2002. Effective diffusion coefficients of soil aggregates with surface skins. *Soil Sci. Soc. A. J.* 66: 1430-1438.
- Lambot, S., Javaux, M., Hupet, F., Vanclooster, M., 2002. A Global Multilevel Coordinate Search procedure for estimating the unsaturated soil hydraulic properties. *Water Resour. Res.* (*in press*).
- Lee, J., Horton, R., Noborio, K., Jayes, D.B., 2001. Characterization of preferential flow in undisturbed, structured soil columns using a vertical TDR probe. *J. Contam. Hydrol.* 51: 131-144.
- Lide, D.(ed.), 1998. *CRC Handbook of Chemistry and Physics*. New York.
- Mallants, D., Vanclooster, M., Meddahi, M., Feyen, J., 1994. Estimating solute transport in undisturbed soil columns using time domain reflectometry. *J. Contam. Hydrol.* 17: 91-109.
- Mallants, D., Vanclooster, M., Toride, N., Vanderborght, J., van Genuchten, M.Th., Feyen, J., 1996. Comparison of three methods to calibrate TDR for monitoring solute movement in undisturbed soil. *Soil Sci. Soc. Am. J.* 60: 747-754.
- Muñoz-Carpena, R., Regalado, C.M., Ritter, A., Alvarez-Benedí, J., Socorro, A.R., 2003. Applicability of time domain reflectometry for simultaneous monitoring of moisture and solute transport in a volcanic soil. *E. J. Soil Sci.* (*in review*).
- Mualem, Y., 1976. A new model for predicting the hydraulic conductivity of unsaturated porous media. *Water Resour. Res.* 12: 513-522.
- Nadler, A., Dasberg, S., Lapid, I., 1991. Time domain reflectometry measurements of water content and electrical conductivity of layered soil columns. *Soil Sci. Soc. Am. J.* 55: 938-943.
- Nelder, J. A., Mead, R., 1965. A Simplex Method for Function Minimization. *Computer Journal* 7: 308-313.
- Persson, M., 1997. Soil solution electrical conductivity measurements under transient conditions using time domain reflectometry. *Soil Sci. Soc. Am. J.* 61: 997-1003.
- Regalado, C.M., Muñoz-Carpena, R., Socorro, A.R., Hernández Moreno, J.M., 2002. Why volcanic soils do not follow Topp's equation?. *Geoderma* (*in press*).
- Rhoades, J.D., Raats, P.A.C., Prather, R.J., 1976. Effects of liquid-phase electrical conductivity, water content, and surface conductivity on bulk soil electrical conductivity. *Soil Science Society of America Journal* 40:651-655.
- Rhoades, J. D., Manteghi, N.A., Shouse, P.J., Alves, W.J., 1989. Soil electrical conductivity and soil salinity: new formulations and calibrations. *Soil Sci. Soc. Am. J.* 53: 433-439.

- Risler, P.D., Wraith, J.M., Graber, H.M., 1996. Solute transport under transient flow conditions estimated using time domain reflectometry. *Soil Sci. Soc. Am. J.* 60: 1297-1305.
- Ritter, A., Hupet, F., Muñoz-Carpena, R., Lambot, S., Vanclooster, M., 2002. Using inverse methods for estimating soil hydraulic properties from field data as an alternative to direct methods. *Agric. Water Manage.* (*in press*).
- Ritter, A., Muñoz-Carpena, R., Regalado, C.M., Vanclooster, M., Lambot, S., 2003. Analysis of alternative measurement strategies for the inverse optimization of the hydraulic properties of a volcanic soil. *J. Hydrol.* (*in review*).
- Roth, K., Flüher, H, Attinger, W., 1990. Transport of a conservative tracer under field conditions: qualitative modeling with random walk in a double porous medium. *Field-scale water and solute flux in soils.* Birkhäuser, Basel, pp 239-248.
- Rousseaux, J.M., Warkentin, B.P., 1976. Surface properties and forces holding water in allophane soils. *Soil. Sci. Soc. Am. J.*, 40: 446-451.
- Rudolph, D.L., Kachanoski, R.G., Celia, M.A., LeBlanc, D.R., Stevens, J.H., 1996. Infiltration and solute transport experiments in unsaturated sand and gravel, Cape Cod, Massachusetts: experimental design and overview of results. *Water Resour. Res.* 32, 519-532.
- van Genuchten, M.Th., Wierenga, P.J., 1976. Mass transfer studies in sorbing porous media. I Analytical solutions. *Soil Sci. Soc. Am. J.* 40: 473-480.
- van Genuchten, M.Th., 1980. A closed-form equation for predicting the hydraulic conductivity of soil. *Soil Sci. Soc. Am. J.* 44: 892-898.
- Vanclooster, M., Mallants, D., Vanderborght, J., Diels, J., Feyen, J., 1993. Determining local-scale solute transport parameters using time domain reflectometry (TDR). *J. Hydrol.* 148: 93-107.
- Vanclooster, M., Mallants, D., Vanderborght, J., Diels, J., van Orshoven, J., Feyen, J., 1995. Monitoring solute transport in a multi-layered sandy lysimeter using time domain reflectometry. *Soil Sci. Soc. Am. J.* 59: 337-344.
- Vanclooster, M., Viaene, P., Christiaens, K., Ducheyne, S., 1996. *WAVE* : a mathematical model for simulating water and agrochemicals in the soil and vadose environment, Reference and user's manual (release 2.1), Institute for Land and Water Management, Katholieke Universiteit Leuven, Leuven, Belgium.

- Vanclooster, M., Ducheyne, S., Dust, M., Vereecken, H., 2000. Evaluation of pesticide dynamics of the WAVE-model. *Agric. Water Manage.* 44: 371-388.
- Vanderborght, J., Timmerman, A., Feyen, J., 2000. Solute transport for steady-state and transient flow in soils with and without macropores. *Soil Sci. Soc. Am. J.* 64: 1305-1317.
- Vogeler, I., Clothier, B.E., Green, S.R., Scotter, D.R., Tillman, R.W., 1996. Characterizing water and solute movement by time domain reflectometry and disk permeametry. *Soil Sci. Soc. Am. J.* 60: 5-12.
- Vrugt, J.A., Bouten, W., Weerts, A.H., 2001. Information content of data for identifying soil hydraulic parameters from outflow experiments. *Soil Sci. Soc. Am. J.* 65: 19-27.
- Ward, A.L., Kachanoski, R.G., Elrick, D.E., 1994. Laboratory measurements of solute transport using time domain reflectometry. *Soil Sci. Soc. Am. J.* 58: 1031-1039.
- Wagenet, R.J., Hutson, J.L., 1989. LEACHM a process-based model of water and solute movement transformations, plant uptake and chemical reactions in the unsaturated zone. *Continuum*, vol. 2. Centre for Environmental Research, Cornell University, New York.
- Wilson, B.N., 2001. Evaluation of hydrologic models using statistical methods. ASAE Paper 01-012207, Presented at 2001 ASAE Annual International Meeting, St. Joseph, MI.

## DISCUSIÓN

Los resultados obtenidos en cada uno de los capítulos tratados en este trabajo se comentan a continuación de manera conjunta.

El estudio detallado de las propiedades físicas y químicas de un suelo de origen volcánico en una parcela agrícola comercial en la isla de Tenerife (Canarias) indicó que éste presenta características ándicas, las cuales se traducen básicamente en baja densidad aparente y fuerte micro-agregación natural que conducen a una porosidad, retención de agua y conductividad hidráulica saturada altas. Estas propiedades condicionan potencialmente el flujo y transporte de contaminantes a través del suelo, especialmente en condiciones de horticultura intensiva y continua (todo el año).

El seguimiento de variables hidrológicas y de diferentes especies de nitrógeno (orgánico, N-NO<sub>3</sub> y N-NH<sub>4</sub>) en dicha parcela, bajo un cultivo de plátanos, permitió evaluar el efecto de las prácticas de riego y abonado sobre este suelo. El balance hidrológico realizado mostró que del agua que se pierde y abandona el perfil del suelo, gran parte se produce durante los meses de mayor aplicación de riego (aspersión) o tras periodos largos de lluvia, alcanzando valores que suponen el 18 % del total del agua aplicada (lluvia + riego). El estudio hidrogeológico de la zona indicó que este suelo, que se haya dispuesto en terrazas, se encuentra situado sobre diversas capas de basalto fracturado, de manera que el agua que abandona el perfil percola rápidamente a través de vías preferenciales con lo que tiene el potencial de recargar el acuífero rápidamente y por lo tanto de contaminarlo. No obstante, antes de alcanzar el acuífero este agua es interceptada por el flujo subterráneo de la zona diluyéndose en una proporción 1:4.

La estimación de los requerimientos de lavado con un sistema de riego por aspersión y para rendimientos potenciales de la platanera entre 90-100%, sugieren fracciones de lavado entre 15-20%. Por lo tanto, en este caso no sería conveniente reducir el volumen de agua aplicado con el riego.

Debido a las elevadas concentraciones de nitratos por exceso de abonado observadas en la disolución del suelo (50-120 mg/l N-NO<sub>3</sub>), el lixiviado transporta entre 48-52% del nitrógeno total aplicado anualmente como fertilizante al cultivo (fertirrigación). Comparando las concentraciones de N-NO<sub>3</sub> en la base del perfil del suelo con aquellas medidas en muestras recogidas en un manantial situado en los acantilados de la zona (a menor altitud sobre el nivel

del mar que la zona de cultivo), se deduce una dilución de N-NO<sub>3</sub> en una proporción de 0.60. Este valor no se corresponde con la relación de 0.25 mencionada anteriormente y obtenida a partir de un estudio isotópico realizado en la zona. Sin embargo, hay que considerar que este último no considera i) la variabilidad temporal, ii) el efecto de escala regional implícito en las muestras recogidas del manantial y iii) el tiempo de tránsito desde la base del perfil del suelo hacia al manantial a través del material volcánico fracturado.

Los resultados mostraron por tanto un exceso de aplicación de abonos nitrogenados al cultivo, que sugiere la revisión de las prácticas de fertilización, siendo recomendables aplicaciones más frecuentes y en menor cantidad. Otra alternativa para reducir las pérdidas de nitrógeno por lixiviación implicaría reducir el volumen de agua que abandona el perfil del suelo. Sin embargo, en este caso, esta práctica no es conveniente debido a la fracción de lavado que se requiere para mantener la salinidad del suelo en niveles adecuados.

La obtención de datos hidrológicos en este escenario agrícola (capítulo 1) permitió la aplicación de un modelo numérico para describir el movimiento de agua a través del perfil del suelo, el cual presentaba tres horizontes (0 – 20; 20 – 50; 50 – 70 cm). El gran número de parámetros que requiere este modelo se determinó en parte de forma experimental y en parte por procedimientos de calibración. La realización de un análisis de sensibilidad aportó información para la selección de aquellos parámetros que son más susceptibles de ser optimizados. Así, se decidió determinar simultáneamente, para los tres horizontes, tres parámetros hidráulicos: humedad residual ( $\theta_r$ ) y los parámetros de forma de la curva de retención de humedad ( $\alpha$  y  $n$ ).

En la estimación de estas propiedades, se realizó una comparación entre el procedimiento directo y dos métodos indirectos de calibración: a) “prueba y error” y b) optimización o simulación inversa. Para estos últimos se usaron las series temporales de humedad de suelo medidas en los tres horizontes. La evaluación de los métodos se hizo cuantitativamente mediante la raíz del error cuadrático medio (RMSE) y de forma cualitativa a través de la inspección visual de las predicciones del modelo frente a los valores medidos. El método directo resultó inadecuado, mientras que con la simulación inversa se obtuvo los mejores resultados.

El procedimiento de “prueba y error”, aunque tiene la ventaja de ser más flexible, presenta los inconvenientes de que consume mucho tiempo; resulta difícil saber en qué

dirección modificar los parámetros (sobre todo si hay interacción entre ellos); el resultado depende de los valores iniciales; es muy subjetivo y no asegura encontrar el mejor conjunto de parámetros. Además, no permite cuantificar la incertidumbre asociada a los parámetros estimados.

Por el contrario, el uso de un algoritmo de optimización inversa potente, como es el Global Multilevel Coordinate Search combinado secuencialmente con un Nelder Mead Simplex (GMCS-NMS), acelera el proceso de calibrado, ya que no depende de valores iniciales y dentro del espacio de búsqueda (definido por los intervalos de los parámetros) no prueba todas las combinaciones, sino aquellas con mayor probabilidad de ser la solución. Es una técnica menos subjetiva y por sus características encontrará de forma más eficiente el mejor conjunto de parámetros.

No obstante, la eficacia de las técnicas de optimización inversa depende del *planteamiento* del problema. El planteamiento está condicionado entre otras cosas por las condiciones del suelo que se investiga, el rango y tipo de condiciones de contorno, la estructura del modelo, la magnitud del error en las mediciones y el número de parámetros a estimar.

Las diferencias observadas entre los parámetros estimados mediante los procedimientos indirectos mencionados y las determinaciones realizadas experimentalmente en laboratorio (método directo) se explican debido a fenómenos relacionados con la estructura del suelo, que generalmente influyen en el movimiento de agua a escala de campo, pero que difícilmente están representados a la escala de pequeñas muestras inalteradas como en las que usualmente se realiza la determinación directa. A esto hay que añadir que los métodos indirectos permiten obtener parámetros efectivos en el rango de aplicación del modelo de simulación.

En consecuencia, el procedimiento de calibración usando técnicas de optimización inversa resulta prometedor frente al procedimiento tradicional de “prueba y error” y a los métodos directos. Sin embargo, para aplicar esta técnica es conveniente disponer de información previa sobre los parámetros a optimizar así como usar datos de varias variables de estado que contengan información suficiente para estimar dichos parámetros.

En el estudio de las variables hidrológicas en la parcela comercial de platanera, se observan discrepancias respecto a la cuantificación de las pérdidas de agua por lixiviación. Por un lado, en el capítulo 1, éstas se estiman en 237 mm a partir del establecimiento del

balance hidrológico mensual en la parcela. Por el contrario, cuando se aplicó el modelo WAVE usando los parámetros hidráulicos optimizados por simulación inversa, la cantidad de agua que abandona el perfil del suelo se cuantificó en 424 mm.

Esta diferencia se explica lógicamente debido a los métodos de cálculo empleados. En primer lugar, el modelo determina el flujo en la base del perfil por resolución numérica de las ecuaciones que gobiernan el movimiento de agua en el suelo. Este valor de 424 mm es 33 mm superior al que se puede obtener por diferencia entre los componentes del balance hidrológico que también proporciona el modelo (error de balance= 33 mm).

En segundo lugar, comparando los componentes hidrológicos acumulados al final del periodo que se estiman en el capítulo 1 con aquellos obtenidos con WAVE, se observa que la diferencia entre los valores de flujo es debida en un 77% al error en el cálculo de la evapotranspiración actual ( $ET_a$ ) y en un 23% al error en la estimación de la variación de la humedad en el suelo. Mientras que el modelo calcula la variación de humedad diariamente, en el capítulo 1, este componente se determinó por diferencia entre los valores de humedad mensuales, que resultan del promedio a partir de datos diarios.

Con respecto a la  $ET_a$ , el modelo la estima con base en una función que describe la extracción de agua por las raíces y que depende del potencial matricial del suelo. En el capítulo 1, sin embargo, la  $ET_a$  se calculó como sigue:

$$ET_a = \begin{cases} ET_c; BAL \geq 0 \\ P + R + \Delta W; BAL < 0 \end{cases} \quad \text{donde } BAL = (P + R) - (ET_c + \Delta W)$$

siendo  $P$  precipitación,  $R$  riego,  $ET_c$  evapotranspiración potencial del cultivo y  $\Delta W$  la variación del contenido de humedad de suelo.

Este hecho ilustra la utilidad que tiene el uso de un modelo de simulación validado para la predicción de los procesos de flujo en el suelo.

Conociendo el potencial y las limitaciones de la calibración por simulación inversa (capítulo 2), resulta interesante estudiar qué variables y en qué cantidad se necesitan medir para realizar la optimización de parámetros con el mínimo coste y esfuerzo. En este contexto, puede aplicarse un procedimiento en el que se analicen alternativas o estrategias basadas en el uso de datos correspondientes a diferentes variables de estado y distintos puntos de medida. La identificación de la estrategia más adecuada se facilita mediante el uso de un

índice basado en el grado de incertidumbre asociado a los parámetros estimados y en el error cuadrático medio entre los datos observados y los valores simulados por el modelo con esos parámetros.

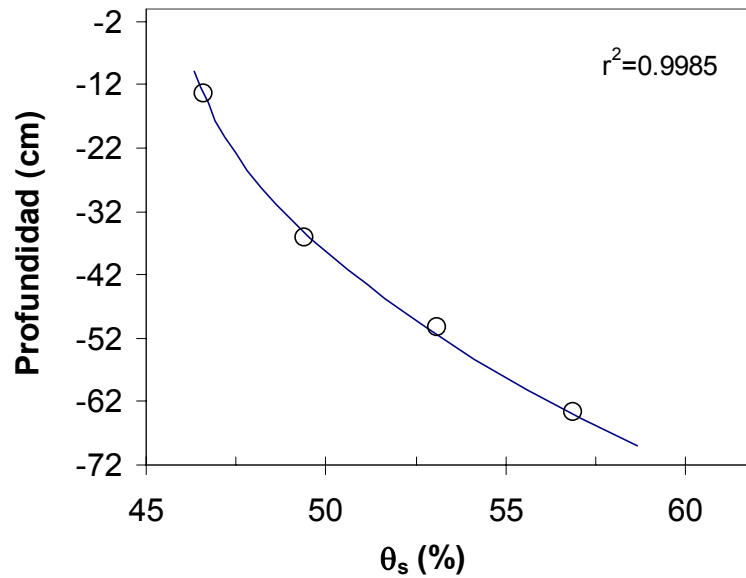
Generalmente las decisiones a la hora de establecer la estrategia de muestreo para obtener la información necesaria para la calibración de parámetros están basadas en simple intuición. Este procedimiento puede servir para fundamentar cuantitativamente esas decisiones. Para ello, durante la fase de diseño, pueden usarse datos sintéticos. Estos datos se generan con el modelo de simulación usando parámetros de referencia obtenidos en la literatura para condiciones similares o a través de funciones de transferencia.

El procedimiento se ilustró y validó con datos reales en la simulación inversa de las propiedades hidráulicas de una columna de suelo inalterado (monolito) a partir de experimentos de flujo. Un primer experimento permitió identificar cuatro horizontes con diferente comportamiento hidrológico, aportando así información útil sobre las propiedades hidráulicas del suelo. Un segundo experimento sirvió para estimar los parámetros por optimización inversa.

Se definieron varias estrategias basadas en el uso de los datos correspondientes a diferentes variables hidráulicas y a distintas profundidades de medida en la columna (hasta siete). Las variables consideradas fueron: contenido de humedad de suelo ( $\theta$ ), succión ( $h$ ) y flujo recogido en la base de la columna ( $q$ ). Con base en un análisis de sensibilidad se seleccionaron un total de 8 parámetros para su optimización: conductividad hidráulica saturada en los cuatro horizontes, humedad a saturación en los dos horizontes superiores y el parámetro de curva  $n$  en los dos horizontes inferiores.

Los mejores resultados se obtuvieron al combinar información de las tres variables hidráulicas. Sin embargo, el uso de mediciones de  $\theta$  conjuntamente con datos de  $h$  o  $q$  conduce también a resultados satisfactorios. Con respecto al número de profundidades de medida, se observó que éstas se pueden reducir hasta cuatro (una por horizonte).

En cuanto a las propiedades hidráulicas estimadas en el monolito, los valores de humedad a saturación ( $\theta_s$ ) en cada horizonte siguen una tendencia cuadrática con la profundidad, como se puede ver en la siguiente gráfica.



Esto puede explicarse por procesos de compresión del suelo que conducen a cambios en su porosidad. La compresión en los suelos agrícolas puede darse de forma natural como consecuencia de su textura y del régimen hídrico al que están sometidos. Por otro lado, este efecto se observa también al aplicar fuerzas mecánicas sobre la superficie del suelo. En este caso la distribución de presiones en el perfil, justo debajo del punto de aplicación, es de tal manera que la presión se reduce de forma cuadrática con la profundidad (Hillel, 1998).

Una vez estimados los parámetros hidráulicos y obtener así una buena descripción de los procesos hidrológicos en el suelo de estudio (capítulo 3), es posible determinar las propiedades que rigen el transporte de solutos en dicho suelo. La descripción de este proceso es complicada y es conveniente simplificar el problema para solutos no-sorbibles y no-reactivos.

En una columna de suelo volcánico inalterado, de grandes dimensiones se lleva a cabo un experimento de desplazamiento de bromuro. El seguimiento mediante TDR del movimiento del bromuro a lo largo del perfil del suelo se realiza con éxito a siete profundidades. Para ello resultó apropiado el uso del modelo de Nadler et al. (1991) junto con el modelo de Rhoades et al. (1976), calibrado para este suelo volcánico.

El grado de simetría que presentan la mayoría de las curvas de ruptura obtenidas sugiere condiciones de equilibrio. Además, el frente abrupto de estas curvas indica que posiblemente el principal mecanismo de transporte sea por convección. Esta hipótesis se confirma estimando las propiedades de transporte mediante la aplicación de técnicas de simulación

inversa usando el modelo WAVE y el algoritmo de optimización global GMCS-NMS. Considerando la aproximación clásica de transporte convectivo-dispersivo (CDE) se obtiene que, con valores de dispersividad bajos, WAVE describe satisfactoriamente el movimiento de bromuro a través del monolito. Por otro lado, al aplicar la aproximación basada en dos regiones (inmóvil-móvil, MIM), se obtiene que una fracción alta de poros contribuye al transporte convectivo.

En la base del monolito se observa una curva de ruptura diferente a lo comentado anteriormente. En primer lugar, ésta muestra un retraso que sugiere que el bromuro está reaccionando con la matriz del suelo. Esto podría explicarse por el alto contenido de oxihidróxidos de hierro y aluminio presentes en este suelo volcánico, que a pH inferiores al punto de carga cero, muestran cargas positivas que pueden retener el bromuro. Sin embargo, no se comprende por qué este fenómeno no se observa en el resto de la columna de suelo. En segundo lugar, la curva de ruptura presenta un tramo ascendente de pendiente no abrupta que puede asociarse a un transporte convectivo dispersivo y en condiciones de no-equilibrio. Esto se deduce igualmente a partir de los parámetros estimados para esta profundidad.

El predominio del transporte convectivo puede estar en contradicción con lo que cabría esperar en suelos volcánicos con alto contenido en arcillas alofanas. En estos suelos el agua se encuentra principalmente retenida en microporos (agua inmóvil). Sin embargo, a contenidos de humedad altos el agua se encuentra también en macroporos. Esta fracción de agua móvil, aunque menor, es la que condiciona en mayor medida el transporte de solutos (Regalado et al., 2002). El rango alto de humedad al que se hace referencia coincide con aquel que se da frecuentemente en estos suelos bajo escenarios agrícolas.

Por otro, lado también se ha citado (Köhne et al., 2002) que el transporte preferencial de solutos en suelos estructurados puede estar favorecido por la presencia de una fina capa arcillosa que recubre la interfase entre las regiones móvil e inmóvil impidiendo la difusión del anión a la zona intragregados. Estas capas son frecuentes en aquellos horizontes de iluviación.

En general, el frente abrupto de las curvas de ruptura observadas en el monolito puede estar relacionado con un transporte preferencial de solutos. En consecuencia se deduce que, en este tipo de suelo, el potencial contaminante por agroquímicos pueda ser mayor.

Como consecuencia de lo estudiado en los diferentes capítulos, la descripción de procesos mediante modelos numéricos y la calibración de los mismos con técnicas de optimización inversa son técnicas prometedoras, sobre todo debido a la disponibilidad de ordenadores cada vez más potentes y al desarrollo de herramientas que permiten el seguimiento de variables de forma automática y con costes relativamente asequibles. La limitación del número de propiedades que se pueden optimizar, sugiere que, de todos los parámetros que necesita un modelo, se determine el mayor número posible de aquellos a los que éste es menos sensible utilizando otros métodos (medición directa, estimación a partir de funciones de transferencia, literatura, etc.) Así, la simulación inversa podrá centrarse en los parámetros para los que el modelo presenta mayor sensibilidad.

### **Referencias citadas**

- Dorel, M., Roger-Estrate, J., Manichon, H., Devaux, B., 2000. Porosity and soil water properties of Caribbean volcanic ash soils. *Soil Use & Management*, 16: 133-145.
- Hillel, D. 1998. *Environmental Soil Physics*. Academic Press: San Diego, pp. 771.
- Köhne, J.M., Gerke, H.H., Köhne, S., 2002. Effective diffusion coefficients of soil aggregates with surface skins. *Soil Sci. Soc. A. J.* 66: 1430-1438.
- Nadler, A., Dasberg, S., Lapid., I., 1991. Time domain reflectometry measurements of water content and electrical conductivity of layered soil columns. *Soil Sci. Soc. Am. J.* 55: 938-943.
- Regalado, C.M., Muñoz-Carpena, R., Socorro, A.R., Hernández Moreno, J.M., 2002. Why volcanic soils do not follow Topp's equation?. *Geoderma (in press)*.
- Rhoades, J.D., Raats, P.A.C., Prather, R.J., 1976. Effects of liquid-phase electrical conductivity, water content, and surface conductivity on bulk soil electrical conductivity. *Soil Science Society of America Journal* 40:651-655.



## CONCLUSIONES

En este trabajo titulado *Optimización de la simulación del transporte de agua y solutos en suelos volcánicos para la evaluación de la contaminación de aguas y suelos por agroquímicos* se han obtenido las siguientes conclusiones:

- El estudio detallado de las propiedades físico-químicas de un suelo agrícola en una zona de platanera en la parte Norte de la isla de Tenerife, así como el seguimiento realizado de las variables hidrológicas y contenidos nitrógeno han permitido estudiar el funcionamiento hidrológico de este escenario y evaluar las prácticas agronómicas.
- El suelo presenta características ándicas que condicionan el flujo y el transporte de nitrógeno a través de la zona no saturada.
- El citado estudio indicó que el 48-52% del total de abono nitrogenado aplicado al cultivo anualmente no es usado por la planta, sino que abandona el suelo hacia el acuífero.
- Estas pérdidas de nitrógeno se concentran en los periodos de lluvia y/o fertirrigación intensos.
- Debido a los requerimientos de lavado necesarios para mantener la salinidad del suelo en niveles adecuados, el control de la contaminación del acuífero por nitratos implica solamente una revisión de las prácticas de abonado (cantidad, frecuencia, técnica de aplicación, etc.) y no la reducción de la fracción de lavado.
- La aplicación de un modelo para la simulación del flujo en un escenario típico agrícola del Norte de Tenerife usando propiedades hidráulicas determinados experimentalmente en laboratorio puede conducir a resultados inexactos.
- Esto es debido a que el uso de parámetros determinados experimentalmente en laboratorio en pequeñas muestras de suelo no reflejan el efecto que los fenómenos estructurales tienen a escala de campo.
- La estimación de esos parámetros por métodos indirectos resulta más apropiada en este contexto.
- Entre los métodos indirectos, el uso de la optimización inversa usando el algoritmo GMCS-NMS resulta ser una técnica eficiente y preferible al procedimiento tradicional de “prueba y error”.

- Para mejorar la efectividad de la calibración mediante optimización inversa, es necesario disponer de información previa sobre los parámetros a optimizar así como usar datos de diferentes variables de estado que contengan información suficiente para estimar dichas propiedades.
- En el diseño de una estrategia adecuada de seguimiento de variables y obtención de datos para simulación inversa, se recomienda aplicar en la fase de diseño experimental un procedimiento que permita analizar diferentes alternativas de muestreo usando datos sintéticos.
- El uso de un índice basado en criterios de evaluación, como el propuesto, facilita la comparación entre estrategias.
- Igualmente, la obtención previa de información sobre las propiedades hidráulicas del suelo a partir de experimentos o cualquier otro método resulta ventajosa para el diseño.
- El procedimiento para establecer la estrategia de muestreo apropiada se ilustró con éxito en la optimización de los parámetros hidráulicos de un monolito a partir de experimentos de flujo y usando el algoritmo GMCS-NMS acoplado al modelo numérico WAVE.
- El análisis de varias estrategias basadas en distintas profundidades de medida y en la combinación de variables de estado (humedad de suelo, succión y flujo en la base del monolito), indicó que para la optimización inversa de las propiedades hidráulicas del suelo, son suficientes solamente cuatro profundidades de medida y la combinación de datos de humedad de suelo junto con datos de succión o de flujo en la base de la columna.
- El seguimiento conjunto del flujo y del transporte de bromuro en un suelo volcánico puede realizarse con éxito mediante la aplicación de la técnica de TDR.
- La caracterización del transporte de bromuro a partir de las curvas de ruptura obtenidas mediante TDR y con la aplicación de técnicas de simulación inversa indica que, bajo las condiciones de contorno aplicadas, el bromuro se mueve en este suelo volcánico principalmente por convección.
- El tipo de curvas de ruptura observadas se asocia con procesos de transporte preferencial, con lo que se puede esperar que el potencial contaminante de los agroquímicos aplicados a este suelo sea mayor.

- La combinación de modelos de simulación con algoritmos de optimización inversa y el uso de mediciones detalladas de diferentes variables de estado, resulta una técnica prometedora para la identificación de procesos y de parámetros.